Inaugural-Dissertation zur Erlangung der Doktorwürde
der Tierärztlichen Fakultät der Ludwig-Maximilians-Universität
München

In vivo evaluation of siRNA-based cancer therapeutics delivered by polymeric nanocarriers

von Eva Kessel

aus Worms

München 2017

Aus dem Veterinärwissenschaftlichen Department der Tierärztlichen Fakultät
der Ludwig-Maximilians-Universität München

Lehrstuhl für Molekulare Tierzucht und Biotechnologie

Arbeit angefertigt unter der Leitung von: Univ.-Prof. Dr. Eckhard Wolf

Angefertigt an: Fakultät für Chemie und Pharmazie, Lehrstuhl für
Pharmazeutische Biotechnologie der Ludwig-Maximilians-Universität München

Mentor: Univ.-Prof. Dr. Ernst Wagner

**Gedruckt mit Genehmigung der Tierärztlichen Fakultät
der Ludwig-Maximilians-Universität München**

Dekan:	Univ.-Prof. Dr. Joachim Braun
Berichterstatter:	Univ.-Prof. Dr. Eckhard Wolf
Korreferent:	Univ.-Prof. Dr. Gerd Sutter

Tag der Promotion: 11. Februar 2017

Meiner Familie

Mona, Xantos und Angelina

TABLE OF CONTENTS

I INTRODUCTION

The rising burden of cancer poses a serious global threat to human development and the well-being of society. As published by the WHO in the Global Cancer Report 2014 [1], 8.2 million people die from cancer each year worldwide, 2 million alone in the US and EU. From 2012 to 2014, the global incidence of cancer increased about 10 percent and this trend is expected to continue in the next decades.[1, 2]

Carcinogenesis is a result of inherent or acquired genetic alterations and subsequently of dysregulated proteins.[3] Historically, the profiling of cancer specimens and subsequent treatment decisions were mainly based on the histopathological evaluation.[4, 5] Recently, advanced molecular biology techniques provided useful tools for the characterization of genetic alterations and the subtyping of cancer specimens.[6, 7] The identification of numerous cancer-related gene expression profiles facilitated a deeper understanding of tumor cell biology and the identification of novel molecular targets for therapeutic intervention.[7-9] These targets may be addressed, for instance by nucleic acid (NA)-based therapies to modulate their gene expression in a desired manner.[10] NAs have been expected to provide high potential for the treatment of various diseases with genetic dysregulation, therefore great efforts have been put into the research on gene therapy.[11] In consequence, the number of clinical trials in this field has constantly risen during the last decades, and the majority of them seek new treatment approaches for cancer diseases (~64% of the trials).[12, 13] However, in this respect, the number of approved gene therapies on the global market seems low, primarily due to obstacles concerning the delivery process, as successful gene therapy is largely dependent on selective and efficient intracellular delivery of the therapeutic NA to the target cell.[14-16] Hence, the experiments illustrated in this thesis evaluate multifunctional carriers designed for efficient and save NA-based therapy.

1 Tumor-selective delivery strategies for siRNA based therapy

For the genetic treatment of diseases, NA are used to either express (e.g. via mRNA or pDNA [17]) or silence (e.g. via antisense oligonucleotides or siRNA [18]) selected genes and consequently promote, or respectively downregulate, the expression of their encoded proteins. Recently, the use of synthetic small interfering RNA (siRNA) emerged as a promising NA-based treatment concept.[19] siRNA presents an attractive tool for the specific downregulation of essential proteins, comprising a wide clinical potential to treat various diseases induced by

genetic alteration [16], especially cancer.[10] Nonetheless, the treatment of cancer with siRNA remains a challenge in clinical trials since the requirements for a successful cure represent multiple demanding tasks to be fulfilled by an efficient delivery system.[20] In this regard, the associated barriers that might limit a tumor-selective siRNA delivery are described first, followed by a customized solution approach, which may increase the overall effectiveness of this NA-based treatment concept.

1.1 siRNA therapy

The small double-stranded RNA (dsRNA) molecules belong to the non-coding RNAs and interfere directly on the level of gene expression, thus offer the opportunity to specifically manipulate, likewise kill or cure affected cells.[21, 22] These abilities are based on a naturally occurring mechanism in eukaryotic cells to regulate gene expression (via microRNAs) which was discovered and published as RNA interference (RNAi) in 1998.[15] The 21-23 base pairs long siRNA molecules need to be located in the cytosol of the target cell to induce the silencing mechanism with synthetic siRNA for the treatment of diseases. The antisense strand of siRNA is incorporated into the RNA-induced silencing complex (RISC) resulting in identification and the subsequent RNase-mediated degradation of the target messenger RNA (mRNA). Thus, the disease-related mRNA is disabled and the expression of its encoded protein prevented (compare figure 1, steps 6 - 9).[15, 18, 23]

For a limited range of indications (e.g. liver disease targets [20]), therapeutic siRNA delivery is already close to entering the clinical market, while hurdles remain to be overcome in the field of tumor-specific siRNA delivery.[16] Nevertheless, the pipeline is filled and the relatively young market of gene therapy is expected to grow at a rapid pace over the next decade.[11, 24, 25]

1.2 Challenges of siRNA *in vivo* delivery

Synthetically designed, sequence-specific siRNAs represent promising treatment opportunities for a wide range of protein expression-associated indications.[11, 22, 26] Nevertheless, the synthetic molecules revealed major pharmacokinetic deficits *in vivo* that have significantly hampered their therapeutic potential.[19, 27] The nanosized (~7 x 2 nm) and negatively charged particles [16] are cleared from the blood circulation rapidly after *in vivo* application, because they underlay renal filtration [28] or nucleases-mediated biodegradation.[20] Thus, vehicles that can stably protect and shield siRNAs from the extracellular environment, enhance their size

to avoid clearance and furthermore circumvent siRNA triggered immune reactions are indispensable.[15, 29] The next challenge to be overcome by multifunctional siRNA carriers, is to selectively address the target tissue, which usually is a specific target cell.[30] Otherwise, severe side effects are likely to occur and may dramatically decrease the clinical potential of delivered siRNA.

Due to their size and charge, siRNAs and other therapeutic nucleic acids, in contrast to common drugs, cannot diffuse passively through likewise charged lipid membranes into the cytosol of cells.[23, 31] As aforementioned, siRNA needs to be transported into the cytosol of the target cell to perform gene silencing. Hence, cell internalization, usually via the endosomal route, followed by endosomal release are key capabilities that have to be provided by the delivery system.[32] The schematic siRNA delivery process is illustrated in the following figure.

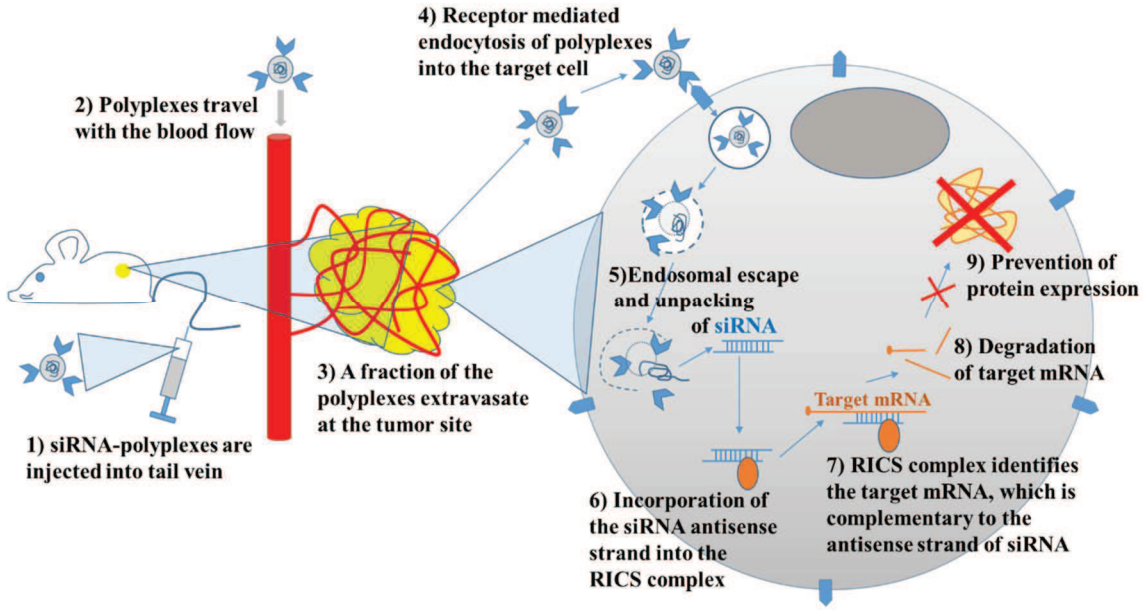

Figure 1: siRNA *in vivo* delivery and mechanism of gene silencing. A simplified scheme of the siRNA delivery process after the intravenous injection of polyplexes in mice is shown. The steps 2 - 5 are commonly known as bottlenecks of siRNA-based treatment approaches. The steps 6 - 9 illustrate the basic mechanism of siRNA-induced gene silencing in the cytosol of a mammalian cell.[18]

1.3 Polymeric carrier systems

Intracellular siRNA delivery can be accomplished with a wide range of different delivery systems.[33] Cationic polymers, cationic peptides and liposomes are used most commonly.[20] The siRNA carriers need to facilitate multiple different tasks in order to successfully silence genes inside the target cell (compare figure 1). In this respect, strategically tailored

nanoparticles provide a number of favourable properties to overcome the aforementioned hurdles.[34] This thesis illustrates and evaluates the *in vivo* performance of precise, sequence-defined, multifunctional siRNA carrier systems (Scheme of siRNA carriers is shown in figure 2), generated by solid phase-assisted synthesis.[35-37] The small peptide-like polymers ('oligomers'), which have been tested *in vivo,* belong to a library containing around 1000 polycations with different structural moieties that were designed to enable gene delivery.[38-40]

General requirements for the *in vivo* usage of structures are the absence of toxic effects [41, 42] and immune reactions induced by the polymer, respectively the formed nucleic acid complex ('polyplex'[43]) itself.[44, 45]

For siRNA delivery, the oligomers are based on a polycationic backbone, made of artificial amino acids (Stp = succinoyl tetraethylene pentamine and Sph = succinoyl pentaethylene hexamine) that contain amino groups which are partly protonated at a neutral pH. These positively charged building blocks complex the negatively charged siRNA, allowing the formation of nanosized polyplexes.[46] Additional structural elements are introduced into the oligomers, establishing structure related activity profiles for the molecules.[47] Promoting particle stability, cysteines were incorporated into the polymeric structure and resulting in the formation of crosslinking disulfide bridges.[48, 49] Additionally, other stability motifs (e.g. tyrosins) were opted for some of the evaluated oligomers.[31]

As aforementioned, the protection of siRNA from undesired interactions with the extracellular environment is essential for the nucleic acid delivery. Hence, polyethylene glycol (PEG) for surface shielding is an integral part of many of the tested polyplexes.[45] Surface protection circumvents aggregation processes and unspecific binding to non-target tissues, enabling passive targeting.[50, 51] Furthermore, PEG may serve as binding domain for targeting-ligands to further promote the specificity of the polyplexes.[52] The following figure illustrates the basic domains of the siRNA polyplexes used in the experiments of this thesis.

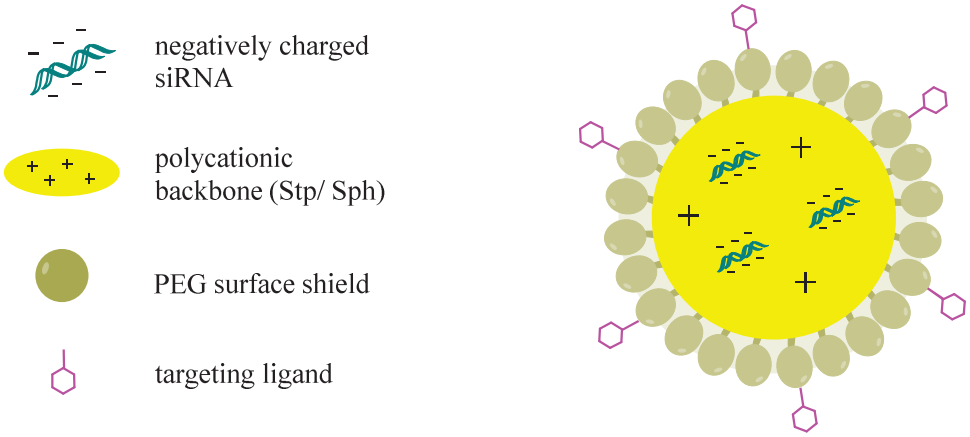

Figure 2: Simplified and schematic illustration of a targeted, polymeric carrier system for siRNA delivery.

Another indispensable capability of the carrier system is to booster endosomal release after cell internalization. Therefore, histidines were integrated optionally for increased endosomal buffering capacity [53], described by Lächelt *et al.* [54], though for most of the illustrated studies additionally the endosomolytic peptide Inf7 was conjugated directly to the siRNA. This synthetic peptide is an analogue to the N-terminus of influenza hemagglutinin membrane protein HA2, ensuring cytosolic release by its high lytic activity at the typically low endosomal pH.[55]

Sizes of polyplexes aimed for systemic delivery have to be in a range of 20-200 nm to circumvent renal filtration and furthermore to become subject of the so called tumor-selective enhanced permeability and retention (EPR) effect.[56] The described enhanced accumulation effect of nanoparticles (> 40kDa) [57] in the tumor tissue is based on the tumor-typical extensive angiogenesis, further supported by the high leakiness of big fenestrated vessels that facilitates extravasation of nanoparticles (varying degree in different tumor types [58]). Simultaneously, tumors provide a poor lymph drainage system. This decreases the chance for already extravasated nanoparticles to be cleared again.[59] The occurrence of EPR-related, enhanced nanoparticle accumulation in tumor tissues allows the “passive targeting” effect and therefore prolongs intratumoral retention.[57] However, in the following projects, “active targeting” strategies (see below) were chosen for additional tumor selectivity of the treatment approaches.

1.4 Receptor-specific targeting

Firstly, carriers for therapeutic siRNA should be capable of reaching the tumor site through blood circulation, including the distribution of critical organs that are associated with degradation processes (e.g. liver, spleen) [20, 30], without sustaining a loss of function. Secondly, cellular uptake and cytosolic release should be influenced in an active as well as controlled manner.[59] Hence, the introduction of targeting ligands that address the typically overexpressed, complementary receptors in tumor tissues, is a promising strategy to increase the efficiency and safety of polyplexes [30, 60], and furthermore represents the active counterpart to the aforementioned 'passive targeting' via hydrophilic shielding domains for surface protection [52] or the EPR-effect.[57]

The folate receptor (FR) has been extensively utilized for tumor targeting.[61, 62] The FR was selected for its striking overexpression in many malignant tumors (especially carcinomas [63]) compared to low or moderate expression in healthy tissues, therefore presenting a convenient target for tumor-specific cell uptake.[64-66] Opted ligands for FR-targeting were folic acid itself as well as its structural analogue methotrexate (MTX). Folate and MTX have a similar chemical structure (see figure 3). Therefore, selective cellular uptake occurs for both ligands via the same two pathways, mediated by either the folate receptors (FR) or the reduced folate carriers (RFC) [67], though the affinity of FR for folate is significantly higher than for MTX.[68]

However, MTX additionally possesses antiproliferative potency [69] in contrast to its natural analogue.[70] Intracellularly, MTX affects nucleic acid biosynthesis and other metabolic reactions by inhibiting the enzyme dihydrofolate reductase. The enzyme is essential to reduce dihydrofolate to its active form. The active tetrahydrofolate is required for the *de novo* biosynthesis of thymidylate and purines, therefore ultimately of DNA and RNA.[71, 72]

Thus, MTX presents a bifunctional alternative to selectively target and additionally affect FR-overexpressing tumor cells.[73] Originally, the clinical use of MTX was focused on the treatment of various types of cancer (e.g. breast cancer, childhood acute leukemia, osteogenic sarcoma).[74, 75] The therapeutic application is nevertheless complicated due to occurring drug resistance, drug-drug interactions, a narrow therapeutic window, strong side effects and low bioavailability in high doses. Development of target specific drug delivery strategies is essential to overcome at least some of the limitations.[71, 73, 75] In low doses, MTX shows an anti-inflammatory effect and plays a crucial role in the treatment of autoimmune diseases (e.g. Crohn's disease, gold standard therapy for rheumatoid arthritis).[71, 74, 75]

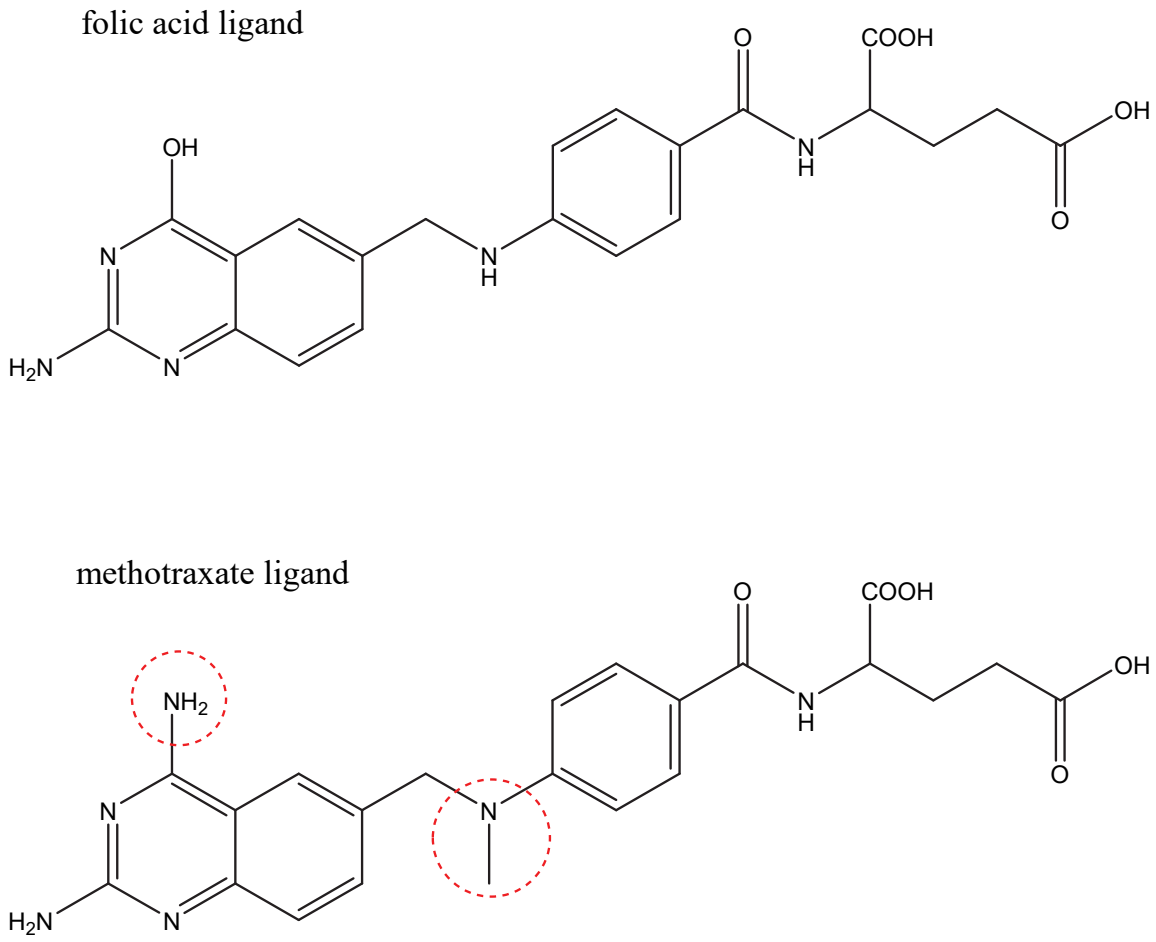

Figure 3: Chemical structure of the FR targeting ligands folic acid and methotrexate. Structural differences are indicated by the red rings.

The serum protein transferrin (Tf) was introduced to siRNA polyplexes in another approach towards receptor-mediated, selective tumor targeting. Tf has served as targeting-ligand in the field of nucleic acid delivery since decades.[76] The iron transporting protein promotes transferrin receptor (TfR)-mediated endocytosis. In addition, the Tf targeting ligand provides additional shielding abilities for the carrier systems.[77] The TfR is overexpressed in many tumor types, as it commonly occurs in proliferating cells. Hence, the TfR is a favorable target for tumor-specific delivery.[77, 78] Recently published, TfR-targeted siRNA delivery systems have so far reached phase I in clinical trials.[24] Furthermore, TfR often showed high expression in malignant tumors with poor prognosis in several studies, therefore TfR expression might be a useful tool as a prognostic marker.[79, 80]

2 Aims of the thesis

The thesis aimed at achieving efficient tumor-specific, intracellular siRNA delivery *in vivo*. The multifunctional polycations that proofed to be most promising in preceding *in vitro* studies had to be chosen for *in vivo* experiments. These carriers had to be screened for their siRNA delivery potential (challenges illustrated in 1.2) with regard to their structural- or surface modifications (structure-activity relationship described in 1.3).

In the first part, the receptor-specific targeting ability of locally applied siRNA polyplexes had to be explored by validating their tumoral retention. In the follow up experiment, cell internalization and endosomal escape had to be evaluated indirectly by the extent of tumor growth inhibition after the local treatment with anti-tumoral siRNA polyplexes in parallel to several controls.

As the systemic delivery is imperative for the treatment of many human tumors, the second part aimed at improving tumor-specific delivery after intravenous application. As basis, a systemically accessible mouse tumor model for FR-targeting had to be established. By intravenous biodistribution studies, tumor-specific siRNA delivery of preselected polyplexes had to be evaluated via Cy7-labeled siRNA and further improved by structural or surface modifications. Consequently, the most promising formulations complexed with therapeutic siRNA had to be applied for subsequent functional verification of gene silencing by qRT-PCR analysis.

II LABORATORY ANIMALS AND HOUSING

1 Mouse strains

1.1 NMRI-nude mice

Female Rj: NMRI-Foxn1^{nu}/Foxn1^{nu} mice were obtained from Janvier Labs (Le Genest-St-Isle, France). This mouse type goes back to an inbred albino stock in the 1960s. Today, the outbred mouse strain is characterized by a mutation in the *Foxn1* gene, which causes thymus aplasia and affects keratinization in the epidermis and the hair follicle. The resulting lack of T-cell immunity and nudeness are key properties for the use as xenograft models and for *in vivo* bioimaging studies.

1.2 BALB/c mice

Female BALB/cByJRj mice were purchased from Janvier Labs (Le Genest-St-Isle, France). The inbred, albino mouse is immuno-potent, calm and simple to keep, thus may serve as sentinel mouse or in syngeneic tumor models (e.g. with M109 cell line).

2 Housing

2.1 Keeping conditions

The animal housing was maintained according to the standards based on §11 (Absatz 1; Satz 1; Nr.1) of the German law for animal protection "Tierschutzgesetz" (TierSchG).[81] Mice were housed in isolated ventilated cages under specific pathogen-free conditions that were verified on a regular basis as described in 2.3. Newly arrived mice were acclimated for at least 7 days prior to experiments. A 12 h day/night interval, optimized temperature (~22°C, respectively ~24°C for nude mice) and humidity (50-70%) were provided and controlled daily. Light and sound intensity were adapted to a maximum of 200 Lux, respectively 40dB. Enriched cages got refreshed once a week with dust-free bedding (ABEDD Vertriebs GmbH, Österreich) and light protected cottages, wooden tubes and nest building material. Mice were kept in groups of 2-5 animals per cage and their welfare was verified daily by an animal care attendant and a veterinarian.

2.2 Nutrition

Food (Teklad laboratory animals diet, ENVIGO, UK) and water were provided sterilized and ad libitum.

2.3 Health monitoring

In order to maintain the specific pathogen-free environment, health monitoring was performed four times a year according to FELASA recommendations. A specified pathogen free environment is essential to exclude unspecific influences on the experiments caused by pathogens and moreover to achieve reproducible results.[82]

3 Research proposal for animal experiments

All animal studies were performed according to the terms stated in the research proposal "Entwicklung von Sequenz-definierten Oligomeren als Träger für die zielgerichtete Einbringung neuer molekularer Therapeutika in Tumore" that was approved by the local animal ethics committee and the government of Oberbayern at the 26th of May 2014, valid for 5 years. The experimental settings and procedures, described in the proposal, were planed according to the guidelines of the German law for animal protection/ TSchG [81] and its by-laws.[83]

Study-specific assessment sheets were designed to score the observed behavior, appearance, and body condition of the mice, as well as the measured weight loss, tumor volume and the frequency of applied sedations. The sum of scores indicates the impairment to health and welfare for each individual animal and defines the rules for the proceeding experiment (e.g. more intense observation or euthanasia).

The approved proposal contains four experimental sections that are aimed to develop and evaluate sequence-defined oligomers for tumor-specific delivery of molecular therapeutics. The first section deals with the establishment of a mouse tumor model, suitable for the systemic delivery of FR-targeted carriers. Since the 15th of October 2015, the newly established L1210 model has partly replaced the KB model in systemic delivery experiments, as KB tumors were found to be less suitable for systemic applications. The relevant authorities were informed about these and any further planned changes in design of the study. The following 3 sections illustrate the settings and procedures of fluorescent biodistribution, gene silencing/ gene expression and consequent treatment experiments.

III MATERIALS AND METHODS

1 Materials

1.1 Cell culture

Material	Source
Folate-free RPMI 1640 medium	Invitrogen, (Karlsruhe, Germany)
DMEM medium	Invitrogen (Karlsruhe, Germany)
PBS (phosphate buffered saline)	Biochrom (Berlin, Germany)
FCS (fetal calf serum)	Invitrogen, (Karlsruhe, Germany)
Trypsin EDTA solution	Biochrom (Berlin, Germany)
Cell culture plates, flasks	TPP (Trasadingen, Switzerland)
L-alanyl-L-glutamine	Biochrom (Berlin, Germany)
Neuro-2a (N2a) cells ATCC® CCL-131™ murine neuroblastoma cell line	American Type Cell Collection (ATCC) (Wesel, Germany)
KB cells ATCC® CCL-17™ human carcinoma cell line	ATCC (Wesel, Germany)
L1210 cells murine leukemia cell line	Kindly provided by Prof. Philip S. Low, Department of Chemistry (Purdue University, USA)
M109 cells murine carcinoma cell line	Kindly provided by Prof. Alberto Gabizon Faculty of Medicine (Hadassah-Hebrew University, Israel)

1.2 *In vivo* experiments

Material	Source
Isoflurane CP®	CP-Pharma (Burgdorf, Germany)
Bepanthen®	Bayer Vital GmbH (Leverkusen, Germany)
Syringes, needles	BD Medical (Heidelberg, Germany)
Multivette 600 (EDTA-coated tubes)	Sarstedt (Nümbrecht, Germany)
HBG (HEPES buffered 5% glucose, pH 7.4)	HEPES: Biomol (Hamburg, Germany) Glucose monohydrate: Merck (Darmstadt, Germany)
Matrigel® Matrix (356231)	Fisher Scientific GmbH (Schwerte, Germany)

1.3 Histology

Material	Source
Mayer's haematoxylin solution	Sigma-Aldrich (Steinheim, Germany)
Eosin Y	Sigma-Aldrich (Steinheim, Germany)

1.4 Polymeric structures

Oligomers were synthesized by Dr. Ulrich Lächelt (postdoc at Pharmaceutical Biotechnology, LMU), Philipp Klein and Dongsheng He (PhD study at Pharmaceutical Biotechnology, LMU).

ID	Sequence
640	K(dPEG$_{24}$-E$_4$-MTX)-K(Stp$_4$-C)$_2$
356	C-Stp$_4$-K-(PEG$_{24}$-FolA)-Stp$_4$-C
188	A-dPEG$_{24}$-K(Stp$_4$-C)$_2$
454	C-Y$_3$-Stp$_2$-[(OleA)$_2$-K]K-Stp$_2$-Y$_3$-C
595	CRC-Y$_3$-Stp$_2$-[(OleA)$_2$-K]K-Stp$_2$-Y$_3$-CRC
386	C-Stp$_3$-K-(Stp$_3$-C)$_2$
873	K-(PEG$_{24}$-FolA)-K-[K-Sph$_4$-C-TNB)$_2$]$_2$
762	K-(PEG$_{24}$-FolA)-K-[H-K-((H-Stp)$_3$-H-C)$_2$]$_2$

1.5 siRNAs

Material	Source
siCtrl AuGuAuuGGccuGuAuuAG dTsdT CuAAuAcAGGCcAAuAcAU dTsdT	Axolabs (Kulmbach, Germany)
siEG5 ucGAGAAucuAAAcuAAcu dTsdT AGUuAGUUuAGAUUCUCGA dTsdT	Axolabs (Kulmbach, Germany)
Cy7-labeled siAHA1 with a hexyl thiol modification at the 5′ end of the sense strand and a Cy7 dye at the 5′ end sense: C6-ss-C6-5′-GGAuGAAGu GGAGAuuAGudTsdT-3′ antisense: 5′-(Cy7) (NHC6)ACuAAUCUC cACUUcAUCCdTsdT-3′)	Axolabs (Kulmbach, Germany)
Inf7 peptide	Biosyntan (Berlin, Germany)

*capital letters: standard RNA ribonucleotides
*small letters: 2′-methoxy-RNA;
*s: phosphorothioate

siRNA-Inf7 conjugates: contain the pH-triggered fusogenic peptide Inf7 [55](sequence: GLFE AIEG FIEN GWEG MIDG WYGC) covalently linked to the 5´-end of the siRNA sense strand as described in Dohmen *et al.*[28]

Conjugates were provided by Dongsheng He and Philipp Klein (PhD study at Pharmaceutical Biotechnology, LMU).

1.6 Instruments

Instrument	Source
Cordless animal shaver GT 420 ISIS	Aesculap Suhl GmbH (Suhl, Germany)
Caliper DIGI-Met	Preisser (Gammertingen, Germany)
IVIS Lumina	Caliper Life Science (Rüsselsheim, Germany)
Tissue embedding Leica EG1150	Leica Microsystems GmbH (Wetzlar, Germany)
Microtome Leica RM2265	Leica Microsystems GmbH (Wetzlar, Germany)
Paraffin floating bath	MEDAX GmbH & Co. KG (Neumünster, Germany)
Olympus BX41	Olympus (Hamburg, Germany)
Zeiss Cell Observer SD	Carl Zeiss AG (Göttingen, Germany)

1.7 Software

Software	Provider
Graph Pad Prism 5 software	Graph Pad Software (San Diego, USA)
Living Image 3.2	Caliper Life Science (Rüsselsheim, Germany)

2 Methods

2.1 Cell culture

Murine neuroblastoma (N2a) cells were cultured in Dulbecco´s modified Eagle´s medium (DMEM 1 g/l Glucose). Whereas human cervix carcinoma cells (KB), murine lymphocytic leukemia cells (L1210) and murine lung carcinoma cells (M109) were cultured in folate-free RPMI 1640 medium at 37 °C in 5 % CO_2 humidified atmosphere. All media were supplemented with 10% FCS and 4 mM stable glutamine.

2.2 *In vivo* experiments

All animal experiments were performed according to guidelines of the German law for the protection of animal life and were approved by the local animal ethics committee (compare II.3).

The tumor volume was measured daily by caliper and calculated as [0.5 x longest diameter x shortest diameter^2] as stated by Xu *et al.*[84] The body weight was recorded every second day until tumors reached a measurable size, then on a daily base.

2.2.1 Intratumoral retention of methotrexate (MTX)-directed siRNA nanoplexes

5 x 10^6 KB cells were injected subcutaneously in the nape of 10 week old female NMRI-nude mice. After sufficient tumor growth (volume: 500-800 mm^3), the animals were randomly divided into 3 groups (n=3) and anaesthetized with 3% isoflurane in oxygen to perform near infrared (NIR) imaging. Polyplexes containing 50 µg of Cy7-labeled siRNA (N/P 16) in 50 µL of HBG were injected intratumorally. Fluorescence was measured with a charge coupled device (CCD) camera after 0, 0.5, 1, 4, 24 h, followed by a daily rhythm until the animals were sacrificed after 144 or 160 h. Color bar scales were equalized by IVIS Lumina system with Living Image software 3.2 (Caliper Life Sciences, Hopkinton, MA, USA) in order to analyze the efficiency of fluorescence signals, subsequently the intratumoral retention of polyplexes was evaluated.

2.2.2 Intratumoral treatment with MTX-directed siRNA nanoplexes

8 week old female NMRI-nude mice were randomly divided into 6 groups (n=6). Left flanks of the animals were subcutaneously injected with 5 x 10^6 KB cells. Two days after tumor inoculation, mice were treated intratumorally with polyplexes containing 50 µg of siRNA at N/P 16, corresponding amount of plain oligomer or MTX, each solved in 50 µL of HBG. One control group remained untreated. Treatments were repeated 3 times a week (on days 2, 4, 7, 10, 14 and 17). Tumor growth was monitored daily and animals were sacrificed after exceeding a tumor volume of 1000 mm^3 or any other animal protection related criteria (e.g. spontaneously occurring tumor ulceration or significant weight loss). Kaplan-Meier survival analysis was performed to compare the lifetime after treatments among different groups.

2.2.3 Cell culture and *in vivo* growth of folate receptor (FR)-overexpressing tumor models

For M109 cells, syngeneic 6 week old BALB/c mice were purchased and injected subcutaneously in 3 groups of 4 mice (n=4) per cell dosage (using 0.5, 1 and 2 x 10^6 M109 cells in 150 µl of PBS). After 4 weeks, 3 animals with bigger tumors were sacrificed for recultivation of the *in vivo* passaged cells *in vitro*. Those cells were reinjected after multiplying with the optimized dose of 2 x 10^6 in 2 groups (n=6). Cells were diluted in 150 µl of PBS for one group, the other group received cells in 75 µl PBS mixed with 75 µl of Matrigel. After sufficient tumor

growth (500-700 mm^3) mice were treated intravenously via tail vein using Cy7-labeled siRNA polyplexes for biodistribution studies.

For L1210 cells, 6 week old NMRI-nude mice were purchased and injected subcutaneously in 3 groups of 4 mice (n=4) per cell dosage (using 0.5, 1 and 2 x 10^6 L1210 cells in 150 µl of PBS). In the follow up growth experiment, optimized doses of 0.5 and 1 x 10^6 (n=6) were injected in 150 µl of PBS. After sufficient tumor growth (500-700 mm^3) mice were injected with Cy7-labeled siRNA polyplexes for biodistribution studies.

2.2.4 Biodistribution studies in FR-overexpressing tumor models

Tumor bearing mice of the growth experiment for M109 and L1210 cell lines were treated in groups of 1 - 5 animals. All polyplexes contained 50 µg of siRNA (50% Cy7-labeled) and were solved in 250 µL HBG. Mice were injected intravenously into the tail vein and anaesthetized in 3% isoflurane in oxygen. NIR fluorescence bioimaging was performed at 0 min, 15 min, 30 min, 1 h, 4h and 24 h after injection by a (CCD) camera using IVIS Lumina system. Color bar scales were equalized by Living Image software 3.2 (Caliper Life Sciences, Hopkinton, MA, USA) for the subsequent analysis of the biodistribution profile.

Mice of one polyplex group were sacrificed at different time intervals after injection to perform *ex vivo* imaging of organs and tumors.

2.2.5 Histologic evaluation of FR-overexpressing tumors

Tumors of M109, L1210 and KB cell lines were harvested, dissected, afterwards fixed in formalin and embedded into paraffin. Embedded tumors were cut with a microtome into 5.0 µm slices and stained with haematoxylin and eosin (HE staining). Results were analyzed and documented using an Olympus BX41 microscope.

2.2.6 Systemic biodistribution of targeted siRNA polyplexes

All biodistribution experiments were performed in 6 - 8 week old NMRI-nude mice.

All polyplexes contained 50 µg of siRNA (50% Cy7-labeled) and were solved in 200-250 µL HBG. Mice were injected intravenously via tail vein and anaesthetized in 3% isoflurane in oxygen. NIR fluorescence bioimaging was performed at 0 min, 15 min, 30 min, 1 h, 4h and 8 h/ respectively 24 h after injection by a (CCD) camera using IVIS Lumina system. Color bar

scales were equalized by Living Image software 3.2 (Caliper Life Sciences, Hopkinton, MA, USA) for the subsequent analysis of the biodistribution profile.

2.2.6.1 Transferrin receptor (TfR)-targeted cationic lipo-oligoamino amide *454*

5×10^6 N2a cells were injected subcutaneously into the left flank of the animals. Imaging experiments were performed in triplicate and 10 days after tumor cell inoculation, when tumor volume reached about 800 mm^3. Polyplexes were prepared and administered as previously described, complexed at N/P 6, using AHA1 siRNA (50% Cy7-labeled) for subsequent quantitative reverse transcription polymerase chain reaction (qRT-PCR).

At 8 h after the systemically applied treatment and in the same narcosis of the final *in vivo* imaging, animals were sacrificed. Organs (including lung, liver, kidney, and spleen) and tumors were collected for further investigation by qRT-PCR.

qRT-PCR was performed with Wei Zhang (postdoc at Pharmaceutical Biotechnology, LMU) using the following method described in *Zhang et al* [85].: Total RNA was isolated from organs and tumors of different groups using peqGOLD TriFast method (PEQLAB, Germany), and cDNA synthesis was performed using 1 µg of total RNA with qScript microRNA cDNA synthesis kit (Quanta BioScience, USA). qRT-PCR was implemented with PerfecTa SYBR Green SuperMix (Quanta BioScience, USA) on a LightCycler 480 system (Roche, Germany) using miR-191 as housekeeper. Primers used are shown as follows; miR-191 forward: GCGCAACGGAATCCCAAAAG, AHA1 forward: GAGACTAATCTCCACTTC (Sigma-Aldrich, Germany). ΔCt is the difference between Ct (threshold cycle) values of the measured RNA of interest and the housekeeper RNA, meaning a normalization to the housekeeper. Thus, $2^{-\Delta ct}$ represents the relative quantity of the target RNA. It assumes an exponential growth and a doubling of product in each PCR cycle.

2.2.6.2 FR-targeted cationic lipo-oligoamino amides *454* and *595*

1×10^6 L1210 cells were injected subcutaneously into the left flank of the animals. Imaging experiments were performed in triplicate as soon as tumor volumes reached about 500-700 mm^3. Polyplexes were prepared and administered as previously described, complexed at N/P 10, using AHA1 siRNA (50% Cy7-labeled) for subsequent qRT-PCR. Animals were sacrificed 8 h after the intravenously applied treatment and in the same narcosis of the final *in vivo* imaging. Organs (including lung, liver, kidney, and spleen) and tumors were collected for further investigation by qRT-PCR.

qRT-PCR was performed with Katharina Müller (PhD study at Pharmaceutical Biotechnology, LMU) using the following method described in Müller *et al.* [86]: RNA was extracted from organs using peqGOLD TriFastTM (PEQLAB Biotechnology GmBH, Germany) according to the manufacturer's protocol. RNA (1 µg) was transcribed with qScript microRNA cDNA synthesis kit (Quanta BioScience, USA) into cDNA. qRT-PCR was performed using PerfecTa SYBR Green SuperMix (Quanta BioScience, USA) on a LightCycler 480 system (Roche, Germany) with miR-191 as a housekeeper. Following primers were used: miR-191 forward, GCGCAACGGAATCCCAAAAG, and AHA1 forward, GAGACTAATCTCCACTTC (Sigma-Aldrich, Germany). Results were analyzed using the ΔC_T method.

2.2.6.3 FR-targeted combinatorial siRNA polyplexes

0.5 – 2 × 10^6 L1210 cells were injected subcutaneously into the left flank of the animals. Imaging experiments were performed in groups of 3 - 4 mice as soon tumor volume reached about 500-800 mm^3. Polyplexes were prepared and administered as previously described, complexed at N/P 16. In the same narcosis of the final *in vivo* imaging, animals were sacrificed for *ex vivo* imaging of tumors and organs at different time intervals (15 min - 24 h) after polyplex injection.

2.2.7 Tumoral gene silencing

In vivo experiments were performed as described in Lee *et al.*[87]: Female 8 week old NMRI-nude mice were injected subcutaneously with 1 × 10^6 L1210 cells.

When tumors reached 500 mm^3, mice were randomly grouped (n=5) and injected with polyplexes into the tail vein. Treatment with siRNA polyplexes containing 50 µg of siEG5-Inf7 or siCtrl-Inf7 at N/P 16, was performed twice, 48 h and 24 h before euthanasia. As a part of terminal procedure, blood samples were obtained by cardiac puncture for blood biochemistry examinations. To isolate plasma, blood samples were collected in EDTA-coated tubes (Multivette 600, Sarstedt, Nümbrecht, Germany) and centrifuged at 3000 rpm for 7 min. The supernatant was analyzed for clinical biochemistry parameters: alanine aminotransferase (ALT), asparate aminotransferase (AST), blood urea nitrogen (BUN) and creatinine in the Clinic of Small Animal Medicine, Faculty of Veterinary Medicine, Ludwig-Maximilian-Universität München.

The tumors were harvested and homogenized, afterwards total RNA was extracted using Trifast (Peqlab, Erlangen, Germany) according to the manufacturer's protocol. The reverse

transcription and qRT-PCR was performed by Dian-Jang Lee (PhD study at Pharmaceutical Biotechnology, LMU) as described in Lee *et al.* [87]: Quantitative real-time polymerase chain reaction (qRT-PCR) was performed to determine the mRNA level of EG5 gene in transfected cells. L1210 cells (1.5×10^5/well) were seeded in 900 µL of medium onto 6-well plates. The cells were treated with 100 µL of polyplexes with siEG5-Inf7 or siCtrl-Inf7 (N/P 16) with a final siRNA concentration of 370 nM and incubated for 24 h. Total RNA was isolated with the miRCURY RNA Isolation Kit (Exiqon, Vedbaek, Denmark) followed by reverse transcription using Transcriptor High Fidelity cDNA Synthesis Kit (Roche, Mannheim, Germany) according to the manufacturers' protocols. Quantitative RT-PCR was performed in triplicates on a LightCycler 480 system (Roche, Mannheim, Germany) using UPL Probes (Roche, Mannheim, Germany) and Probes Master (Roche, Mannheim, Germany) with GADPH as housekeeping gene. The following probes and primer sequences were used: murine GAPDH (ready-to-use in UPL), and EG5 (UPL Probe #100) forward: TTCCCCTGCATCTTTCAATC, reverse: TTCAGGCTTATTCATTATGTTCTTTG). Results were analyzed by the ΔC_T method. C_T values of GAPDH were subtracted from C_T values of EG5. ΔC_T values of siRNA-transfected cells were calculated as percentage relative to untreated control cells.

2.3 Statistical analysis

Statistical analysis is calculated using GraphPadPrism™ software. Results are presented as mean value ± S.E.M (if not indicated elsewise). Unpaired T-tests were performed and p-values < 0.05 were considered as significant (*$p < 0.05$; **$p < 0.01$; ***$p < 0.001$, NS = no significance).

IV RESULTS

1 Intratumoral administration of MTX-directed siRNA nanoplexes

Based on promising *in vitro* efficacy of the MTX-directed polymer K(dPEG$_{24}$-E$_4$-MTX)-K(Stp$_4$-C)$_2$ [73] (see scheme 1), in combination with the therapeutic EG5 siRNA (siEG5) [88] and endosomolytic peptide Inf7 [55], the following experiments investigate the *in vivo* performance and the therapeutic potential of these polyplexes after intratumoral application. The experiments were performed together with Dian-Jang Lee (PhD study at Pharmaceutical Biotechnology LMU) in folate receptor overexpressing KB tumor-bearing NMRI-nude mice.

In line with previous intratumoral administration studies, doses of 50 µg of siRNA per injection solved in 50 µL of HBG were applied intratumorally.[28, 47, 88]

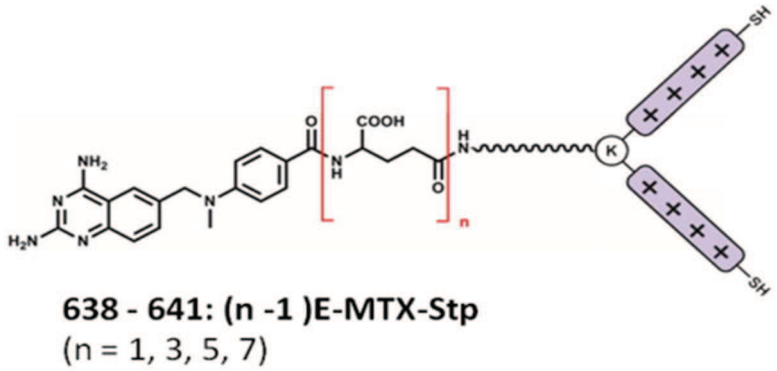

Scheme 1: Illustration of MTX-conjugates for siRNA delivery. Overview of the *in vitro* evaluated polymeric structures with different glutamylation degree (n) of MTX.[73] For *in vivo* experiments, the tetraglutamylated (n=5) ***640*** conjugates were selected for polyplex formation. Stp-units (+); lysine (K); PEG shielding domain (∿∿∿). The graphic illustration is provided by Dr. Ulrich Lächelt (postdoc at Pharmaceutical Biotechnology, LMU) [73] and Dian-Jang Lee (PhD study at Pharmaceutical Biotechnology, LMU).[89]

1.1 Intratumoral retention - efficacy of MTX as targeting-ligand

Folate receptor targeted, polymeric carrier-based siRNA delivery concepts already achieved promising results in the previous work of Dohmen *et al.*[28]

The following imaging experiment was set to evaluate targeting ability and intratumoral retention time of MTX-directed siRNA polyplexes *in vivo*. The MTX-oligomer conjugate ***640*** proofed to perform best *in vitro* compared to other tested MTX formulations [89] and was subsequently chosen to compete against folate-directed (positive control, ***356***) and untargeted

(negative control, ***188***) polyplex analogs *in vivo*. Intratumoral retention was measured time dependent by detection of polyplex-incorporated Cy7-labeled siRNA via near infrared (NIR) fluorescence imaging after a single intratumoral application of polyplex-groups.

In order to save animals, previously tested intratumoral retention of free siRNA (as additional negative control) was omitted, as we already found proof for it being washed out of tumor tissue in less than 24h.[28]

The acquired imaging results confirm the targeting ability of MTX *in vivo* and provide evidence that both targeted siRNA polyplexes (folate-based ***356*** and MTX-based ***640***) remained in the tumor site 5 days longer than untargeted siRNA polyplexes (***188***). The retention time of MTX- and folate-conjugates was comparable (Figure 4A).[89]

Interestingly, 7 days after treatment, the *ex vivo* imaging (Figure 4B) even revealed a prolonged residue of labeled siRNA in the ***640*** group compared to the fully cleared siRNA polyplexes of the ***356*** group.

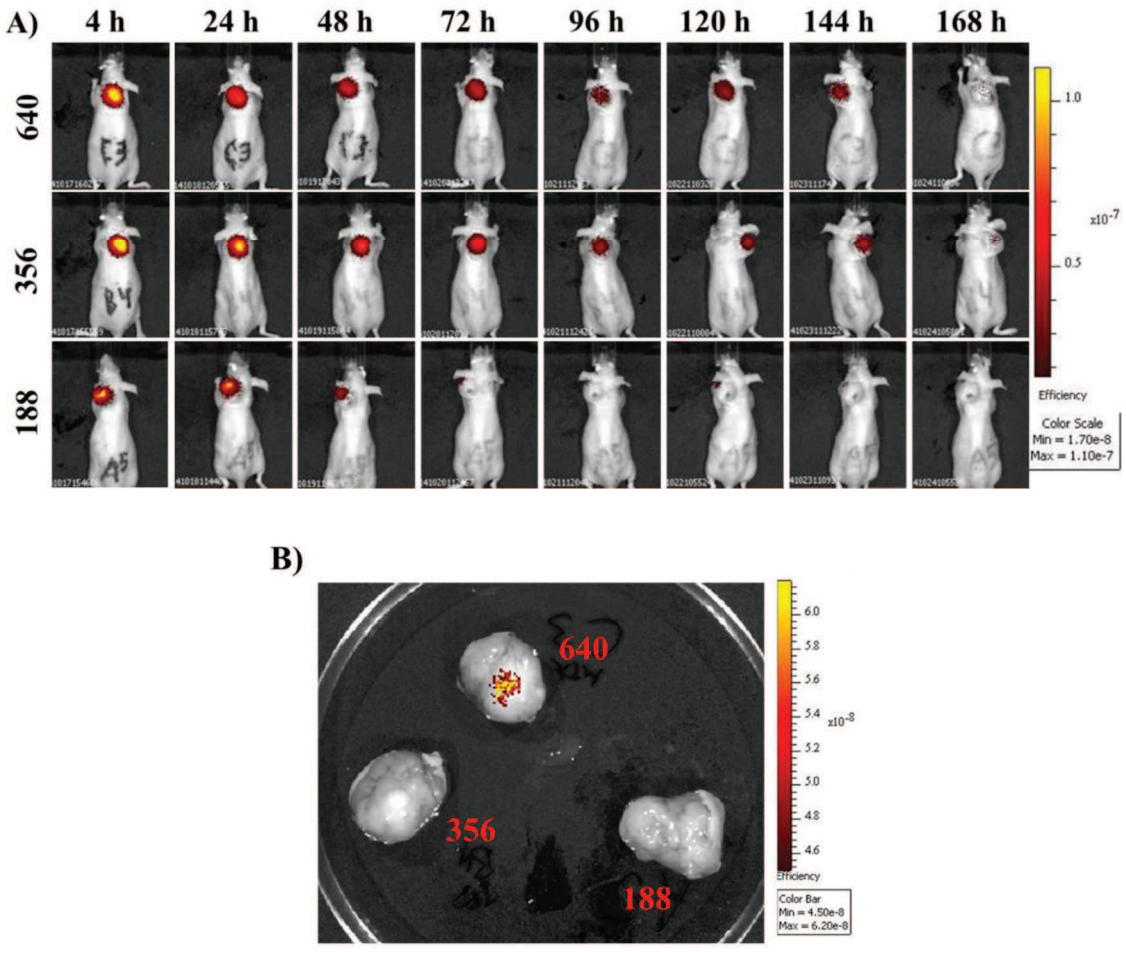

Figure 4: Intratumoral biodistribution of siRNA polyplexes in NMRI-nude mice bearing subcutaneous KB tumors determined by NIR fluorescence bioimaging. A) Time-dependent retention of Cy7-labeled siRNA after intratumoral application with MTX-conjugated oligomer

640 (upper panel), folate-conjugated positive control ***356*** (middle panel) or untargeted negative control ***188*** (lower panel) serving as carriers. B) *Ex vivo* imaging of harvested tumors at 168 h after injection of siRNA polyplexes. Experiments were performed in triplicate; a representative animal of each group is shown. Illustrations are provided by Lee *et al.*[89]

Clearance occurred as expected via renal filtration (Figure 5), due to the small particle size (~ 6 nm).[90] Bladder and kidney signals were detectable for the first 4 h after intratumoral treatment.[89]

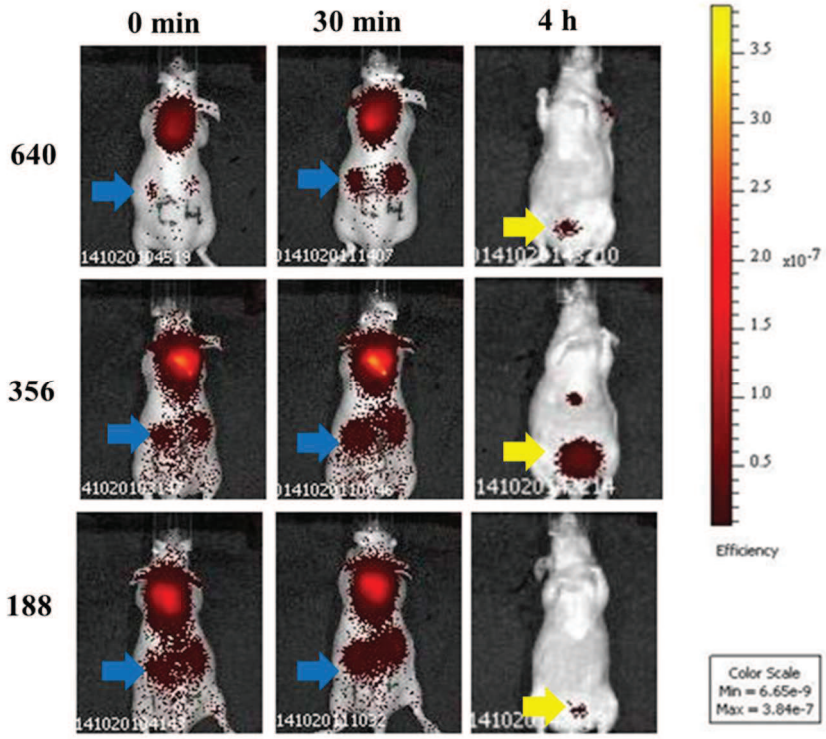

Figure 5: Renal clearance of siRNA polyplexes observed over 4 h after intratumoral injection, detected by NIR imaging in KB tumor-bearing nude mice. The upper panel represents MTX-conjugated polyplex ***640***, then the folate-conjugated ***356*** in the middle panel followed by untargeted negative control ***188*** (lower panel). The polyplex-incorporated Cy7-labeled siRNA was detected in the kidneys (blue arrows) and the bladder (yellow arrows) as indicated. Experiments were performed in triplicate; one representative mouse per group is shown. The illustration is adapted from Lee *et al.*[89]

1.2 Intratumoral treatment of MTX-directed EG5 siRNA nanoplexes

The intratumoral retention study did not reveal any significant advantage of either MTX-based, or folate-based conjugates. Both targeting strategies did significantly prolong intratumoral retention of Cy7-labeled siRNA polyplexes compared with untargeted polyplexes, displayed in

figure 4. Nevertheless, tetraglutamyl-MTX targeting ligand is expected to improve tumor cell killing ability of polyplexes after incorporation in cells in contrast to folate.[73]

Consequently, the following study was set to investigate the antitumoral potency of the bifunctional MTX targeting ligand combined with anti-mitotic EG5 siRNA in comparison to structurally similar folate-based siEG5 polyplexes.

Using the subcutaneous KB tumor model and intratumoral application mode, we treated mice repetitively starting 2 days after tumor inoculation. Five different treatment/ control groups were formulated to further distinguish between the possible therapeutic effects of selected conjugate components. On the one hand, there was the MTX conjugate ***640*/siEG5-Inf7** complex, and on the other hand the same oligomer conjugate but complexed with siCtrl-Inf7, to analyze the therapeutic potency of mitosis inhibiting siEG5 in combination with the cytotoxic MTX targeting ligand. Moreover, this should validate the contribution of siEG5 to the antitumoral efficacy of the polyplex. In addition, free MTX in the equivalent dose as incorporated inside the polyplexes was applied in one control group. The folate-based conjugate ***356*/siEG5-Inf7** served as a further important control to investigate the therapeutic influence of MTX targeting ligand (negative control) and siEG5. To evaluate a possible effect of the small MTX-targeted polymers itself, we used free ***640*** (without siRNA dependent complexation). All groups were compared with untreated, tumor-bearing control animals. Aside from tumor growth and weight development, we recorded the survival of mice post treatment for Kaplan-Meier statistical survival analysis.[89]

Treatment with all siRNA polyplex groups resulted in significantly reduced tumor growth compared to untreated control group, evaluated 5 days after treatment and illustrated in figure 6B. Encouragingly, the combination of dual-functional MTX targeting ligand with siEG5-Inf7 proved to be the most effective. By the end of the treatment period, the combinatorial formulation strikingly reduced the subcutaneous tumor to a nearly not palpable size. On day 25, eight days post the last treatment, there were only little scars left where the tumors used to be (Figure 6C).[89]

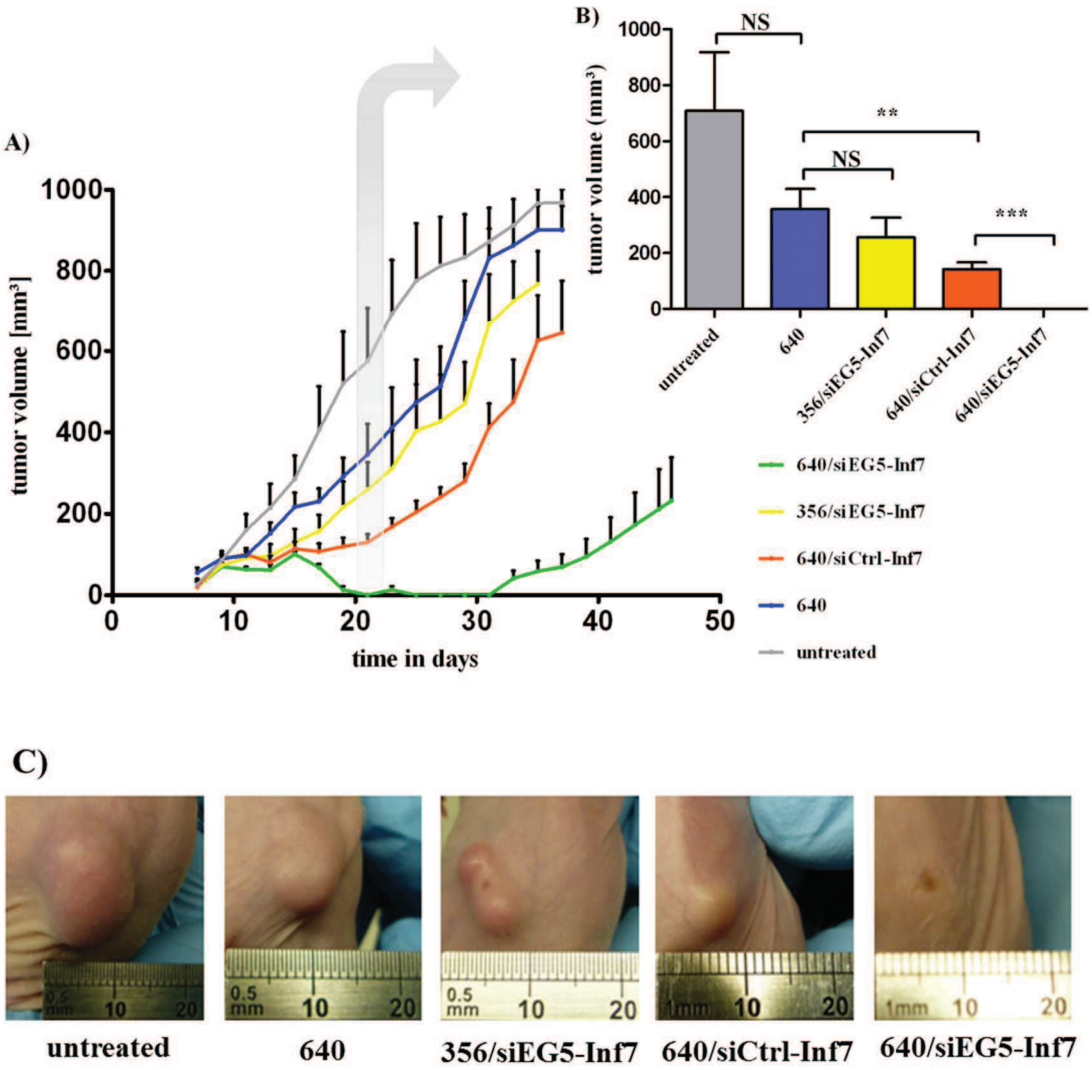

Figure 6: *In vivo* evaluation of the antitumoral potential of MTX-conjugated siRNA polyplexes after local application in KB xenograft model. A) Therapeutic efficacy illustrated by tumor growth curve of MTX-directed ***640***-based polyplexes (with siEG5-Inf7 or siCtrl-Inf7), free ***640*** oligomer or folate-directed ***356*/siEG5-Inf7** polyplexes and compared with untreated animals (n=6 per group). B) The tumor volume of indicated groups measured and compared 5 days after the last treatment (day 22). C) Representative subcutaneous KB tumors grown, respectively inhibited under indicated treatment procedure, pictures taken 8 days after the last treatment (day 25). Illustrations and graphs are adapted from Lee *et al.*[89]

Half of the ***640*/siEG5-Inf7** group survived until the study was ended (day 70) without any sign of recurrence, others showed returning tumor growth from day 32 on (Figures 6A and 7).[89]

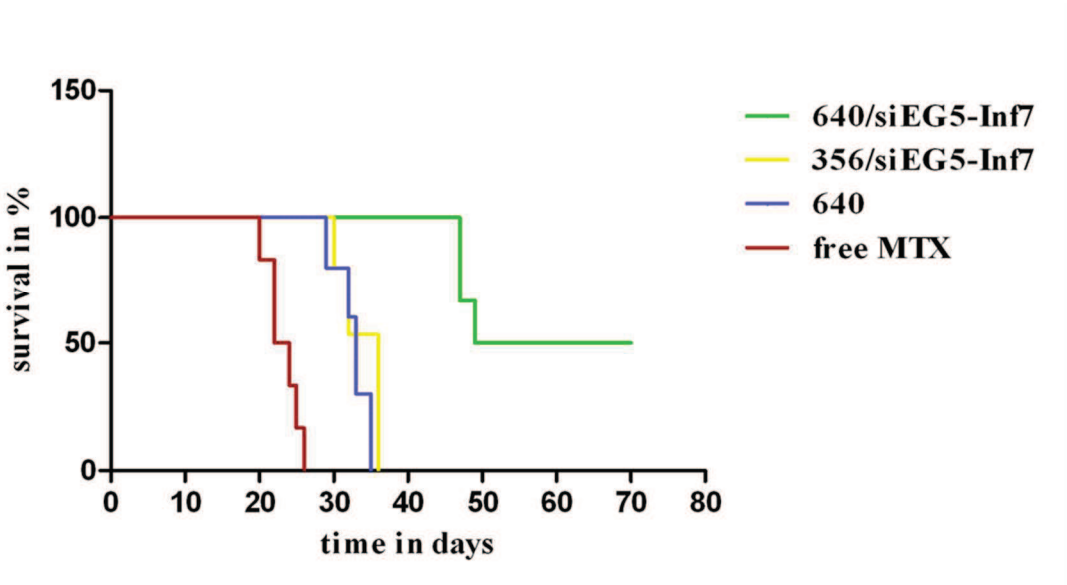

Figure 7: The Kaplan-Meier survival curve of the mice, treated as indicated. Tumors of **640**/siEG5-Inf7 treatment group, largely disappeared by day 22. Three of six mice did not show recurrence until the end of the study (day 70). The graph is adapted from Lee *et al.*[89]

According to the varying inhibition of tumor growth in the different control groups, it seems that binding MTX to a carrier and even more complexation with siRNA increases antitumoral potential.

Free MTX of equivalent doses did not inhibit the rapid tumor growth [89] (up to 1000 mm^3 of volume in ~25 days), whereas polymer bound MTX at least revealed some minor retardation, reaching the final tumor volume within ~35 days (Figure 7). Interestingly, complexation of ***640*** with siCtrl-Inf7 achieved significant inhibition of tumor growth compared with free ***640*** polymers, illustrated in figure 6B.

In summary, these findings suggest a therapeutic advantage of MTX in polyplexes over the free or only polymeric bound form. The folate-based ***356*/siEG5-Inf7** group did not result in a significant tumor growth retardation (comparable to free ***640***). Nevertheless, pronounced necrosis of tumor tissue occurred in both siEG5-Inf7 containing conjugate groups (***356*** and ***640*** polyplexes). Tumor necrosis transitioned into an active healing process, especially in the animals with clearly inhibited tumor growth of ***640*/siEG5-Inf7** group. Remaining scars in these animals' flanks gradually faded only days after the last treatment (day 17) [89], illustrated in the following figure.

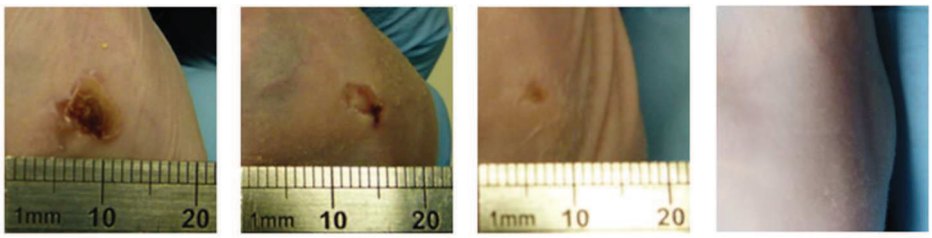

Figure 8: Course of the active healing process after KB tumors "melted" in a necrotic manner. The phenomenon occurred in relation with treatments in ***640***/siEg5-Inf7 group (or ***356***/siEg5-Inf7 group, though without healing as tumors continued to grow). The healing time was different for individual mice, however the wounds eventually disappeared as shown in the representative pictures from the tumor site treated with ***640***/siEg5-Inf7. The illustration is provided by Lee *et al.*[89]

Animal welfare was monitored every day and summing up by evaluation of behavior, outward appearance and of the body weight curve, the treatment was tolerated well. Though we observed a temporary stagnation of body weight in the animals treated over the second half of treatment period, an encouraging weight gain followed after the last treatment at day 17 (compare figure 9).[89] The quick recovery indicates the absence of macroscopically detectable, subacute or chronic side effects during the observed post treatment period.

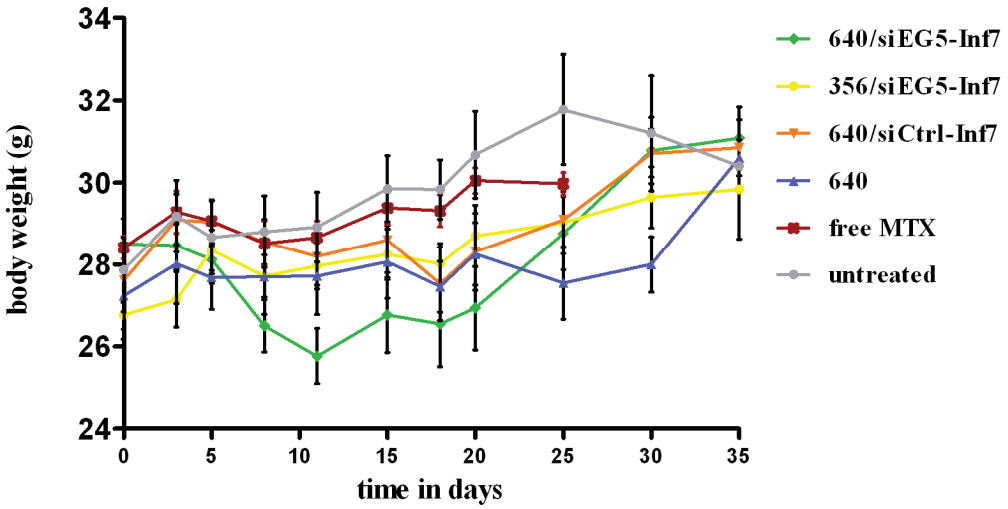

Figure 9: Body weight course displayed for all groups over the treatment period, followed by recovery time. Differences between treatment groups and controls approximated progressively within 18 days after the last treatment, which was performed at day 17. The graph is adapted from Lee *et al.*[89]

Summarizing, these results suggest promising therapeutic potential of siEG5-Inf7 polyplexes, illustrated in figure 10A. Importantly, their antitumoral efficacy can be significantly boosted by introducing the FR-responsive, tetraglutamyl-MTX targeting-ligand (Figure 10B).[89]

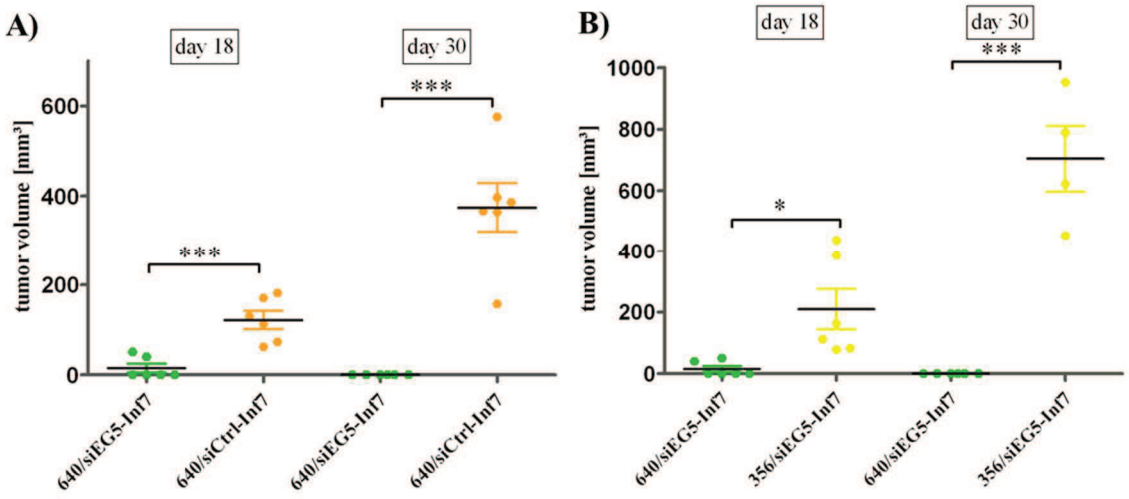

Figure 10: Indirect validation of the anti-tumor efficiency determined for polyplex components, augmented to bear therapeutic potential. Therefore, growth inhibition was compared by group means of tumor volume, measured 1 day (day 18) or 13 days (day 30) after the last treatment. Panel A) shows the evaluation of growth inhibition caused by siEG5, comparing ***640***/siEg5-Inf7 and ***640***/siCtrl-Inf7 group, while B) presents the therapeutic influence of the cytotoxic MTX-targeting-ligand, comparing bifunctional MTX-conjugated ***640***/siEG5-Inf7 with the folate-conjugated equivalent. Graphs are adapted from Lee *et al.*[89]

2 Evaluation of a FR-responsive *in vivo* tumor model for systemic delivery

In the following experiments, we compared attributes (growth, shape, structure and vascularization) of two FR-overexpressing cell lines [91] *in vivo*. Receptor status of utilized cell lines was verified by Dian-Jang Lee (PhD study at Pharmaceutical Biotechnology, LMU) and confirmed to be comparable with the FR-overexpressing, cervix carcinoma KB cell line (already established and used *in vitro*/ *in vivo* in our lab).

Both of the selected cell lines are of murine origin, M109, a lung carcinoma cell line syngeneic to BALB/c mice [92, 93] and L1210 lymphocytic leukemia cells derived from DBA-2 mice [94, 95]. The study was aimed to establish a FR-overexpressing tumor model with high taking rates, simultaneous growth development and reproducible growth rates. Furthermore, a well vascularized tumor increases the chances for polyplexes to extravasate into tumor tissue after intravenous injection.[58] Experiments were performed together with Dian-Jang Lee (PhD study at Pharmaceutical Biotechnology LMU).

2.1 *In vivo* growth properties

The growth experiment was split in two parts to optimize the settings of procedure in terms of applied cell dose (first doses based on [91, 96, 97]), necessity of possible growth booster like *in vivo* passaging, or the application with Matrigel.[98, 99] For the M109 cell line, an *in vivo* passaging was required to enhance taking rates and growth speed of the tumor cells before starting with the second part of the *in vivo* growth experiment (formerly routinely used to maintain M109 cell line [93, 100]). Recultivated cells were injected with the optimized dose of 2 million cells per animals, additionally Matrigel was used for one group in the second part to further improve their *in vivo* growth. This resulted in an increase of the taking rate for M109 tumors from 58% in the first to 100% in the second part of the experiment. However, M109 cells injected with Matrigel still grew much slower (size of 500 mm^3 from day 29) than L1210 cells in NMRI-nude mice (size of 500 mm^3 from day 12), though Matrigel quickened growth of M109 tumors compared to the group with PBS only.

L1210 tumors presented taking rates of 100% through all parts of the experiments without the need of *in vivo* passaging or Matrigel. They grew reliably in low cell doses of 0.5 - 1 million cells, furthermore displaying superiority over the M109 tumors in BALB/c mice in terms of homogenous, simultaneous and reproducible growth.

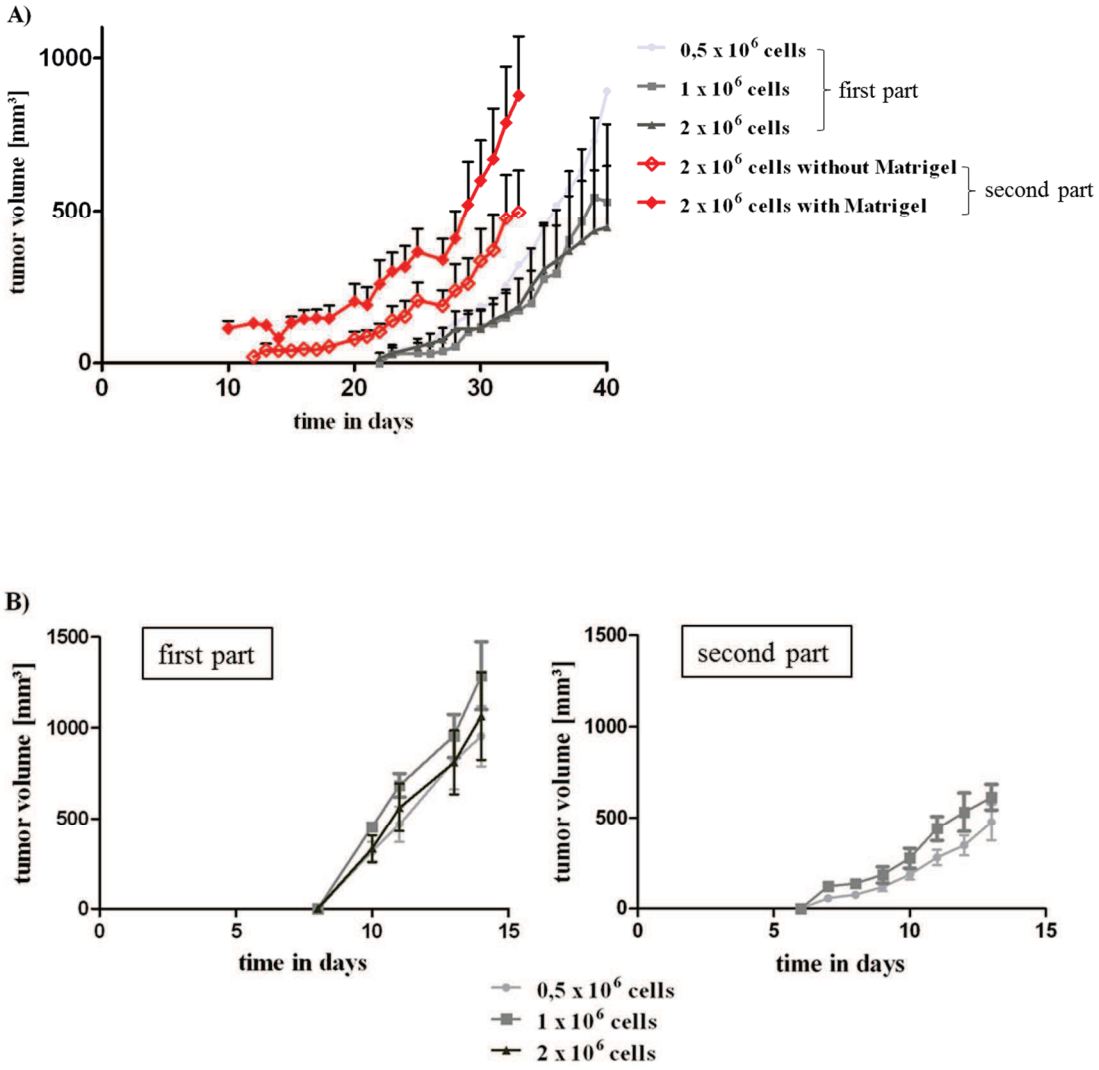

Figure 11: Tumor growth experiments of two FR-overexpressing cell lines. For each cell line, experiments were split in two parts (n=4 - 6 mice per group) in order to optimize experimental settings (e.g. cell dose). A) M109 cells of different doses were injected subcutaneously in BALB/c mice. The first and second part are displayed in the same graph. After the first part of growth experiment, tumors were harvested for re-cultivation *in vitro*, subsequently, the *in vivo* passaged cells were reinjected in the second approach, additionally, Matrigel was opted as growth booster. B) L1210 cells grew well with all applied cell numbers, though 0.5 and 1 million cells per mice were chosen in the second step, as these doses exhibited slightly more homogeneity in their growth profile.

2.2 *Ex vivo* tumor imaging and histology

To evaluate the *in vivo* performance of both tumor models and examine the bioaccessibility/permeability of tumors for our carriers, Cy7-labeled siRNA polyplexes were applied intravenously and tumor signals were measured *in vivo* and *ex vivo*. There was a limited number of tumor bearing mice for M109 cell line, since the taking rate was only 58% and tumors were used for *in vivo* passaging in the first part, as well as for histology in the second

part of the growth experiment. Therefore, the siRNA accumulation comparing biodistribution were performed to a smaller extend than originally expected. However, we compared one formulation carrying Cy7-labeled siRNA for *ex vivo* tumor signals in both models. The exhibited tumor signal was measurable after 15 min comparable for both tumor models (Figure 12A). Though with another conjugate the *ex vivo* tumor signal was measurable for L1210 tumors only, displayed in figure 12B.

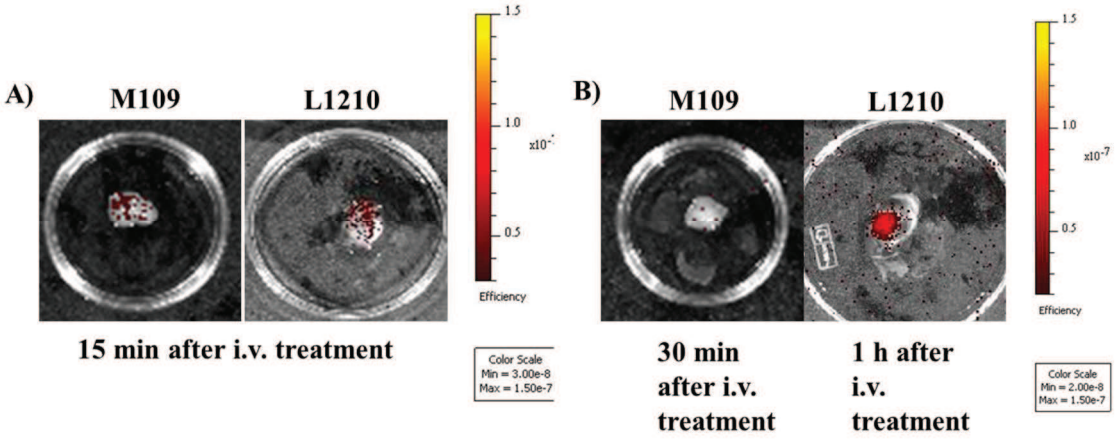

Figure 12: Tumoral biodistribution after intravenous (i.v.) administration of different FR-targeted polyplex formulations carrying 50% Cy7-labeled siRNA, detected via NIR bioimaging. A) Tumoral signals were measured *ex vivo*, 15 min after systemic application of a combinatorial polyplex (**386+873**/ Cy7-siRNA). B) After administration of ***762***-based polyplex, *ex vivo* signals were detectable only for L1210 tumors.
This study was of an explorative character, as group sizes were limited for M109 tumor model, due to reasons described above.

After animals were sacrificed, tumors with sizes of about 600-800 mm^3 were dissected and examined macroscopically. M109 cells built round-shaped tumors, definitely delimited from other mouse tissues, showing only rarely skin adhesions. Besides, tumors appeared as a pale white-rose and solid mass, though many fine red hairlines indicating blood vessels already on a macroscopic level. The leukemia cell line instead, presented flat but more extensively growing tumors with irregular shapes, showing high tendency for adhesions to skin and connective tissue of the mice. Already visible through the skin, harvested L1210 tumors appeared to be more intensively dark blue colored than M109 tumors, indicating more widely distributed blood residues in the leukemia cell based tumor (Figure 13).

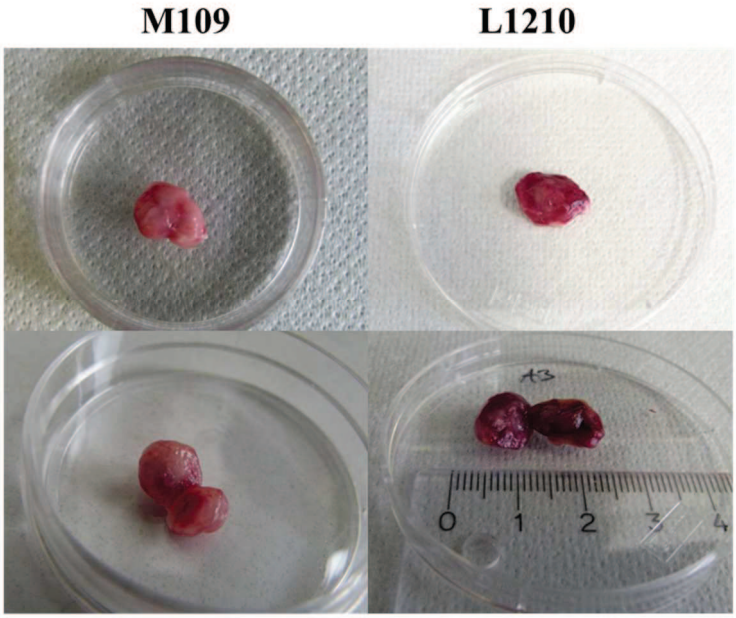

Figure 13: The pictures display the **macroscopic examination of harvested tumors**, comparing both cell lines. The upper panel presents tumors straight after harvesting, while the lower panel shows the tumors in cross-section.

Histologic evaluation was performed with paraffin embedded, eosin-haematoxylin (HE) stained tumor slices and aimed to compare tissue-structure and vascularization of both tumor types on a microscopic level. As additional control, slices of the folate-overexpressing KB tumors (also used for intratumoral application in the former experiments) of a similar size were harvested and screened. KB tumors have already been shown to be poorly vascularized by Smreka *et al.* [58], therefore they are a useful tool to compare the provided degree of vasculature to the other tumors. Not surprisingly, the M109 and KB tumors, both solid carcinomas, exhibited similarities of structure, while the leukemia cell line presented different features. Both *in vivo* round-shaped, well-delimited carcinomas displayed an "organ-like" structure with capsule (yellow arrows in figure 14) and rudimentarily indicated compartmentation (yellow curly brackets in figure 14) in the histologic view. The L1210 tumors were not equipped with a capsule or any other organizational structures (Figure 14, upper panel).

In terms of vascularization, erythrocytes were found all over the tissue sample, disseminated in small capillaries or even less organized in the intercellular matrix of L1210 tumors (dissemination of multiple 'free' erythrocytes found in most of the L1210 sections, figure 14). The M109 tumors displayed a more organized, "organ-like" form of perfusion, providing proper blood vessels of different sizes (blue arrows in figure 14), that were distributed well in the tissue. The KB tumor samples presented a similar perfusion system (blue arrows in figure 14,

middle panel), but the distribution of blood vessels was not as frequently as in M109 tumors (Figure 14, lower panel).

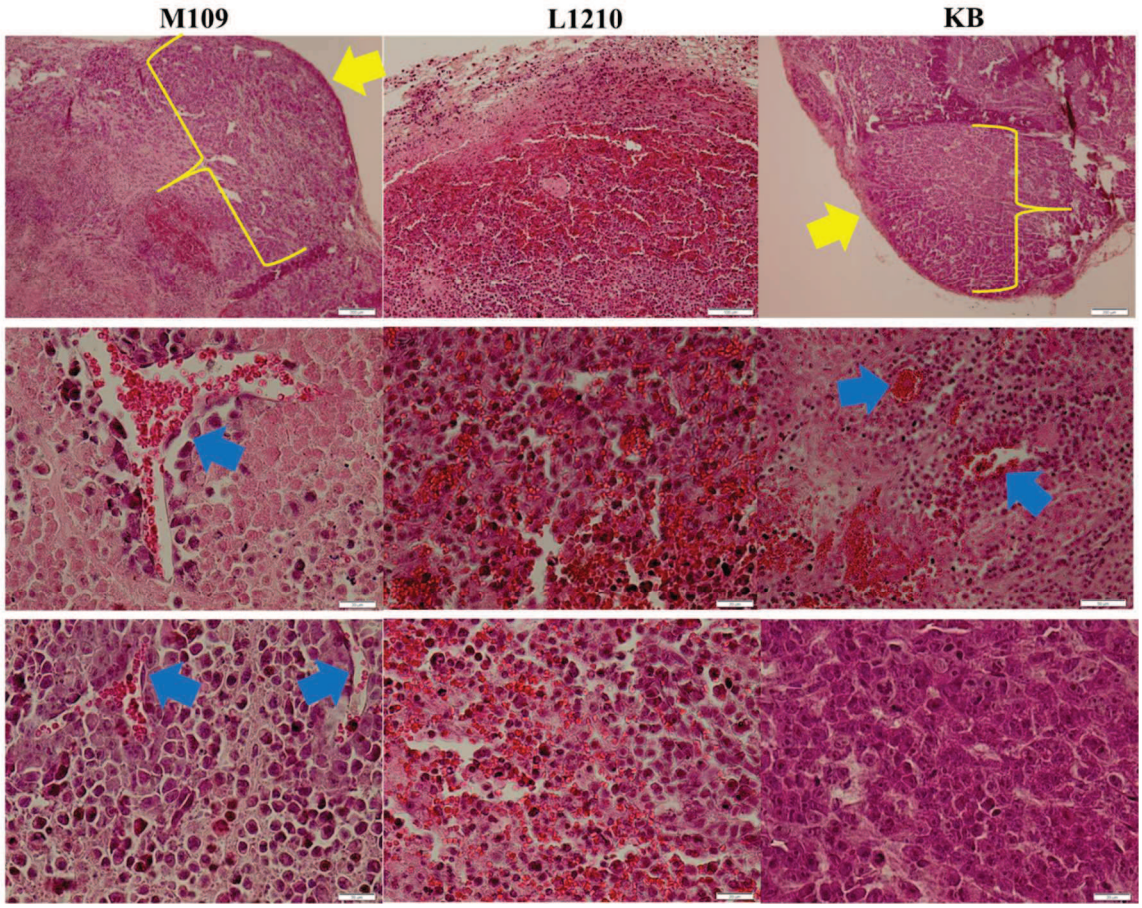

Figure 14: Histologic examination of FR-overexpressing tumor types based on either the M109, L1210 and or KB cell line. HE-stained tumor cross-sections were analyzed with an Olympus BX41 microscope. The upper panel displays an overview of structure, while the middle and lower panel includes representative sections for the different types and degrees of tumor vascularization The scale bars represent 200 µm in the upper panel, 20 µm in the middle and lower panel for M109 sections, while for L1210 they show 100 µm in the upper panel, 20 µm in the middle and lower panel. In the KB sections, the scale bars express 200 µm in the upper panel, 50 µm in the middle panel and 20 µm in the lower panel.

To sum up the outcome of performed experiments, both the carcinoma and leukemia originated tumors, provided sufficient connection to the circulatory system of the mice and presented comparable accessibility for one of the tested polyplex formulations, though L1210 displayed higher tumor accumulation for the other tested formulation.

3 Systemic tumor-targeted siRNA delivery

The systemic evaluation of targeted carriers for *in vivo* siRNA delivery presented the consequent step after confirming the therapeutic potential of intratumorally applied siRNA nanoparticles. Tumor-specific delivery was aimed at by the intravenous administration of exclusively surface-shielded and receptor targeted formulations. The provided mouse tumor models were selected for their overexpressed receptor status and favorable bioaccessibility.

In line with previous systemic applications, doses of 50 µg of siRNA per injection solved in 200 - 250 µL of HBG were applied intravenously. [28, 47] The targeted formulations selected for experiments in 3.1 – 3.3 all were previously found to be very effective in gene silencing *in vitro* in tumor cell culture.[85-87]

3.1 TfR-targeted cationic lipo-oligoamino amide *454*

In the following experiment, the systemic *in vivo* biodistribution profile of TfR-targeted, T-shaped lipo-oligomer ***454*** [C-Y_3-Stp_2-[$(OleA)_2$-K]K-Stp_2-Y_3-C] siRNA polyplexes was investigated in N2a tumor-bearing nude mice. This mouse tumor model was chosen for its reliable vascular permeability and TfR overexpression. Two polyplex groups were injected intravenously together with a free siRNA group (n=3). Distribution profiles were analyzed via NIR imaging and qRT-PCR, both. One injection group contained TfR-targeted ***454***/siRNA polyplexes, whereby siRNA was further conjugated with endosomolytic peptide Inf7 (***454*/Tf&Inf7**) (see scheme 2). The second group was injected with unmodified ***454***/siRNA polyplexes (***454*)** to evaluate the influence of multifunctional Tf targeting ligand and Inf7 polyplex modification.[85]

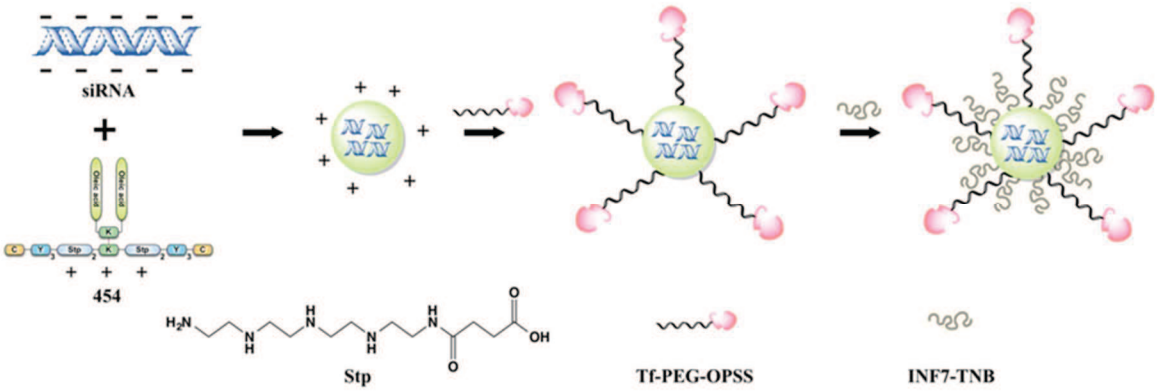

Scheme 2: The formation of Tf&INF7-modified siRNA polyplexes, based on lipo-oligomer ***454*** presented in a simplified scheme. K, Y, and C in ***454*** represent the corresponding (L) α-amino acids in one-letter code. The graphic illustrations are provided by Dr. Wei Zhang (postdoc at Pharmaceutical Biotechnology, LMU).[85]

The initial biodistribution was observed via NIR fluorescence bioimaging over the first 8 h and is displayed in figure 15A, with regard to intratumoral accumulation of the Cy7-labeled siRNA (tumor site is indicated by yellow arrows). In the first 15 min after administration, siRNA polyplexes of ***454*** and ***454*/Tf&Inf7** spread throughout the whole body along with the blood circulation. After 30 min, polyplexes of both groups mainly accumulated in liver and lung, indicated by the detection of Cy7-labeled siRNA. Nonetheless, there was no acute toxicity observed in any of the groups.[85]

Unfortunately, an early decrease of fluorescent signals was measured, although slightly slower than in the free siRNA control group (presented in figure 15B). Intact siRNA polyplexes display a size of 107 nm for ***454*** to 244 nm for ***454*/Tf&Inf7** group that would not allow renal clearance.[16] Therefore, this remarkable decay of fluorescence plus the early prominent bladder signals point out a lack of *in vivo* stability and dissociation of the polyplexes.[85] Nonetheless, ***454*/Tf&Inf7** group presented an observable tumor-associated siRNA accumulation, detectable via NIR over the first hour, in contrast to the unmodified ***454*** polyplex group (Figure 15A). At 8 h after injection, Cy7 signals had largely disappeared (Figure 15B), presumably due to the early decay of polyplexes and the subsequent renal clearance of the small Cy7-labeled siRNA (~7 x 2 nm size, 14 kDa molecular weight).[16]

The AHA1-siRNA distribution profile via qRT-PCR at 8 h after the treatment in figures 15 C and D presents the more sensitive siRNA quantification method. As already indicated by fluorescence imaging results, the siRNA mainly accumulated in liver and lung, while less lung accumulation was observed for the shielded ***454*/Tf&Inf7** group than for ***454*** group.[85] For liver accumulation, results were reverse (Figure 15 D).

The tumoral siRNA quantification confirmed the NIR-detected superiority of ***454*/Tf&Inf7** group over the ***454*** group with a twofold enhanced AHA1-siRNA dose in the tumors, displayed in figure 15C.[85]

Tumoral accumulation of additional controls (including 5% albumin modified ***454*/albumin** and Tf-targeted without Inf7 polyplex-group which is indicated as ***454*/Tf**) were measured and compared to ***454*/Tf&Inf7**, unmodified ***454*** and free siRNA. In figure 15D), the controls indicate a possibly TfR-independent passive accumulation of siRNA in the tumor site, as the ***454*/Tf** group could not reach the enhanced intratumoral siRNA amount of ***454*/Tf&Inf7**.[85] Interestingly, polyplexes with control protein albumin showed higher siRNA accumulation than ***454*/Tf**, too. Nevertheless, only the Tf-containing polyplexes would be expected to be actively endocytosed (as demonstrated in prior *in vitro* work). In summary, the observed lack of *in vivo* stability overshadowed encouraging tumor accumulation of ***454*/Tf&Inf7** group.[85]

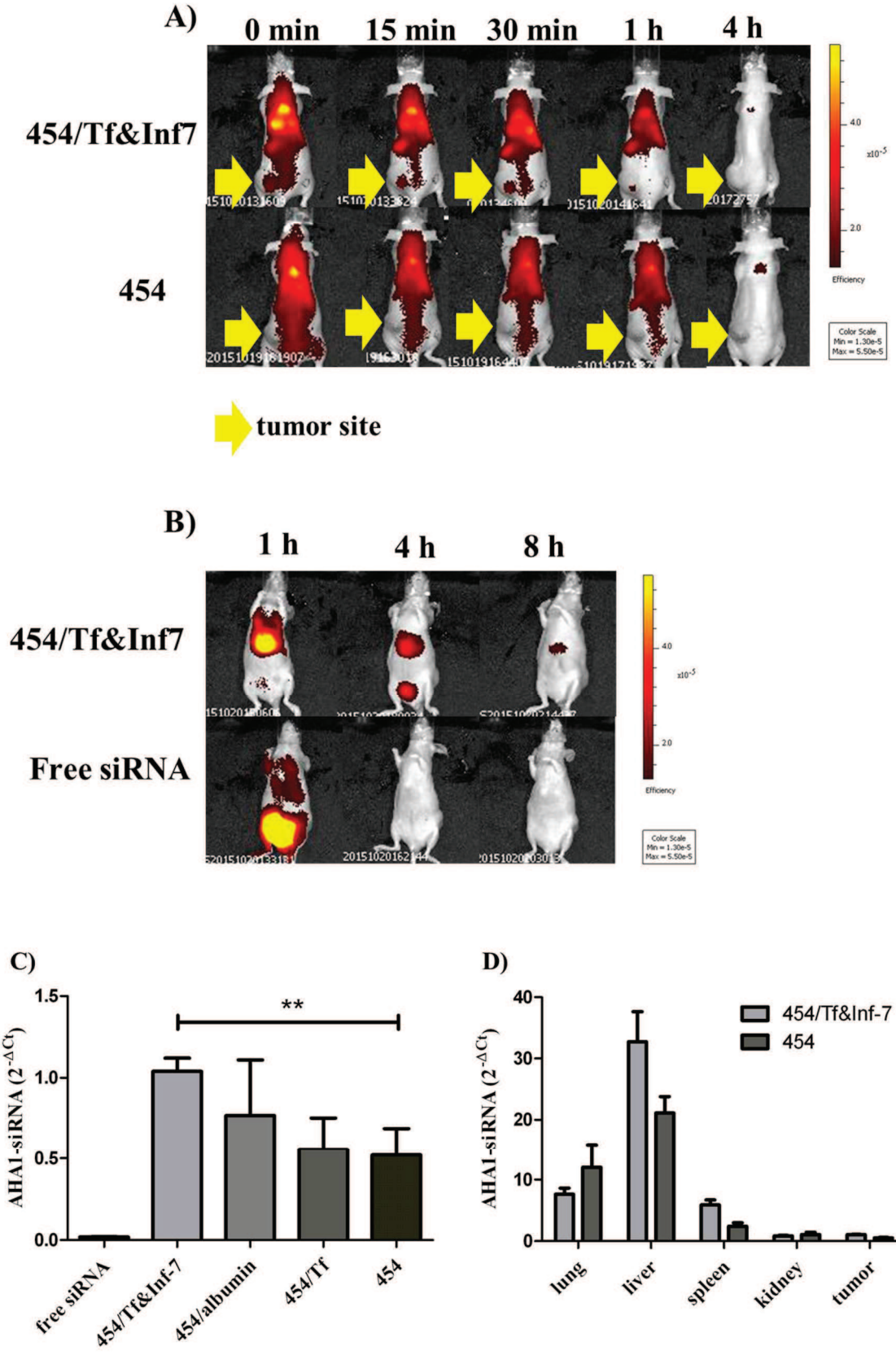

Figure 15: *In vivo* distribution of 50% Cy7-labeled AHA1 siRNA in N2a tumor-bearing mice. The performed bioimaging of systemic administration experiments is displayed in A) images

for ***454*/Tf&Inf7** are shown in the upper panel and for ***454*** polyplexes in the lower panel. The dorsal view is presented and the tumor site is indicated by yellow arrows. In B), the ventral view shows siRNA clearance probably caused by the dissociation of ***454*/Tf&Inf7** polyplexes (upper row), but slower as compared to the clearance profile of free siRNA (lower row). Bioimaging experiments were performed in triplicate, one representative mouse of each group is shown. Graphs in C) and D) (generated by Dr. Wei Zhang, postdoc at Pharmaceutical Biotechnology, LMU) illustrate the accumulation of siRNA in tumors and organs determined by qRT-PCR (ΔCt method) at 8 h after intravenous injection. C) represents the tumor accumulation comparing all groups. In D), the siRNA accumulation in organs of ***454*/Tf&Inf7** treated animals compared to ***454*** treated group is shown. Data is presented as relative quantity of AHA1 RNA, mean + SD (*n=3*). Illustrations and graphs are adapted from Zhang *et al.*[85]

3.2 FR-targeted cationic lipo-oligoamino amide *454* and *595*

The analogous experimental setting in L1210 tumor mice was chosen to examine the systemic biodistribution performance of siRNA polyplexes of ***454*** (C-Y_3-Stp_2-[$(OleA)_2$-K]K-Stp_2-Y_3-C) and **595** (CRC-Y_3-Stp_2-[$(OleA)_2$-K]K-Stp_2-Y_3-CRC), modified with a novel post-PEGylation strategy and folate as targeting ligand (see scheme 3). In addition, the stabilizing influence of the twin disulfide-forming cysteine–arginine–cysteine (CRC motif) [49] on polyplex-based siRNA delivery was investigated *in vivo*.[86]

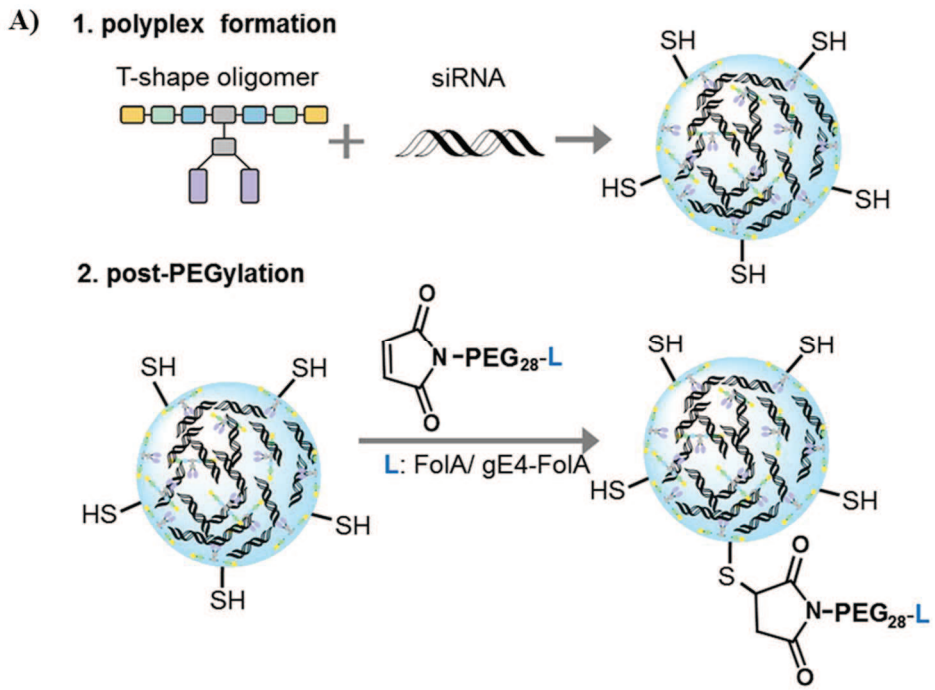

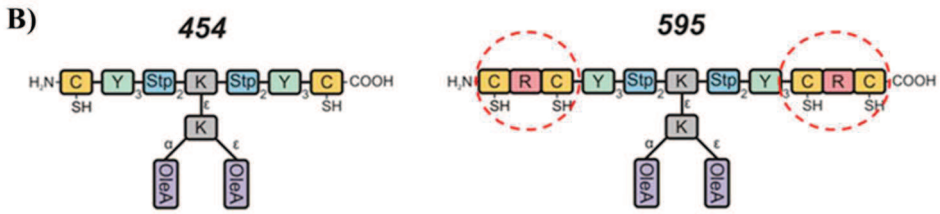

Scheme 3: A) Simplified and schematic illustration of **the lipo-oligomer based polyplex formation** (1.), **followed by a post-PEGylation process** (2.). As the T-shaped lipo-oligomer may serve ***454*** or the CRC-motif (indicated by red rings in B) stabilized ***595***, likewise. B) The structural schemes for both lipo-oligomers are shown. K, Y, and C in the represent the corresponding (L) α-amino acids in one-letter code; OleA = oleic acid; Stp = succinoyl tetraethylene pentamine. The graphic illustrations are provided by Katharina Müller (PhD study at Pharmaceutical Biotechnology, LMU).[86]

NIR imaging and qRT-PCR were used to acquire distribution profiles of both post-PEGylated conjugates ***454***/AHA1-siRNA and ***595***/AHA1-siRNA (50 % Cy7-labeled siRNA). The FR-overexpressing L1210 tumor model (as established in Results, section 2) was selected for the systemic application of the folate-containing nanoparticles.

A distribution pre-experiment was performed via NIR bioimaging in tumor free mice, using 3 equivalents of gE4-FolA-PEG for both oligomers. The initial distribution images displayed a rather short circulation time, due to rapid decay of polyplexes indicated by massive siRNA elimination via kidneys (Figure 16 A) upper panel, yellow arrows indicate bladder signals of differing intensity). Surprisingly, the degradation of the post-PEGylated, FolA-modified polyplexes (N/P 10) appeared to be faster than the clearance of TF-modified ***454*** siRNA polyplexes (N/P 6) as evaluated in parallel (Figure 16A). The early and prominent bladder signals (yellow arrows) of the post-PEGylated conjugates were even reminiscent of those of free siRNA. Moreover, fluorescence mostly disappeared within 1 h, corresponding to the systemic application of free siRNA (Figure 17A).[85, 86]

To investigate the relation between post-PEGylation and decreased stability, we continued the experiment by evaluating the previously used 3 equivalents against lower PEGylation degrees (2 and 1.5 equivalents) for both oligomers. Lower PEGylation degrees gradually improved stability, as shown in figure 16B. Encouragingly, the 1.5 equivalents of gE4-FolA-PEGylation enhanced *in vivo* stability remarkably, while the *in vitro* efficacy kept unaffected by the modification of the PEGylation degree.[86] Subsequently, *ex vivo* measured Cy7-signals in liver and lung were still detectable at 8 h after application, when the 1.5 equivalents of gE4-FolA were used for PEGylation, in contrast to the first *in vivo* approaches using the 3

equivalents PEGylation degree (Figure 16C) Unfortunately, we could not test lower degrees than 1.5 as they resulted in particle agglomeration *in vitro* and therefore were ruled out for *in vivo* use.[86]

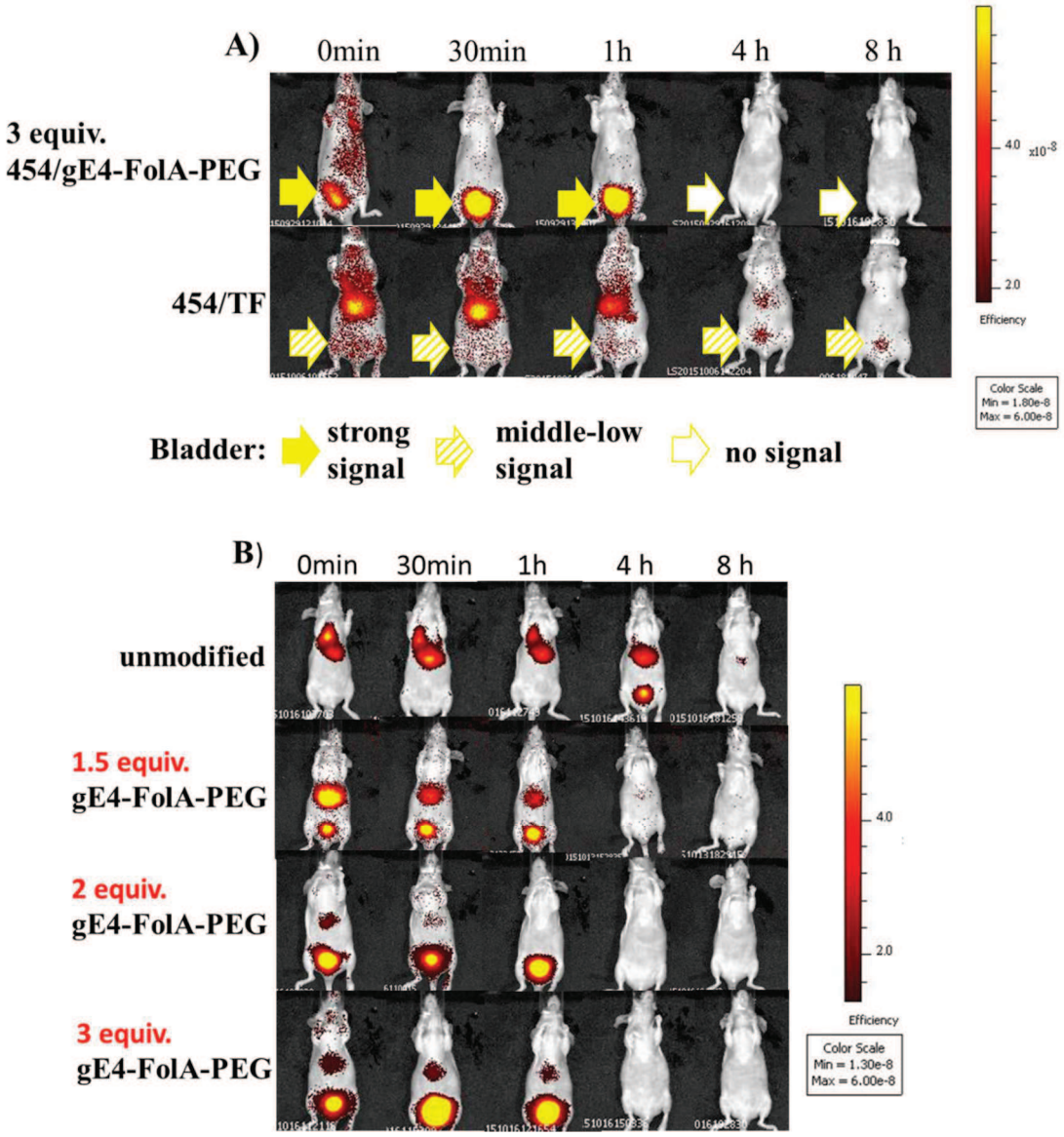

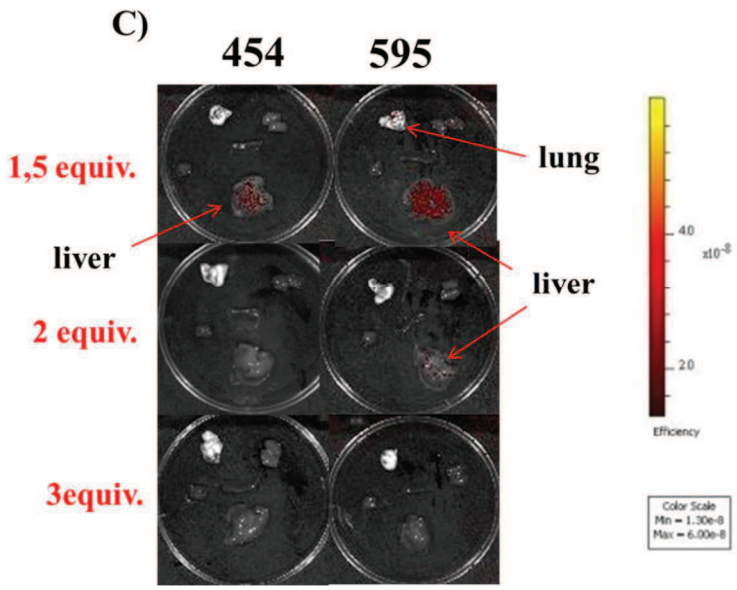

Figure 16: Time-dependent biodistribution of Cy7-siRNA polyplexes based on ***454*** or ***595*** after intravenous administration (n=3) in tumor-free mice. Signals were measured via NIR imaging *in vivo* and *ex vivo* and the results of one representative mouse of each group is shown. In A), differently modified and prepared polyplexes based on lipo-oligomer ***454*** were compared for their stability, represented through bladder signals of differing intensity (yellow arrows) in the ventral view. In the upper panel core ***454*** polyplexes were formed at N/P 10 and post-PEGylated with 3 equivalents (equiv.) of gE4-FolA. The lower panel shows animals treated with ***454*/Tf** polyplexes. In the latter case, the ***454*** oligomer was prepared at N/P 6 and surface-modified with transferrin via a PEG linker.
In B) the CRC-motif stabilized ***595***-based polyplexes present the gradual improvement of stability by lowering the degree of post-PEGylation from 3 to 1.5 equivalents of gE4-FolA. The ventral view allows the comparison of the elimination of dissociated polyplexes via the fluorescence degree of Cy7-labeled siRNA in the bladders.
The *ex vivo* imaging of organs at 8 h after injection, comparing ***595*** with ***454***-based post-PEGylated polyplexes prepared with 1.5 to 3 equivalents of gE4-FolA is displayed in C). In terms of stability, a moderate superiority of post-PEGylated ***595*** over post-PEGylated ***454*** polyplexes was indicated by higher efficiency of the Cy7-signals in liver and lung observed for 1.5 and 2 equivalents of gE4-FolA. Illustrations are adapted from Müller *et al.*[86]

Throughout the presented pre-experiments, CRC-motif stabilized ***595***-based siRNA polyplexes were found to be slightly superior to ***454***-based polyplexes in terms of stability (compare figure 16C). Therefore, ***595*** with a 1.5 equivalents gE4-FolA-PEGylation degree was subsequently applied in L1210 tumor-bearing mice for the qRT-PCR supported measurement of siRNA distribution.[86]

Free siRNA**,** ***595***-based polyplexes without PEGylation (***595***) and PEGylated polyplexes without targeting ligand (***595*/Mal-PEG**) served as controls. Cy7-signals were present for up to 8 h post treatment, detected via NIR imaging for all ***595***-based conjugates (Figure 17A).

Whereas for free siRNA, the signal completely disappeared between 1 h and 4 h after the treatment, due to renal clearance, presented in the lowest panel of figure 17A.[86]

Unmodified ***595*** polyplexes appeared to be the most stable of all tested siRNA carriers, while pronounced bladder signals of ***595*/Mal-PEG** and ***595*/gE4-FolA-PEG** still indicated a stability issue, probably related to their surface-modification.[86] Finally, the animals were sacrificed for subsequent qRT-PCR analysis of organs and tumors.

Consistent with previously published distribution data [31, 85] and NIR imaging results (blue and red arrows, figure 17A), all polyplexes mainly accumulated in liver and lung. Nonetheless, the reduced lung accumulation of shielded versus unshielded polyplexes (already presented in Results, section 3.1) was reproducible. qRT-PCR even confirmed that lung accumulation of ***595*/gE4-FolA-PEG** was lower than of ***595*/Mal-PEG** (Figure 17C), indicating decrease of undesired accumulation in vital organs like lungs through advanced shielding and targeting strategy.[86]

Tumoral Cy7-signals were observed in all ***595***-based groups at some point in the first hour after polyplex application as presented in figure 17B, but were not measurable anymore at 4 h after treatment. Quantified via qRT-PCR and normalized to lung accumulation, the highest siRNA residue was detected in the unmodified and most stable ***595*** group, followed by the targeted ***595*/gE4-FolA-PEG** polyplexes, that were superior to the untargeted equivalents ***595*/Mal-PEG** (Figure 17D).[86]

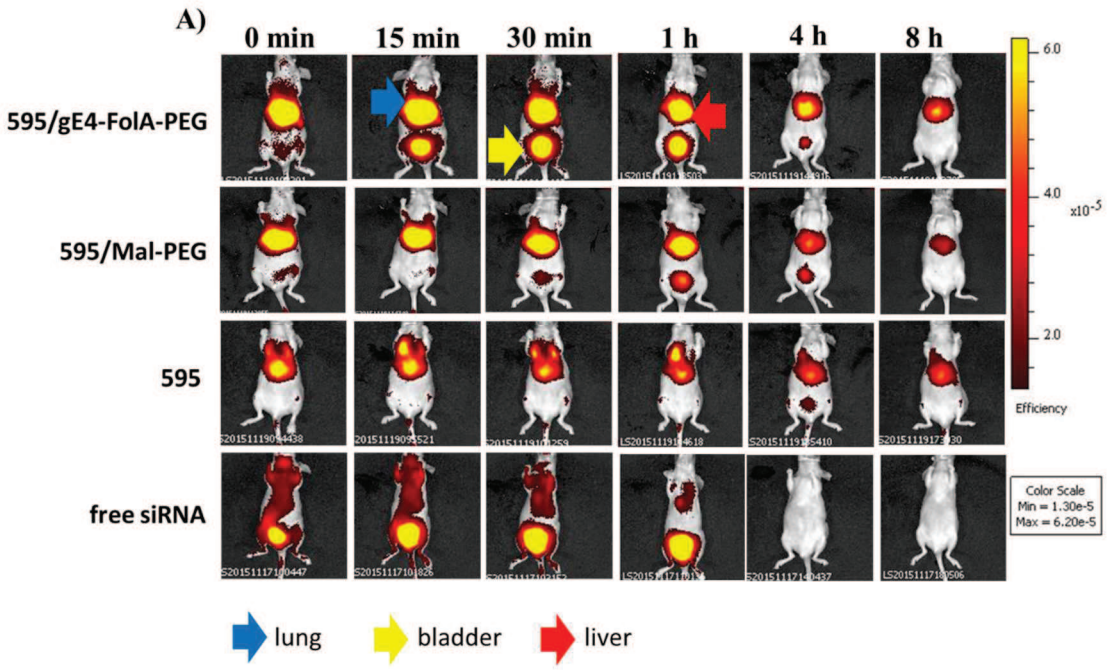

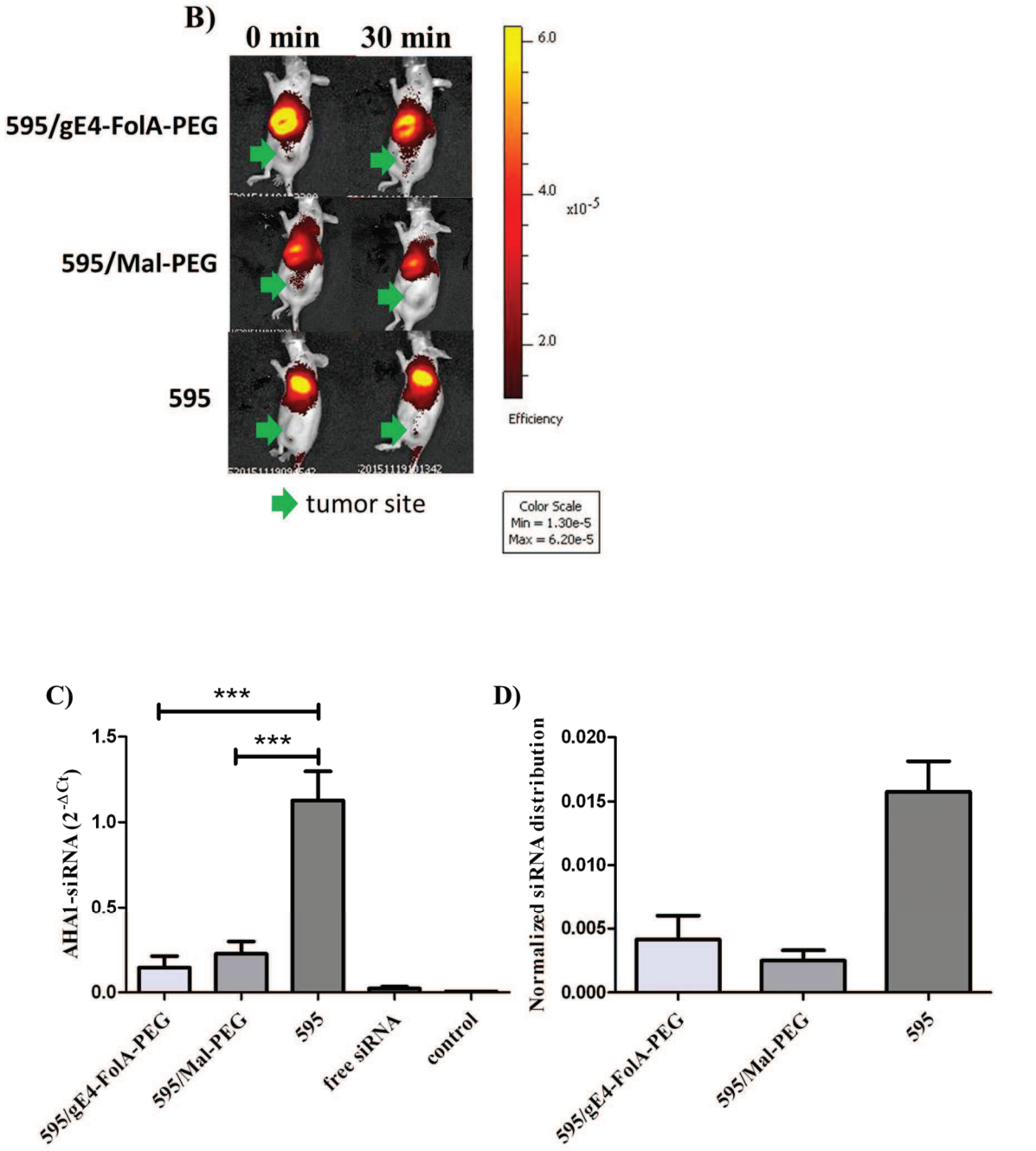

Figure 17: Final distribution experiment using ***595***-based siRNA polyplexes which were applied into the tail vein of NMRI-nude mice, bearing subcutaneous FR-overexpressing L1210 tumors. The optimized post-PEGylation degree of 1.5 equivalent was used to prepare the ***595*/gE4-FolA-PEG** formulation**.** (n=3 mice per group)
In A), the time-dependent biodistribution is illustrated for ***595*/gE4-FolA-PEG,** control polyplexes and free siRNA, using 50% Cy7-labeled siRNA which was detected via NIR imaging. Ventral view of one representative mouse per group is shown. The blue arrow indicates a lung signal, the red one a liver signal, and the yellow one a bladder signal. The lateral view in B) presents the tumor site of all ***595***-based siRNA polyplex groups at 0 min and 1 h after injection. Graphs in C) and D) (generated by Katharina Müller, PhD study at Pharmaceutical Biotechnology, LMU) show the distribution of AHA1 siRNA in organs and tumors as quantitated by qPCR analysis, at 8 h after the treatment with indicated formulations.

The graph in C) provides information on the siRNA accumulation in lungs. Data is presented as relative quantity of AHA1 RNA, mean + SD (n=3) while the bars in D) represent the normalized tumor to lung distribution ratio of quantified siRNA for the differently modified variations of ***595***-based polyplexes. Illustrations and graphs are adapted from Müller *et al.*[86]

Acute toxicity was not observed in any of the treatment groups. However, consistent with the Tf-targeted lipo-oligomers (Results, section 3.1) which were tested in parallel to the described pre-experiment, the *in vivo* performance of post-PEGylated polyplexes was still limited by lacking particle stability, despite the encouraging improvement through CRC motif integration and optimized PEGylation degree.[86]

3.3 FR-targeted combinatorial polyplexes

The described experiments were performed to evaluate the *in vivo* performance of polypex-combinations designed out of a library containing sequence-defined polycationic, oligoaminoamide-based oligomers.[38, 101] Physicochemical properties of polyplexes were optimized by covalent coupling of two oligomer-types (see scheme 4) with different favourable structural moieties (e.g. target-specificity, surface-protection, strong siRNA binding activity), hence uniting required properties for efficient and tissue specific siRNA delivery, enabling *in vivo* gene silencing.[87]

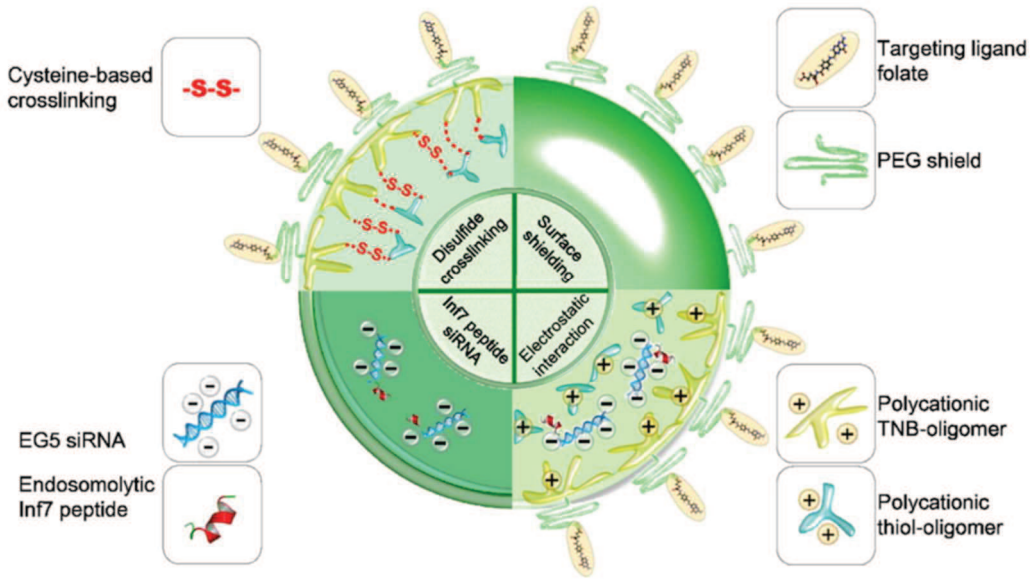

Scheme 4: FR-targeted combinatorial polyplexes. The functional elements are presented in a simplified, schematic illustration that is provided by Dian-Jang Lee and Dr. Dongsheng He (PhD study at Pharmaceutical Biotechnology, LMU).[87]

The NIR-imaging of Cy7-labeled polyplex combinations was terminated at varying time-intervals after systemic treatment to perform *ex vivo* imaging of harvested tumors (and organs), in order to confirm the origin of the *in vivo* detected signals in a more sensitive and precise way. Encouragingly, the described covalent coupling of oligomers, resulting in combinatorial polyplexes, improved the *in vivo* performance in comparison to polyplexes which were based on the single oligomers. The *in vivo* imaging in figures 18A and B shows tumor accumulation profiles of the targeted combinatorial polyplexes (TCPs) **386+873**/Cy7-siRNA [87] and **356+454**/Cy7-siRNA, and furthermore the 'single' polyplexes-components in the co-formulations (***386***/Cy7-siRNA, ***873***/Cy7-siRNA, ***356***/Cy7-siRNA and ***454***/Cy7-siRNA). While the untargeted ***386***-based polyplexes appeared to literally detour around the tumor region, the PEGylated and FR-targeted, DTNB-modified ***873***-based polyplexes displayed moderate tumor-associated signals at 30 min post the intravenous application. Those signals, however, could not be confirmed by *ex vivo* imaging.[87] In contrast, the co-formulation of aforementioned polymers presented tumor-signals for up to 1 h after the intravenous treatment (confirmed also by *ex vivo* imaging, figure 18A). Furthermore, the combinatorial optimization of polyplexes resulted in prolonged circulation time due to enhanced stability as illustrated figures 18C and D. For both TCPs, the 'single' polyplexes were fully cleared at 4 h after the treatment, while the co-formulations where still detectable, though mainly in liver and bladder.[87] Encouragingly, the co-formulation of the surface-shielded and folate-directed ***356*** with the cationic lipo-oligomer ***454*** which promotes siRNA binding and increases the polyplexes size, even displayed less bladder signals than TCP **386+873**/Cy7-siRNA. The same applied to 'single' polyplex-components of own components, indicating increased stability (Figure 18D). However, as presented in Figures 18A and B, the *in vivo* signals of TCPs completely disappeared at 24 h after the treatment, thus causing no residue.[87]

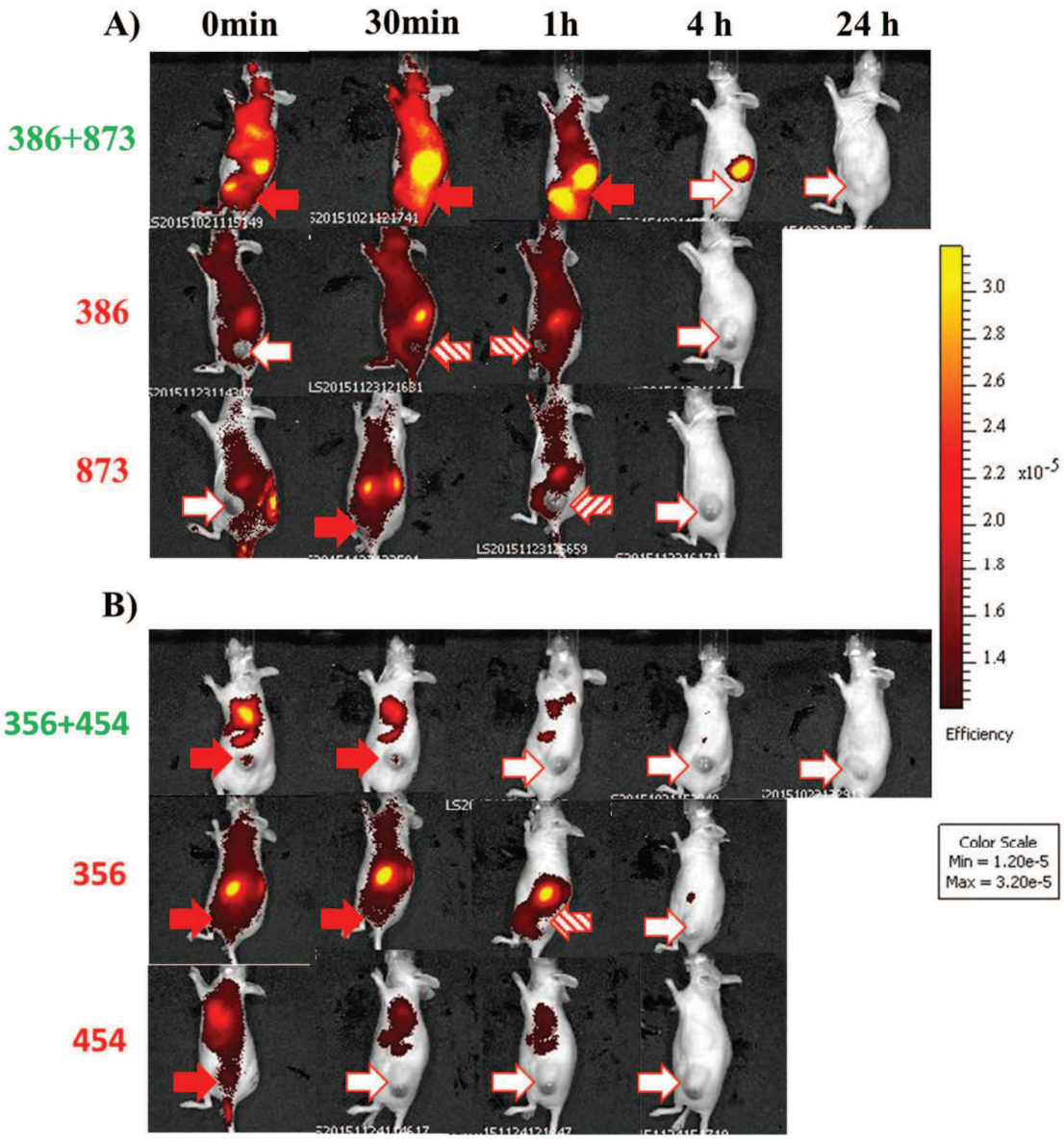
A)
0min
30min
1h
4 h
24 h
386+873
386
873
B)
356+454
356
454
3.0
2.8
2.6
2.4
2.2 x10-5
2.0
1.8
1.6
1.4
Efficiency
Color Scale
Min = 1.20e-5
Max = 3.20e-5

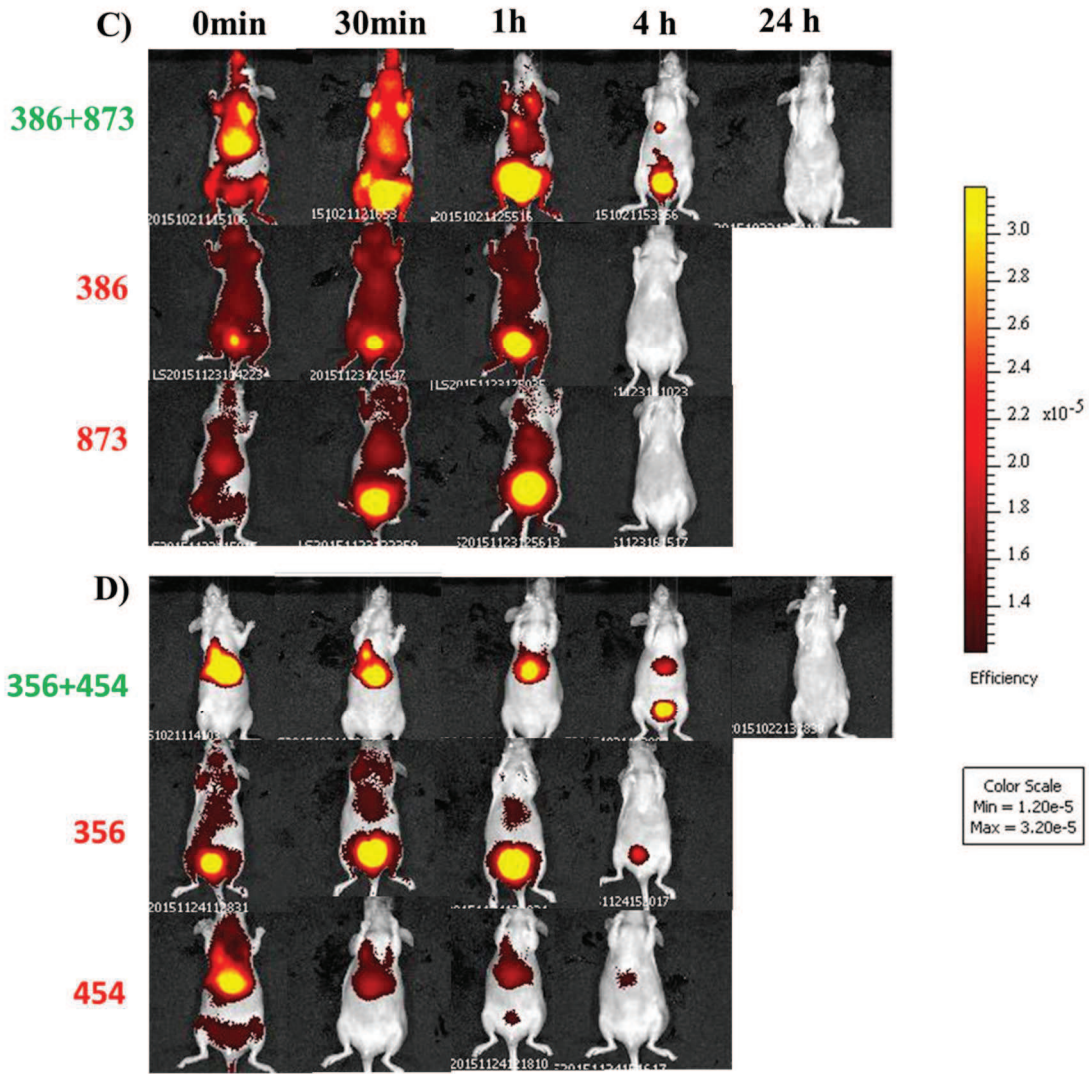

Figure 18: Biodistribution of optimized combinatorial siRNA polyplexes in L1210 tumor-bearing nude mice determined by NIR fluorescence imaging. A) and B) present time-dependent distribution of Cy7-labeled siRNA after intravenous injection. The lateral view of animals allows to observe the tumor site, while arrows with different fillings indicate the degrees of tumor accumulation. The results for co-formulation of the untargeted oligomer ***386*** with the DTNB-modified, surface-shielded, FR-targeted oligomer ***873*** as well as the respective single oligomer-based control polyplexes are shown in A), while biodistributions of co-formulation of PEG-shielded, FR-targeted ***356*** with lipo-oligomer ***454*** and respective controls are illustrated in B).
The respective ventral view of animals presented in A) and B) is provided in figures C) and D). This perspective allows to observe the accumulation of Cy7-siRNA in liver and lungs, and moreover their elimination via bladder signals for up to 24 h.
Experiments were performed with 3–4 animals per group; a representative mouse of each group is shown. The illustrations presented in A) and C) are adapted from Lee *et al.*[87]

Interestingly, a tumor-specific Cy7-signal was observed *in vivo* for up to 30 min after injection of **356+454**/Cy7-siRNA co-formulation (Figure 18B). These *in vivo* signals were verified by *ex*

vivo measurement of harvested tumors that detected a strong fluorescence which was present for over 2 h post the treatment, illustrated in figure 19B.

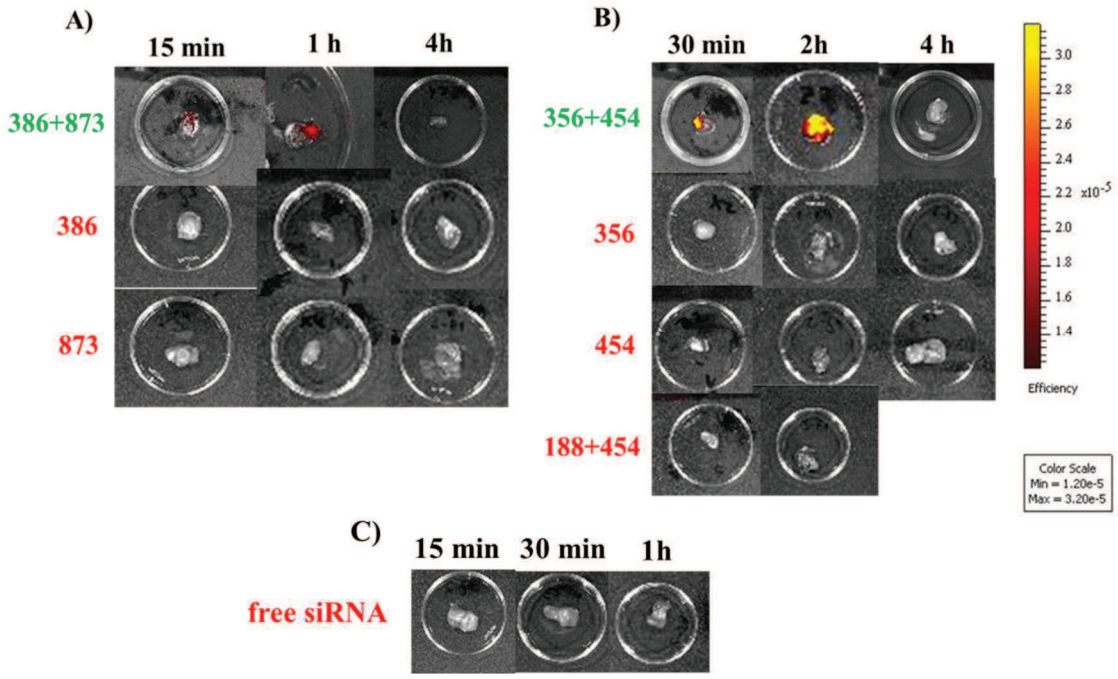

Figure 19: *Ex vivo* imaging of harvested tumors at different time intervals after the treatment with optimized combinatorial Cy7-siRNA polyplexes in L1210 tumor-bearing nude mice determined by NIR fluorescence imaging. A) Tumors were harvested at 15 min, 1 h or 4 h after intravenous injection of TCP **386+873** and its respective controls. B) Tumors were harvested at 30 min, 2 h or 4 h after intravenous injection of TCP **356+454** and its respective controls, including an untargeted combinatorial polyplex (**188+454**), that exhibits a similar structure to **356+454** but is missing the folate-conjugation. C) Tumors were harvested at 15 min, 30 min and 1 h after injection of 50µg of free Cy7-siRNA.
Experiments were performed with 3–4 animals per formulation. The illustrations presented in A) and C) are adapted from Lee *et al.*[87]

In sum, the poor pharmacokinetics of free siRNA got enhanced remarkably through complexation in TCPs. While free siRNA did not accumulate in the tumor site as shown in figure 19C, NIR-measured *ex vivo* signals of TCPs were detectable for up to 2 h (compare figures 19A and B). These encouraging results provided ground to experiment *in vivo* gene silencing as the following step.[87]

For qRT-PCR-based evaluation of gene silencing, Inf7 modified EG5-siRNA was used to complex TCPs for treatment groups. Additionally, TCPs were formulated with siCtrl-Inf7 as control groups. Intravenous treatments were performed twice in a 24 h interval and mice were euthanized 48 h after the first treatment. The tumors were harvested for siRNA extraction and

mRNA expression levels of EG5 gene were compared to untreated animals. The TCP **386+873** complexed with siEG5-Inf7 reduced the EG5 gene expression by 46% [87], while **356+454** silenced the EG5 gene expression with twofold significance by 65%. (Figure 20). However, the equivalent formulation with siCtrl-Inf7 showed only trifling effects on the mRNA level of EG5 in comparison to tumors of untreated control mice [87], excluding unspecific effects on gene expression caused by the polyplexes themselves.

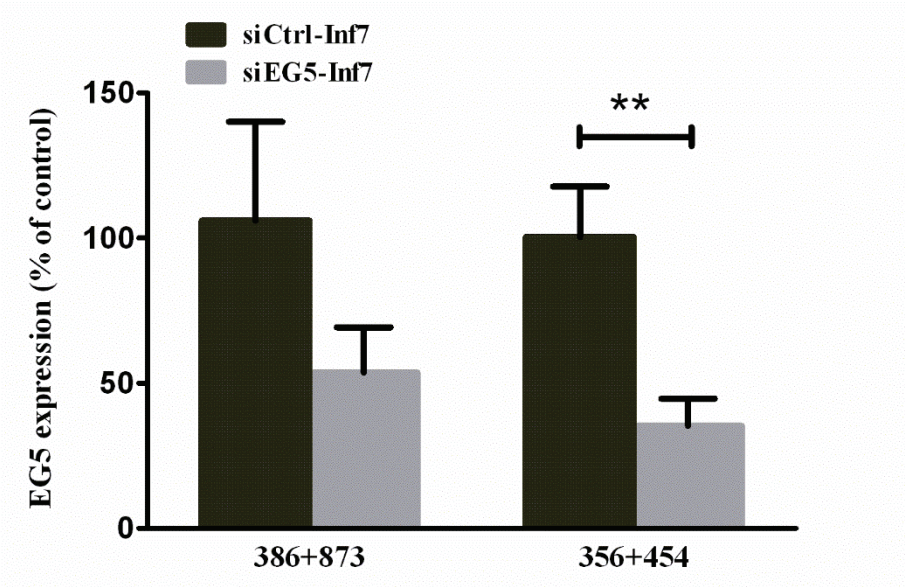

Figure 20: Gene silencing efficiency of FR-targeted combinatorial polyplexes in L1210 tumor-bearing mice. The mRNA level of EG5 gene was measured via qRT-PCR of harvested tumors after twofold intravenous treatments. EG5 gene expression is expressed in % of untreated controls. The groups (n=5) were treated with **386+873/siEG5-Inf7** respectively **siCtrl-Inf7** [87] or **356+454/siEG5-Inf7** respectively **siEG5-Inf7**. The qRT-PCR analysis was performed by Dian-Jang Lee (PhD study at Pharmaceutical Biotechnology, LMU).

To monitor the animals' well-being during the treatment process, we measured bodyweight daily and examined blood parameters (ALT, AST BUN, creatinine) to observe possible side effects on the vital organs liver and kidney (Figure 21). Both presented high Cy7 accumulation observed via NIR imaging of TCPs (Figure 18). An elevation, compared to untreated control mice, was only found for creatinine in the **386+876/siEG5-Inf7** group.[87] None of the other parameters were influenced by the treatment (Figure 21b). The weight courses were not affected by the treatments with any of the formulations either (Figure 21a).

In conclusion, TCP siEG5-Inf7 treatment reduced gene expression remarkably, in absence of any acute side effects.[87]

A)

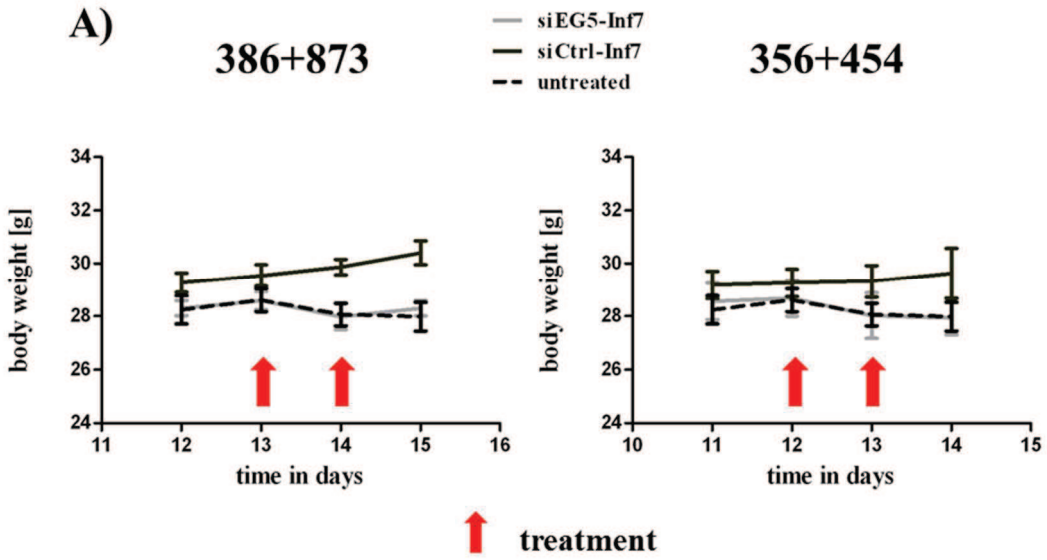

B)

	ALT (U/L)	AST (U/L)	creatinine (mg/dL)	BUN (mg/dL)
reference range	60±11	161±60	0.63±0.05	40±10
untreated control	46±15	113±23	0.07±0.01	38±7
386+873/ siEG5-Inf7	34±15	80±28	0.11±0.01 *	43±13
386+873/ siCtrl-Inf7	39±2	115±36	0.08±0.02	39±6
356+454/ siEG5-Inf7	39±2	120±31	0.09±0.01	40±8
356+454/ siCtrl-Inf7	57.4±25	130±46	0.09±0.01	39±7

Figure 21: Health analysis and screening for possible side effects in mice that were treated with TCPs. A) Body weight course over the treatment period observed for both TPCs and compared to that of untreated but tumor-bearing mice. The intravenous injections were performed at day 13 and 14, respectively 12 and 13 as indicated by the red arrows. The table in B) presents clinical biochemistry parameters (ALT, AST, creatinine and BUN). When animals were sacrificed for RNA extraction of tumors (48 h after the first and 24 h after the second treatment), the plasma was obtained and analyzed. Indicated reference range at the top of the table is provided by the breeder Janvier Labs and is valid for female NMRI-nu/nu mice of the same age that are not treated or tumor-bearing.[102] The second row of the table presents the internal untreated control that contains L1210 tumor-bearing mice which were otherwise handled in the same way and time schedule. N=5 for TCP groups and n=3 for untreated group. The graphs and table regarding **386+873** are adapted from Lee *et al.*[87]
* shows a significant difference between the untreated control and **386+873**/siEG5-Inf7 treated group.

V DISCUSSION

1 Intratumoral administration of MTX-directed siRNA nanoplexes

The efficiency of siRNA therapy is mainly hampered by its poor pharmacokinetic properties (compare Introduction, section 1.2.). To achieve the goal of tumor-specific, intracellular siRNA delivery *in vivo*, an optimized combination of recent *in vitro* and *in vivo* findings was developed and tested. Dohmen *et al.*[28] presented a significantly prolonged retention of folate targeted siRNA polyplexes compared to untargeted siRNA polyplexes and free siRNA after intratumoral injection in KB tumors. A similar structure but conjugated with FR-responsive methotrexate (MTX) instead of folic acid (FolA) was chosen for the current work.

The *in vivo* stability of structurally similar FolA-PEG siRNA polyplexes was already investigated by retrieval of these polyplexes from the urine of intravenously injected mice (Fig. S16 and S17 in Dohmen *et al.* [28]). Therefore, we could exclude a major degradation of the polyplexes after intratumoral injection.[89] This finding was quite helpful as we can only detect Cy7-labeled siRNA using near infrared imaging, consequently have no information about the intactness of the polyplexes. The observed particle stability is provided by disulfide formation of cysteines which stabilize the polycationic oligomer backbone necessary for siRNA polyplex formation by intermolecular crosslinking.[46, 48, 89]

To increase the solubility of the polyplexes and prevent undesired immune reactions, a polyethylene glycol (PEG) chain had been introduced into the carrier oligomer for surface-shielding against undesired interactions with body fluids in the extracellular tumor matrix (e.g. blood components, collagens, proteoglycans or hyaluronic acid).[45, 50, 51]

MTX was opted in respect of its FR-responsiveness [67] and to additionally increase the therapeutic potential of EG5-siRNA nanoplexes by its cytotoxic power.[71] Thus, the folate analogue had to accomplish two major tasks. Firstly, MTX was needed to direct the nanoplexes towards their intended site of action and to facilitate cell entry via the folate receptor or folate carrier. Secondly, once inside the target cell, MTX is expected to deploy its anti-proliferative effect [70] that is enhanced through synthetic polyglutamylation of MTX, as proven by Lächelt *et al.*[73] (compare scheme 1).[89]

The bioimaging study in the current work provided evidence for a comparable targeting ability of MTX and FolA, this was ascertained by equally enhanced retention times of both structurally analogous siRNA polyplexes (***640***/Cy7-siRNA-Inf7 and ***356***/Cy7-siRNA-Inf7, compare figure 4A). However, these imaging results only evidenced the increased tumor retention of the

polyplexes due to the targeting ligand, whereas no information about the polyplex internalization, endosomal release and subsequent therapeutic siRNA efficiency was provided. The subsequent treatment experiment was performed to proof the assumed therapeutic potential of MTX-directed ***640*/siEG5-Inf7**. EG5-siRNA (siEG5) is known to inhibit mitosis after cytosolic release, by knockdown of an essential cell-cycle protein (kinesin spindle protein = KSP, also referred to as eglin-5, EG5).[89, 103, 104] Therefore, siEG5 represents a powerful tool to fight rapidly dividing cancer cells.[105] However, in the first place, the synthetic siEG5 needs to be delivered into the cytosolic compartment of the target cells, before its gene silencing effect can actually be exploited for antitumoral efficacy.[106]

2'OMe-modified siRNAs were chosen to circumvent toll-like receptors (TLR)-mediated immune responses, so called off-target effects [105, 107], which consequently excluded undesired inflammatory reactions that could have influenced tumor growth in an unspecific way.[89, 105] Furthermore, conjugation of endosomolytic peptide Inf7 (established by Plank *et al.* [55]) to siRNA was performed in order to overcome the hurdle of endosomal release and to enable cytosolic release of both the combinatorial anti-tumor weapons siEG5 and MTX. Many cancer therapies are hampered by toxicity in non-target tissues or intrinsic, respectively acquired drug resistance.[108, 109] Hence, combinatorial treatment with different antitumor agents is a common strategy to overcome those kind of limitations.[110, 111] Combinatorial treatment strategies facilitate lower doses and subsequently reduce toxicity without influencing effectiveness.[89, 112] Additionally, they increase the chances of circumventing intrinsic resistance and minimize acquired drug resistance by combining two different cell-killing pathways, consequently augmenting cytotoxicity.[113, 114]

In our approach to combine two antitumor weapons that work inside the same target cell and for the same goal but with different mechanisms, we united a RNAi based therapeutic with the standard cancer drug methotrexate in one multifunctional nanoparticle.[89]

The significant superiority of ***640*/siEG5-Inf7** over ***640*/siCtrl-Inf7** (compare figures 6B and 10A) displays the expected mitosis inhibiting effect of EG5 siRNA. Furthermore, the presented results confirm the augmented combinatorial effect of MTX with RNAi based therapy (Figures 6 - 8).

Moreover, the results suggest that siRNA complexation generally improves the antitumoral efficacy (Figures 6 and 7) by presumably prolonged retention in the tumor tissue, dependent on nanoparticle formation.[89] Free ***640*** polymer might be cleared more rapidly (as well as previously experienced with free siRNA [28]), as no nanoparticle formation is possible without the negatively charged siRNA for complexation (or positively charged polymer in respect of

free siRNA).[36] The enhanced endosomolytic release boosted by Inf7 peptide could be another advantage of the polyplex formation.[55]

Figure 7 indicates that therapy with an equivalent dose of cytotoxic DHFR inhibitor MTX in unbound form did not retard the tumor growth at all, further highlighting the improved pharmacokinetics of the standard drug due to polyplex linkage.[70, 89, 115]

The stressful treatment process or tumor necrosis associated discomfort in siEG5-treated groups likely caused the temporary stagnation of body weight recorded in most animals over the treatment period, displayed in figures 8 and 9.[89] Besides that, we encouragingly did not observe any medical condition or side effects caused by the treatment (over 70 days observation time for the surviving animals of ***640*/siEG5-Inf7**), indicating a target-tissue specific effect of our formulation.

Finally, this experimental treatment setting highlighted the advantage of ***640*/siEG5-Inf7** over formerly used ***356*/siEG5-Inf7** (illustrated in figure 10B), therefore evidences the improved efficacy of the combinatorial treatment strategy.[89] The dual antitumoral power of methotrexate plus EG5 siRNA even resulted in a recurrence-free healing process of 50 percent of the ***640*/siEG5-Inf7** group until the end of the study (Figure 7).

Despite these encouraging results, there are still remaining challenges of successful siRNA delivery left to cope with.[16, 23] We chose the local application path to circumvent rapid renal filtration of our small sized nanoparticles (only ~ 6 nm), experienced with analogous Fol-PEG siRNA polyplexes after intravenous administration in Dohmen *et al.*[28] However, most tumor types are not accessible via local application, consequently tissue-specific, stable polymeric carriers with increased sizes and sufficient surface-shielding need to be evaluated for systemic siRNA-based treatment.

2 Folate receptor-overexpressing *in vivo* tumor model for systemic delivery

The utilization of animals in scientific and medical research is a subject of heated debate in many industrial countries.[116] A lot of times, reliable predictions for the translation into humans cannot be provided by animal models, due to genetic or physiological differences, especially for cancer research. Nevertheless, animal models serve as powerful tools for the development of novel treatment approaches, by collection of indispensable preclinical *in vivo* information.[117, 118]

The selection of a suitable mouse tumor model is one key factor in the design of an animal-based cancer research studies and may facilitate rapid scientific progress in the optimization of therapeutic strategies.[117, 119]. In the previous project, FR-overexpressing subcutaneous human KB tumors were treated intratumorally with small FR-targeted nanoparticles, achieving promising results (Figures 6 and 7). For the local application, a solid, well-encapsulated tumor with less frequent blood vessels, indicating poor vascularization [58], was a suitable model to support the retention of injected FR-targeted particles, subsequently enhancing the chance for cell targeting and internalization of therapeutic components. As aforementioned, local application of therapeutics is not suitable for most of the human cancer types. However, for systemic delivery of siRNA, not only the abilities of the developed carriers but also the bioaccessibility of the induced tumors influences the outcome of the study.[120] Therefore, the following project was aimed to establish a mouse tumor model in our lab, which would be suitable for systemic delivery of FR-targeted siRNA carriers.

The newly evaluated FR-overexpressing cell lines are of murine origin. The M109 cell line is syngeneic to the BALB/c mouse strain, as it is based on a spontaneous neoplasm in an 18-month-old BALB/c mouse that occurred in 1964, eventually called the Madison lung carcinoma.[92, 93] The suspension growing L1210 cell line was originally derived from lymphocytic leukemia in ascites from in an 8-month old, female DBA-2 mouse.[94, 95, 121]

The validated folate receptor status (performed by Dian-Jang Lee, PhD study at Pharmaceutical Biotechnology, LMU) was found comparable and sufficiently high for both cell lines. For the following experiments with intravenously applied FR-targeted formulations (illustrated in Results, sections 3.2 and 3.3), we finally chose the leukemia L1210 cell line to induce subcutaneous tumors in immunodeficient NMRI-nu/nu mice. Since the reliable, simultaneous and homogenous growth, requiring only a low number of cells (0,5 - 1 x 10^6) for inoculation (Figure 11B), was considered to be advantageous for the reproducibility of the desired FolA-responsive mouse tumor model. Multiple factors are known to influence the delivery of particles into the tumor tissue [58], for instance tumoral vascularization [122], occurring necrosis [123]

and interstitial pressure in solid tumors, though all these factors are more or less interrelated with tumor size.[120] As shown in Harrington *et al.* [120], there is a relation between liposome uptake and the variation of tumor vascular volume with tumor size. Therefore, a homogeneity of tumor size in treatment experiments is desired. However, the M109 tumors grew at different speeds for the individual mice, and therefore caused high standard deviations in terms of tumor volume observed over the growth course. Thus L1210 tumors were selected over M109, though the described issues could be mitigated by *in vivo* passaging and support through Matrigel (Figure 11A).

Nevertheless, the caliper measurement of L1210 cell line appeared more inconvenient as the shape of tumors is quite flat and irregular in comparison to the round shaped M109 tumors (compare figure 13). The explorative biodistribution results could not sufficiently proof superiority of one over the other tumor model, however, confirmed the essential permeability for nanosized polyplexes (Figure 12A) **386+873** co-formulation: 104 nm [87] and B) ***762***-based polyplexes: 576 nm [101]). Histology of middle sized tumors reasserted distinct vascularization for both models, though by a differently structured vasculature as illustrated in figure 14. The chaotic structure and highly leaking vasculature (many free erythrocytes disseminated in the intercellular matrix in figure 14) of L1210 was not surprising for a leukemia cell line. The M109 tumor presented a similarly strong vasculature but showed a more ‘organ-like’ organization of structure. Moreover, the M109 tumor mass kind of resembled the KB carcinoma structure, though the density of blood vessels was found higher in the M109 tumor sections compared to those of KB tumors (Figure 14).

3 Receptor-responsive systemic siRNA delivery

In the intratumoral treatment experiment as described before, we successfully treated mice with multifunctional, targeted siRNA nanoparticles which displayed a size of ~ 6 nm.[89] Despite the encouraging results, most of human tumors actually are not accessible via local application route. However, the systemic and tumor-specific delivery of RNAi-based therapeutics is still in its infancy [16, 25, 85], yet reaching a relatively low number of representatives in clinical studies, though steadily growing.[124, 125]

Consequently, our next step was the evaluation of enlarged, well-defined, multifunctional siRNA carriers for systemic delivery, which avoid renal filtration and biodegradation, and thus show enhanced circulation time.[38, 39] Prolonged circulation time is favorable to improve the polyplexes' chances for extravasation into the tumor tissue [29, 30], moreover, well-sized nanoparticles (in the range of ~20 - 200 nm) may additionally promote the aforementioned EPR effect.[57, 126]

3.1 TfR-targeted cationic lipo-oligoamino amide *454*

The *in vivo* performance of TfR-targeted cationic lipo-oligoamino amide ***454*** complexed with siRNA (size: ~100 nm) and equipped with varying surface modifications (size: up to ~250 nm) was investigated after systemic application. The targeted TfR is overexpressed on the surface of malignant cells in many tumor types [79, 80], including the surface of the N2a cell line, employed in the current experiment. N2a is of murine origin, derived from a spontaneous neuroblastoma in a strain A albino mouse [121] and commonly known to induce well vascularized tumors [58], thus providing sufficient permeability for nucleic acid delivery systems. The multifunctional Tf-ligand was introduced to the polyplexes via PEG linkage in order to increase their specificity for TfR-overexpressing N2a tumor cells, thus preventing side effects in non-target cells. Recently, systemic *in vivo* application of Ran siRNA delivered by Tf-modified, oligoethylenimine derivative polyplexes resulted in 80% gene silencing, inducing apoptosis in N2a tumors of mice.[127] Even more encouraging, cyclodextrin polymer-based siRNA carriers have reached human clinical testing for tumor-targeted therapy. Here, the Tf-targeted nanoparticles were administrated intravenously into patients.[124]

Tf is not only an efficient and time-tested natural targeting-ligand [24, 76-78], but additionally proved surface protecting abilities.[77] For the evaluated system, the large human serum-protein (80 kDa) could not be linked directly to the oligomeric structure without sustaining a loss of nucleic acid binding ability, therefore the surface has been post-modified with Tf-PEG after siRNA complexation by the lipo-oligomer.[85, 128] In combination, PEGylation and Tf-

modification represent a useful shielding domain to prevent unspecific reactions with body fluids that can lead to deadly aggregation processes [129] or biodegradation.[44, 130] For enhanced cytosolic release the endosomolytic peptide Inf7 was opted to further improve the targeted siRNA carrier, even though the repeated 1,2-diaminoethane motifs for stable siRNA binding and enhanced endosomal release by proton sponge effect [54, 131] were already integrated in the T-shaped lipo-oligomer.[85]

Additional shielding domains of ***454*/Tf&Inf7** group resulted in reduced lung accumulation of siRNA compared with the unmodified ***454*,** as presented in figure 15D. However, highest overall siRNA accumulation was found in the liver.[85] This finding is consistent with previous imaging studies of ***454*** polyplexes [31] and presumably related to the uptake by the reticuloendothelial system (RES) which's components (e.g. phagocytic cells in liver and spleen) represent a commonly known obstacle for the successful delivery of nanoparticles. This phenomenon of RES-dependent degradation of polyplexes should be contained by surface modifications (e.g. PEG-shield).[20, 29, 30] Though, the higher liver accumulation in the shielded and Tf-targeted ***454*/Tf&Inf7** group compared to unmodified ***454*** polyplexes might be related to the receptor status of the tissue, as the liver exclusively expresses a high number of TfR-2 receptors that may play a role in the accumulation processes.[132]

Encouragingly, the quantified tumor accumulation was highest for the ***454*/Tf&Inf7** group. Interestingly, the ligand-independent, passive targeting plays an important role since controls like shielded but untargeted ***454*/Albumin** group attained a better accumulation effect than ***454*/Tf** (Figure 15C).[85] The shielded and targeted ***454*/Tf** formulation only accomplished a tumoral siRNA accumulation comparable to unmodified ***454*** polyplexes. This is not surprising as similar biodistribution of nontargeted and TfR-targeted polyplexes has been reported before in Bartlett *et al.*[133] The main role of Tf is in active endocytosis into the cell after receptor binding, a step which takes place after polyplexes have already located to the tumor.

Polyplex formation increased the retention of siRNA remarkable (for up to 7h) compared to the application of free siRNA as shown in figure 15B. However, stability issues still were observed throughout the imaging process, especially for the surface modified ***454***-based polyplexes.[85] Presumably, therefore, the general efficiency of the siRNA delivery into tumors occurred limited by the relatively short circulation performance.[29, 59] Increased *in vivo* stability of siRNA carrier systems is vital for successful treatment approaches [134] with systemic RNAi based therapy, therefore needs to be optimized for future delivery approaches.[85]

3.2 FR-targeted cationic lipo-oligoamino amides *454* and *595*

The *in vivo* performance of FR-targeted cationic lipo-oligoamino amide ***454*** in comparison to the twin disulfide-forming cysteine–arginine–cysteine (CRC motif) stabilized analog ***595*** was investigated after systemic application. The siRNA polyplexes obtained surface protection to avoid unspecific reactions with e.g. blood components [44, 135], by a novel post-PEGylation strategy. Optionally, the *in vitro* optimized tetra-γ-glutamyl folic acid (gE4-FolA) was introduced to specifically target FR-overexpressing L1210 tumor cells.[86] The surface modifications resulted in precise nanoparticles with sizes between 100 and 200 nm that are well-adapted for systemic application, as both, biodegradation processes followed by rapid renal clearance [90] and also inadvertant *in vivo* aggregation [129] processes should be prevented.[86] Furthermore, the size range is suitable for polyplexes to become subject of the EPR effect, additionally enhancing chances for accumulation in the tumor site.[57] However, consistent with the observations of in parallel tested TfR-targeted polyplexes, *in vivo* destabilization turned out to be the limiting factor for the systemic siRNA delivery by these lipo-oligomer based carrier-systems, which operated efficiently and specifically *in vitro*.[85, 86] Oligomer ***454*** was replaced by the CRC-motif stabilized ***595***. The stabilizing effect of this twin disulfide-forming cysteine–arginine–cysteine motif relies on covalent interactions via disulfide bridge formation.[49] In addition, the PEGylation degree was adapted, all in respect to improved stability. As illustrated in figure 16B, lower PEGylation degrees gradually improved stability, though 1.5 equivalents were the lowest degree that still allowed the forming particles of suitable sizes for *in vivo* application. Particle formation using lower degrees lead to formation of large aggregates *in vitro* [86], which could possibly clog capillaries of vital organs, inducing severe side effects or even a deadly pulmonary embolism. However, in spite of the described optimizations for the *in vivo* setup**, *595*/gE4-FolA-PEG** still degraded too quickly to reach proper circulation times, thus sufficient siRNA accumulation in the tumor site could not be achieved.[29, 59]

Nevertheless, the *in vivo* performance of currently tested lipo-oligomers displayed detectable signals for up to 8 h, whereas ***356*** nanoparticles were completely cleared by kidneys after only half of the circulation time, as shown in the previously published systemic application of the smaller (~ 5.8 nm) siRNA polyplexes based on polymer ***356***.[28] This indicates a desirable size related avoidance of renal clearance. Encouragingly, sufficient surface-protection through the post-PEGylation strategy, improving the ‘passive targeting’[50, 51, 57], plus the tissue specific targeting-ligand FolA for ‘active targeting’[52], reduced an undesired accumulation in the lung

(consistent with ***454*/Tf&Inf7** in 3.1) and liver for ***595*/gE4-FolA-PEG** polyplexes compared to unmodified ***595*** group (Figures 17A and C).[86]

In conclusion, the presented lipo-oligomer based, tumor-targeted conjugates provide a favorable size and efficient surface-protection, resulting in reduced siRNA residues in lung and liver compared to their unmodified analogs. However, an improvement in terms of particle stability is necessary to increase the efficiency of polyplexes for tumor-specific delivery [23, 86, 134], though tumor-associated accumulation was temporarily observed via NIR imaging as displayed in figure 17B.

3.3 FR-targeted combinatorial siRNA polyplexes

The systemic siRNA treatment is hampered by poor pharmacokinetics of the small particles [19, 27], therefore polymeric carrier-based siRNA delivery was evaluated in previous distribution experiments. Polyplexes were based on one well defined oligomer (e.g. ***356*** or ***454***) which met the requirements for siRNA delivery *in vivo* more or less [28, 31], and therefore presented advantages and disadvantages in their biodistribution profiles.[85, 86] Forming stable and well-shielded, targeted particles, ***356*** polyplexes were too small in size and resulted in immediate renal clearance after intravenous application.[28] ***454***-based polyplexes were sized more favorably but could not profit from enhanced circulation time, due to insufficient *in vivo* stability which was partly caused by the integration of surface shielding and targeting components.[85, 86] In the current approach, single polymers were mixed or covalently coupled in co-formulations and screened in biodistribution experiments using subcutaneous L1210 mouse tumor models. Confirmed by NIR-imaging, the co-formulation of ***386*** for efficient siRNA binding covalently coupled with PEG-folate-conjugated ***873*** for surface shielding and FR-targeting (respectively the mixing of lipo-oligomer ***454*** with the shielding and targeting oligomer ***356***) proofed the concept's validity.[87] Both types of combinations achieved prolonged circulation times for up to 4h, compared with their 'single polyplex' components or free siRNA which Cy7-signals were mostly disappeared 4h after systemic application (Figures 18 and 15B). As indicated by the NIR imaging experiment, additionally, both polyplex combinations did not cause residues in other organs that could induce subacute or chronic side effects on non-target tissues (no detectable signals at 24 h after intravenous application as displayed in figure 18). The *ex vivo* NIR-imaging revealed notable intratumoral siRNA accumulations for up to 1 h after the treatment with **386+873** and up to 2 h after the application of **356+454** co-formulation. Whereas figure 19 further presents that *ex vivo* tumor signals could not be detected for free siRNA or single polymer-based polyplex-controls. Encouraged by these

promising results, *in vivo* gene silencing was evaluated with both polyplex-combinations (**386+873** and **356+454**). To enhance the chance of endosomal escape of the FR-targeted formulations, Inf7-conjugated siRNA was chosen for all polyplex-groups.[87] Impressively, the combination of PEG-folate-conjugate **356** with lipo-oligomer ***454*** knocked down more than half (65%) of the EG5-gene expression on mRNA level compared to untreated control animals, followed by **386+873** co-formulation that reached 46%. Moderate superiority of **356+454** over **386+873** could be explained by a slightly advanced distribution profile (less immediate bladder signals and prolonged intratumoral retention, figure 18 and 19), indicating higher *in vivo* stability.[134] The treatment with polyplexes containing siCtrl-Inf7 resulted in EG5 gene expression which was comparable to the untreated control, excluding unspecific influence caused by the carriers themselves.[87]

Thus, there were no observations signaling acute toxicity or any impairment to health. We additionally performed blood biochemistry to exclude side effects on non-target tissues. Analyzed parameters ALT and AST (ALT = alanine aminotransferase and AST = aspartate aminotransferase), also called 'liver enzymes', are indicators for damage of liver cells [136, 137], while elevation of blood urea nitrogen (BUN) or creatinine signal renal dysfunction related issues.[138] The evaluation of clinical blood parameters did not show any alarming elevations, despite of detected siRNA accumulation in liver and kidney during the first hours (fully cleared after 24 h, figure 18). Though the creatinine measured for **368+873/siCtrl-Inf7** group was increased compared to the untreated internal control animals, it was still far lower than the creatinine reference range provided by the breeder of the employed mouse strain (data sheet of NMRI-nu/nu mice by Janvier Labs [102]).[87] Therefore, the health analysis, summing up weight observation, behavior and blood biochemistry, did not indicate formulation-related acute toxicity or malfunction of liver and kidney.

Taking together the measured tumoral gene silencing activity and further the absence of acute toxicity in vital organs, the tested carrier-systems proved efficient siRNA delivery into target cells, as well as cytosolic release, and therefore are covering bottlenecks of siRNA delivery.[16, 23, 87]

VI SUMMARY

Cancer represents a global threat to human well-being as it is a leading cause of death worldwide and its incidence is steadily increasing. The development of new therapeutic modalities is imperative as common treatment strategies often lack efficiency and the prevention remains difficult for this wide field of multifactorial caused diseases. The research of this thesis aimed at the evaluation and improvement of novel treatment approaches based on therapeutic nucleic acids. However, the successful treatment of cancer with genetic therapeutics such as based on a synthetic, short interfering RNA (siRNA) which operates through an intracellular mechanism, is dependent on intracellular and furthermore target-specific delivery. Therefore, we investigated the *in vivo* performance of sequence-defined and highly functionalized polymeric carrier systems in regard to their required capabilities for tumor-specific and intracellular siRNA delivery.

The first set of experiments demonstrated the capabilities of the standard drug methotrexate as a targeting-ligand and subsequently the therapeutic potential of 6 nm sized, targeted siRNA nanoparticles upon intratumoral administration. The combined cytotoxic effect of methotrexate and the anti-mitotic EG5 (eglin-5) siRNA resulted in efficient tumor growth inhibition. Impressively, tumors disappeared recurrence-free in half of the treatment group.

The next project describes the evaluation and establishment of a FR-overexpressing mouse tumor model suitable for systemic delivery. Two murine cell lines, M109 and L1210, provided comparable bioaccessibility validated by histologic examination and explorative biodistribution data based on NIR fluorescence imaging. Since L1210 leukemia cells presented favorable and convenient growth properties, this cell line was selected for future FR-targeted systemic delivery experiments.

The third part of the thesis assessed several tumor-targeted siRNA delivery systems for intravenous, systemic delivery. Lipo-oligomeric carriers formed with siRNA 100-200 nm sized nanoparticles which were equipped with different surface modification. These were screened for their *in vivo* distribution profiles comparing the time-dependent accumulation of fluorescently labeled siRNA in the organs and the tumor site via NIR bioimaging. Some of the surface modification strategies required further *in vivo* optimization, before the amount of delivered siRNA was quantified by a qRT-PCR method. The bioimaging results indicated instability issues, limiting the circulation time and consequently the efficient siRNA delivery to the tumor site. Nevertheless, encouragingly, the developed strategies for surface modification achieved a decreased siRNA accumulation in non-target tissues, like lung or liver.

In the final experiments, polycationic oligomers and lipo-oligomers with complementary capabilities were co-formulated to combine their strengths, while simultaneously resolving their weaknesses. These combinatorial ternary polyplexes exhibited tumor specific accumulation of the delivered, fluorescently labeled siRNA after intravenous application. Consequently, the most promising combinatorial polyplexes were selected for a tumoral gene silencing assay using the anti-mitotic and thus antitumoral EG5 siRNA. Encouragingly, the two tested formulations resulted in a significant knockdown (46% and 65%, respectively) of the EG5 gene in the harvested tumors, as confirmed by qRT-PCR analysis.

Summarizing, the thesis deals with the *in vivo* evaluation of innovative polymeric carrier systems for tumor-specific siRNA delivery, with the aim to perform therapeutic gene silencing in a safe and efficient manner. The encouraging results represent a promising starting point to improve the RNAi based cancer treatment by further investigations.

VII ZUSAMMENFASSUNG

Mit stetig steigender Tendenz repräsentieren Krebserkrankungen die häufigste Todesursache weltweit und stellen folglich eine globale Bedrohung für das menschliche Wohl dar. Die Entwicklung von neuen therapeutischen Modalitäten ist zwingend notwendig, da es vorhandenen Behandlungsstrategien oft an Effizienz mangelt und sich die Prävention für dieses weite Feld multifaktoriell bedingter Erkrankungen als äußerst schwierig erweist.
Die Dissertation „In vivo Bewertung von polymerischen Nano-Trägersystemen für auf siRNA basierende Krebstherapeutika“ präsentiert Forschungsprojekte, welche innovative, auf Nukleinsäure-Therapie (z.B. siRNA) beruhende Behandlungsansätze im Maus-Tumormodell evaluieren und optimieren.

Die erfolgreiche Behandlung von Krebs, mittels auf RNA-Interferenz (RNAi) basierender Modulation der Genexpression, ist von der spezifischen Einschleusung therapeutischer siRNA ins Zytosol der Zielzelle abhängig. Folglich lag der Untersuchungsschwerpunkt hinsichtlich der *in vivo* Wirksamkeit von Sequenz-definierten und hoch funktionalisierten Polymeren in der tumorspezifischen und intrazellulären siRNA Anlieferung.

Das erste Experiment demonstriert die Fähigkeit des Standard-Therapeutikums Methotrexat in innovativer Form als Polymer-gebundenen Targeting Liganden zu fungieren, und das therapeutische Potential der damit hergestellten 6 nm großen, Rezeptor-spezifischen siRNA-Nanopartikeln nach intratumoraler (lokaler) Verabreichung. Die kombinierte zytotoxische Wirkung von Methotrexat als bifunktionellen Targeting Liganden und der anti-mitotischen EG5 (eglin-5) siRNA führte zu einer effizienten Hemmung des Tumorwachstums. Bei der Hälfte der behandelten Tiere erfolgte eine eindrucksvolle Tumor-Eradikation unter Ausbleiben von Rezidiven innerhalb der Beobachtungszeit.

Der nächste dargestellte Schritt beschreibt die Etablierung eines Folat Rezeptor (FR)-überexprimierenden Maus-Tumormodells, welches der nachfolgenden Evaluierung von intravenös (systemisch) verabreichten Teststrukturen dienen soll. Die Tumore von zwei murinen Zelllinien (M109 und L1210) erwiesen eine relativ vergleichbare Zugänglichkeit für getestete Strukturen, jeweils validiert durch histologische Untersuchungen und explorative Bioverteilungsstudien, die mittels Nah-Infrarot (NIR) Fluoreszenz-Bildgebung durchgeführt wurden. Die L1210-Zelllinie präsentierte jedoch günstigere Wachstums-Eigenschaften und wurde daher für künftige Experimente mit FR-gezielten, intravenösen Applikationen von Teststrukturen ausgewählt.

Folglich untersucht der dritte Teil der Dissertation die Tumor-gerichteten siRNA Transport-Systeme nach deren intravenösen Applikation. Lipo-Oligomere als Trägerstrukturen wurden

mit unterschiedlichen Oberflächenmodifikationen ausgestattet. Die *in vivo* Verteilung in Organen und Tumor wurde zeitabhängig mittels fluoreszenzmarkierter siRNA und NIR Bioimaging untersucht und verglichen. Einige der Oberflächenmodifikationsstrategien erforderten weitere *in vivo*-Optimierung bevor die endgültige Quantifizierung von siRNA Anreicherung in verschiedenen Organen mittels qRT-PCR durchgeführt wurde. Die Bioimaging Ergebnisse wiesen auf Stabilitätsprobleme hin, welche die Zirkulationszeit der Träger begrenzten und somit auch einen effizienten siRNA Transport zum Tumor beeinträchtigten. Trotz der Stabilitätseinbußen ist hierbei die verminderte siRNA Anreicherung in Nicht-Zielgeweben (z.B. Lunge, Leber), erreicht durch entsprechende Oberflächenmodifikationsstrategien, positiv zu bewerten.

Im letzten Experiment wurden Co-Formulierungen von siRNA mit je zwei verschiedenen Oligomeren, beziehungsweise Lipo-Oligomeren eingesetzt und die Tumor-spezifische Anreicherung nach intravenöser Applikation der fluoreszenzmarkierten siRNA Polyplexe mittels NIR-Bildgebung detektiert. Für die verwendeten ternären Co-Formulierungen wurden Oligomere mit komplementären Fähigkeiten kombiniert, um deren Stärken in Summe zu nutzen und gleichzeitig eventuelle Schwächen zu kompensieren. In Folge wurden die beiden vielversprechendsten Kombinations-Formulierungen für Gen-Silencing Experimente mittels der anti-mitotischen EG5 siRNA ausgewählt. Die qRT-PCR Analyse der entnommenen Tumore zeigte erfreulicherweise einem signifikanten Knockdown der EG5 Gen Expression (46%, beziehungsweise 65%) durch beide getesteten Formulierungen.

Zusammengefasst beschäftigt sich die Arbeit mit der *in vivo* Evaluation von innovativen Polymer-basierenden Trägersystemen für tumorspezifischen siRNA Transport. Zielsetzung war ein sowohl sicheres, als auch effizientes therapeutisches Gen-Silencing. Die ermutigenden Ergebnisse stellen sowohl einen vielversprechenden Ansatz für eine auf RNAi basierende Krebsbehandlung, als auch einen Ausgangspunkt für weitere Untersuchungen dar.

VIII REFERENCES

1. Stewart BW, Wild, CP. *World cancer report 2014*. International Agency for Research on Cancer, **2014**
2. Peto J. *Cancer epidemiology in the last century and the next decade*. Nature **2001**, 411, 390-395.
3. Sadikovic B, Al-Romaih K, Squire J, Zielenska M. *Cause and consequences of genetic and epigenetic alterations in human cancer*. Curr Genomics **2008**, 9, 394-408.
4. Pao W, Girard N. *New driver mutations in non-small-cell lung cancer*. Lancet oncol **2011**, 12, 175-180.
5. Kodama T, Biyajima S, Watanabe S, Shimosato Y. *Morphologic Variations of Small Cell Lung Cancer. A Histopathologic Study of Pretreat-ment and Posttreatment Specimens in 104 Pa-tients. Sehested, M., Hirsch, FR, Osterlind, K*. Cancer **1986**, 57, 804-807.
6. Bastien RR, Rodríguez-Lescure Á, Ebbert MT, Prat A, Munárriz B, Rowe L, Miller P, Ruiz-Borrego M, Anderson D, Lyons B. *PAM50 breast cancer subtyping by RT-qPCR and concordance with standard clinical molecular markers*. BMC Med Genomics **2012**, 5, 1.
7. Roychowdhury S, Chinnaiyan AM. *Translating genomics for precision cancer medicine*. Annu rev Genomics and Hum Genet **2014**, 15, 395-415.
8. The Cancer Genome Atlas Research Network. *Integrated genomic analyses of ovarian carcinoma*. Nature **2011**, 474, 609-615.
9. Ding L, Getz G, Wheeler DA, Mardis ER, McLellan MD, Cibulskis K, Sougnez C, Greulich H, Muzny DM, Morgan MB*, et al. Somatic mutations affect key pathways in lung adenocarcinoma*. Nature **2008**, 455, 1069-1075.
10. Sana J, Faltejskova P, Svoboda M, Slaby O. *Novel classes of non-coding RNAs and cancer*. J Transl Med **2012**, 10, 103.
11. Ginn SL, Alexander IE, Edelstein ML, Abedi MR, Wixon J. *Gene therapy clinical trials worldwide to 2012 - an update*. J Gene Med **2013**, 15, 65-77.
12. http://www.wiley.com//legacy/wileychi/genmed/clinical/
13. Wirth T, Parker N, Ylä-Herttuala S. *History of gene therapy*. Gene **2013**, 525, 162-169.
14. Li S-d, Huang L-y. *Nonviral gene therapy: promises and challenges*. Gene Ther **2000**, 7, 31-34.
15. Wagner E. *Biomaterials in RNAi therapeutics: quo vadis?* Biomat Sci **2013**, 1, 804-809.
16. Haussecker D. *Current issues of RNAi therapeutics delivery and development*. J Control Release **2014**, 195, 49-54.
17. Zhang G, Budker V, Wolff JA. *High levels of foreign gene expression in hepatocytes after tail vein injections of naked plasmid DNA*. Hum Gene Ther **1999**, 10, 1735-1737.
18. Bartlett DW, Davis ME. *Insights into the kinetics of siRNA-mediated gene silencing from live-cell and live-animal bioluminescent imaging*. Nucleic Acids Res **2006**, 34, 322-333.
19. Soutschek J, Akinc A, Bramlage B, Charisse K, Constien R, Donoghue M, Elbashir S, Geick A, Hadwiger P, Harborth J*, et al. Therapeutic silencing of an endogenous gene by systemic administration of modified siRNAs*. Nature **2004**, 432, 173-178.

20. Lorenzer C, Dirin M, Winkler A-M, Baumann V, Winkler J. *Going beyond the liver: Progress and challenges of targeted delivery of siRNA therapeutics*. J Control Release **2015**, 203, 1-15.
21. Scott DW, Lozier JN. *Gene therapy for haemophilia: prospects and challenges to prevent or reverse inhibitor formation*. Brit J Haematology **2012**, 156, 295-302.
22. Ashtari M, Cyckowski LL, Monroe JF, Marshall KA, Chung DC, Auricchio A, Simonelli F, Leroy BP, Maguire AM, Shindler KS, Bennett J. *The human visual cortex responds to gene therapy-mediated recovery of retinal function*. J Clin Invest **2011**, 121, 2160-2168.
23. Lachelt U, Wagner E. *Nucleic Acid Therapeutics Using Polyplexes: A Journey of 50 Years (and Beyond)*. Chem Rev **2015**, 115, 11043-11078.
24. Davis ME, Zuckerman JE, Choi CH, Seligson D, Tolcher A, Alabi CA, Yen Y, Heidel JD, Ribas A. *Evidence of RNAi in humans from systemically administered siRNA via targeted nanoparticles*. Nature **2010**, 464, 1067-1070.
25. Haussecker D. *The business of RNAi therapeutics in 2012*. Mol Ther Nucleic Acids **2012**, 1, e8.
26. Nathwani AC, Tuddenham EG, Rangarajan S, Rosales C, McIntosh J, Linch DC, Chowdary P, Riddell A, Pie AJ, Harrington C*, et al. Adenovirus-associated virus vector-mediated gene transfer in hemophilia B*. N Engl J Med **2011**, 365, 2357-2365.
27. Juliano R, Bauman J, Kang H, Ming X. *Biological Barriers to Therapy with Antisense and siRNA Oligonucleotides*. Mol Pharm **2009**, 6, 686-695.
28. Dohmen C, Edinger D, Frohlich T, Schreiner L, Lachelt U, Troiber C, Radler J, Hadwiger P, Vornlocher HP, Wagner E. *Nanosized multifunctional polyplexes for receptor-mediated siRNA delivery*. ACS nano **2012**, 6, 5198-5208.
29. Moghimi SM, Hunter AC, Murray JC. *Long-circulating and target-specific nanoparticles: theory to practice*. Pharmacol Rev **2001**, 53, 283-318.
30. Brannon-Peppas L, Blanchette JO. *Nanoparticle and targeted systems for cancer therapy*. Adv Drug Deliv Rev **2004**, 56, 1649-1659.
31. Troiber C, Edinger D, Kos P, Schreiner L, Kläger R, Herrmann A, Wagner E. *Stabilizing effect of tyrosine trimers on pDNA and siRNA polyplexes*. Biomaterials **2013**, 34, 1624-1633.
32. Dominska M, Dykxhoorn DM. *Breaking down the barriers: siRNA delivery and endosome escape*. J Cell Sci **2010**, 123, 1183-1189.
33. Mintzer MA, Simanek EE. *Nonviral vectors for gene delivery*. Chem Rev **2009**, 109, 259-302.
34. Reinhard S, Wagner E. *How to Tackle the Challenge of siRNA Delivery with Sequence-Defined Oligoamino Amides*. Macromol Biosci **2016**
35. Hartmann L, Krause E, Antonietti M, Börner HG. *Solid-Phase Supported Polymer Synthesis of Sequence-Defined, Multifunctional Poly(amidoamines)*. Biomacromolecules **2006**, 7, 1239-1244.
36. Schaffert D, Troiber C, Salcher EE, Fröhlich T, Martin I, Badgujar N, Dohmen C, Edinger D, Kläger R, Maiwald G. *Solid-Phase Synthesis of Sequence-Defined T-, i-, and U-Shape Polymers for pDNA and siRNA Delivery*. Angew Chemie Int Ed **2011**, 50, 8986-8989.
37. Lee DJ, Wagner E, Lehto T. *Sequence-defined oligoaminoamides for the delivery of siRNAs*. Methods Mol Bio **2015**, 1206, 15-27.
38. Weber J, Lachelt U, Wagner E. *Multifunctional Oligoaminoamides for the Receptor-Specific Delivery of Therapeutic RNA*. Methods Mol Bio **2015**, 1324, 369-386.
39. He D, Wagner E. *Defined polymeric materials for gene delivery*. Macromol Biosci **2015**, 15, 600-612.

40. Wagner E. *Polymers for nucleic acid transfer-an overview*. Adv Genet **2014**, 88, 231-261.
41. Fischer D, Li Y, Ahlemeyer B, Krieglstein J, Kissel T. *In vitro cytotoxicity testing of polycations: influence of polymer structure on cell viability and hemolysis*. Biomaterials **2003**, 24, 1121-1131.
42. Meyer M, Dohmen C, Philipp A, Kiener D, Maiwald G, Scheu C, Ogris M, Wagner E. *Synthesis and biological evaluation of a bioresponsive and endosomolytic siRNA-polymer conjugate*. Mol Pharm **2009**, 6, 752-762.
43. Felgner P, Barenholz Y, Behr J, Cheng S, Cullis P, Huang L, Jessee J, Seymour L, Szoka F, Thierry A. *Nomenclature for synthetic gene delivery systems*. Hum Gene Ther **1997**, 8, 511-512.
44. Plank C, Mechtler K, Szoka FC, Jr., Wagner E. *Activation of the complement system by synthetic DNA complexes: a potential barrier for intravenous gene delivery*. Hum Gene Ther **1996**, 7, 1437-1446.
45. Merkel OM, Urbanics R, Bedocs P, Rozsnyay Z, Rosivall L, Toth M, Kissel T, Szebeni J. *In vitro and in vivo complement activation and related anaphylactic effects associated with polyethylenimine and polyethylenimine-graft-poly(ethylene glycol) block copolymers*. Biomaterials **2011**, 32, 4936-4942.
46. Salcher EE, Kos P, Frohlich T, Badgujar N, Scheible M, Wagner E. *Sequence-defined four-arm oligo(ethanamino)amides for pDNA and siRNA delivery: Impact of building blocks on efficacy*. J Control Release **2012**, 164, 380-386.
47. Fröhlich T, Edinger D, Kläger R, Troiber C, Salcher E, Badgujar N, Martin I, Schaffert D, Cengizeroglu A, Hadwiger P*, et al. Structure–activity relationships of siRNA carriers based on sequence-defined oligo (ethane amino) amides*. J Control Release **2012**, 160, 532-541.
48. McKenzie DL, Kwok KY, Rice KG. *A potent new class of reductively activated peptide gene delivery agents*. J Biol Chem **2000**, 275, 9970-9977.
49. Klein PM, Müller K, Gutmann C, Kos P, Krhac Levacic A, Edinger D, Höhn M, Leroux J-C, Gauthier MA, Wagner E. *Twin disulfides as opportunity for improving stability and transfection efficiency of oligoaminoethane polyplexes*. J Control Release **2015**, 205, 109-119.
50. Romberg B, Hennink WE, Storm G. *Sheddable coatings for long-circulating nanoparticles*. Pharm Res **2008**, 25, 55-71.
51. Meyer M, Wagner E. *pH-responsive shielding of non-viral gene vectors*. Expert Op Drug Del **2006**, 3, 563-571.
52. Philipp A, Meyer M, Wagner E. *Extracellular targeting of synthetic therapeutic nucleic acid formulations*. Curr Gene Ther **2008**, 8, 324-334.
53. Chang KL, Higuchi Y, Kawakami S, Yamashita F, Hashida M. *Efficient gene transfection by histidine-modified chitosan through enhancement of endosomal escape*. Bioconjug Chem **2010**, 21, 1087-1095.
54. Lächelt U. *Proton-sponge activity and receptor-targeting of sequence-defined nucleic acid carriers*. LMU, **2014**
55. Plank C, Oberhauser B, Mechtler K, Koch C, Wagner E. *The influence of endosome-disruptive peptides on gene transfer using synthetic virus-like gene transfer systems*. J Biol Chem **1994**, 269, 12918-12924.
56. Maeda H, Wu J, Sawa T, Matsumura Y, Hori K. *Tumor vascular permeability and the EPR effect in macromolecular therapeutics: a review*. J Control Rel **2000**, 65, 271-284.
57. Maeda H, Bharate GY, Daruwalla J. *Polymeric drugs for efficient tumor-targeted drug delivery based on EPR-effect*. Eur J Pharm Biopharm **2009**, 71, 409-419.

58. Smrekar B, Wightman L, Wolschek MF, Lichtenberger C, Ruzicka R, Ogris M, Rodl W, Kursa M, Wagner E, Kircheis R. *Tissue-dependent factors affect gene delivery to tumors in vivo*. Gene Ther **2003**, 10, 1079-1088.
59. Cho K, Wang X, Nie S, Chen Z, Shin DM. *Therapeutic Nanoparticles for Drug Delivery in Cancer*. Clin Cancer Res **2008**, 14, 1310-1316.
60. de Bono JS, Ashworth A. *Translating cancer research into targeted therapeutics*. Nature **2010**, 467, 543-549.
61. Xia W, Low PS. *Folate-targeted therapies for cancer*. J Med Chem **2010**, 53, 6811-6824.
62. Sudimack J, Lee RJ. *Targeted drug delivery via the folate receptor*. Adv Drug Del Rev **2000**, 41, 147-162.
63. Parker N, Turk MJ, Westrick E, Lewis JD, Low PS, Leamon CP. *Folate receptor expression in carcinomas and normal tissues determined by a quantitative radioligand binding assay*. Anal Biochem **2005**, 338, 284-293.
64. Weitman SD, Lark RH, Coney LR, Fort DW, Frasca V, Zurawski VR, Kamen BA. *Distribution of the folate receptor GP38 in normal and malignant cell lines and tissues*. Cancer Res **1992**, 52, 3396-3401.
65. Ross JF, Chaudhuri PK, Ratnam M. *Differential regulation of folate receptor isoforms in normal and malignant tissues in vivo and in established cell lines. Physiologic and clinical implications*. Cancer **1994**, 73, 2432-2443.
66. Low PS, Henne WA, Doorneweerd DD. *Discovery and development of folic-acid-based receptor targeting for imaging and therapy of cancer and inflammatory diseases*. Chem Res **2007**, 41, 120-129.
67. Zhao R, Diop-Bove N, Visentin M, Goldman ID. *Mechanisms of membrane transport of folates into cells and across epithelia*. Annu Rev Nutr **2011**, 31, 177-201.
68. Patri AK, Kukowska-Latallo JF, Baker JR. *Targeted drug delivery with dendrimers: comparison of the release kinetics of covalently conjugated drug and non-covalent drug inclusion complex*. Adv Drug Del Rev **2005**, 57, 2203-2214.
69. Fekry B, Esmaeilniakooshkghazi A, Krupenko SA, Krupenko NI. *Ceramide Synthase 6 Is a Novel Target of Methotrexate Mediating Its Antiproliferative Effect in a p53-Dependent Manner*. PloS One **2016**, 11, e0146618.
70. Thomas TP, Huang B, Choi SK, Silpe JE, Kotlyar A, Desai AM, Zong H, Gam J, Joice M, Baker Jr JR. *Polyvalent dendrimer-methotrexate as a folate receptor-targeted cancer therapeutic*. Mol Pharm **2012**, 9, 2669-2676.
71. Abolmaali SS, Tamaddon AM, Dinarvand R. *A review of therapeutic challenges and achievements of methotrexate delivery systems for treatment of cancer and rheumatoid arthritis*. Cancer Chemother Pharmacol **2013**, 71, 1115-1130.
72. Rajagopalan PR, Zhang Z, McCourt L, Dwyer M, Benkovic SJ, Hammes GG. *Interaction of dihydrofolate reductase with methotrexate: ensemble and single-molecule kinetics*. Proc Natl Acad Sci **2002**, 99, 13481-13486.
73. Lachelt U, Wittmann V, Muller K, Edinger D, Kos P, Hohn M, Wagner E. *Synthetic polyglutamylation of dual-functional MTX ligands for enhanced combined cytotoxicity of poly(I:C) nanoplexes*. Mol Pharm **2014**, 11, 2631-2639.
74. Saibeni S, Bollani S, Losco A, Michielan A, Sostegni R, Devani M, Lupinacci G, Pirola L, Cucino C, Meucci G. *The use of methotrexate for treatment of inflammatory bowel disease in clinical practice*. Digest Liver Disease **2012**, 44, 123-127.
75. Breedveld P, Zelcer N, Pluim D, Sönmezer Ö, Tibben MM, Beijnen JH, Schinkel AH, van Tellingen O, Borst P, Schellens JH. *Mechanism of the pharmacokinetic interaction between methotrexate and benzimidazoles potential role for breast cancer resistance protein in clinical drug-drug interactions*. Cancer Res **2004**, 64, 5804-5811.

76. Wagner E, Zenke M, Cotten M, Beug H, Birnstiel ML. *Transferrin-polycation conjugates as carriers for DNA uptake into cells*. Proc Natl Acad Sci USA **1990**, 87, 3410-3414.
77. Kircheis R, Wightman L, Schreiber A, Robitza B, Rössler V, Kursa M, Wagner E. *Polyethylenimine/DNA complexes shielded by transferrin target gene expression to tumors after systemic application*. Gene Ther **2001**, 8, 28-40.
78. Kircheis R, Schuller S, Brunner S, Ogris M, Heider KH, Zauner W, Wagner E. *Polycation-based DNA complexes for tumor-targeted gene delivery in vivo*. J Gene Med e **1999**, 1, 111-120.
79. Miyamoto T, Tanaka N, Eishi Y, Amagasa T. *Transferrin receptor in oral tumors*. International journal of oral and maxillofacial surgery **1994**, 23, 430-433.
80. Singh M, Mugler K, Hailoo DW, Burke S, Nemesure B, Torkko K, Shroyer KR. *Differential expression of transferrin receptor (TfR) in a spectrum of normal to malignant breast tissues: implications for in situ and invasive carcinoma*. Appl Immunohistochem Mol Morphol **2011**, 19, 417-423.
81. http://www.gesetze-im-internet.de/tierschg/
82. http://www.felasa.eu/recommendations
83. https://www.gesetze-im-internet.de/tierschversv/BJNR312600013.html
84. Xu X-M, Chen Y, Chen J, Yang S, Gao F, Underhill CB, Creswell K, Zhang L. *A peptide with three hyaluronan binding motifs inhibits tumor growth and induces apoptosis*. Cancer Res **2003**, 63, 5685-5690.
85. Zhang W, Müller K, Kessel E, Reinhard S, He D, Klein PM, Höhn M, Rödl W, Kempter S, Wagner E. *Targeted siRNA Delivery Using a Lipo-Oligoaminoamide Nanocore with an Influenza Peptide and Transferrin Shell*. Adv Healthc Mater **2016**, 5, 1493-1504.
86. Müller K, Kessel E, Klein PM, Hoehn M, Wagner E. *Post-PEGylation of siRNA lipo-oligoamino amide polyplexes using tetra-glutamylated folic acid as ligand for receptor-targeted delivery*. Mol Pharm **2016**, 13 2332–2345.
87. Lee D-J, He D, Kessel E, Padari K, Kempter S, Lächelt U, Rädler JO, Pooga M, Wagner E. *Tumoral gene silencing by receptor-targeted combinatorial siRNA polyplexes*. J Control Release **2016**,
88. Edinger D, Klager R, Troiber C, Dohmen C, Wagner E. *Gene silencing and antitumoral effects of Eg5 or Ran siRNA oligoaminoamide polyplexes*. Drug Deliv Transl Res **2014**, 4, 84-95.
89. Lee D-J, Kessel E, Edinger D, He D, Klein PM, von Voithenberg LV, Lamb DC, Lächelt U, Lehto T, Wagner E. *Dual antitumoral potency of EG5 siRNA nanoplexes armed with cytotoxic bifunctional glutamyl-methotrexate targeting ligand*. Biomaterials **2016**, 77, 98-110.
90. Choi HS, Liu W, Liu F, Nasr K, Misra P, Bawendi MG, Frangioni JV. *Design considerations for tumour-targeted nanoparticles*. Nature Nanotechnology **2010**, 5, 42-47.
91. Paulos CM, Reddy JA, Leamon CP, Turk MJ, Low PS. *Ligand binding and kinetics of folate receptor recycling in vivo: impact on receptor-mediated drug delivery*. Mol Pharmacol **2004**, 66, 1406-1414.
92. Schultz RM, Papamatheakis JD, Luetzeler J, Ruiz P, Chirigos MA. *Macrophage involvement in the protective effect of pyran copolymer against the Madison lung carcinoma (M109)*. Cancer Res **1977**, 37, 358-364.
93. Bousquet PF, Paulsen LA, Fondy C, Lipski KM, Loucy KJ, Fondy TP. *Effects of cytochalasin B in culture and in vivo on murine Madison 109 lung carcinoma and on B16 melanoma*. Cancer Res **1990**, 50, 1431-1439.

94. Mihich E. *Combined effects of chemotherapy and immunity against leukemia L1210 in DBA/2 mice*. Cancer Res **1969**, 29, 848-854.
95. Mihich E, Kitano M. *Differences in the Immunogenicity of Leukemia L1210 Sublines in DBA/2 Mice*. Cancer Res **1971**, 31, 1999-2003.
96. Reddy JA, Xu L-C, Parker N, Vetzel M, Leamon CP. *Preclinical evaluation of 99mTc-EC20 for imaging folate receptor–positive tumors*. J Nuc Med **2004**, 45, 857-866.
97. Duncan R, Hume IC, Kopečková P, Ulbrich K, Strohalm J, Kopeček J. *Anticancer agents coupled to N-(2-hydroxypropyl) methacrylamide copolymers. 3. Evaluation of adriamycin conjugates against mouse leukaemia L1210 in vivo*. J Control Release **1989**, 10, 51-63.
98. Fridman R, Kibbey MC, Royce LS, Zain M, Sweeney TM, Jicha DL, Yannelli JR, Martin GR, Kleinman HK. *Enhanced tumor growth of both primary and established human and murine tumor cells in athymic mice after coinjection with Matrigel*. J Natl Cancer Inst **1991**, 83, 769-774.
99. Pretlow TG, Delmoro CM, Dilley GG, Spadafora CG, Pretlow TP. *Transplantation of Human Prostatic Carcinoma into Nude Mice in Matrigel*. Cancer Res **1991**, 51, 3814-3817.
100. Rose WC, Reed FC, Siminoff P, Bradner WT. *Immunotherapy of Madison 109 lung carcinoma and other murine tumors using lentinan*. Cancer Res **1984**, 44, 1368-1373.
101. He D, Müller K, Krhac Levacic A, Kos P, Lächelt U, Wagner E. *Combinatorial Optimization of Sequence-Defined Oligo(ethanamino)amides for Folate Receptor-Targeted pDNA and siRNA Delivery*. Bioconjug Chem **2016**, 27, 647-659.
102. http://www.janvier-labs.com/par-especes/souris-mutantes/product/nmri-nu.html
103. Weil D, Garcon L, Harper M, Dumenil D, Dautry F, Kress M. *Targeting the kinesin Eg5 to monitor siRNA transfection in mammalian cells*. Biotechniques **2002**, 33, 1244-1248.
104. Valentine MT, Fordyce PM, Krzysiak TC, Gilbert SP, Block SM. *Individual dimers of the mitotic kinesin motor Eg5 step processively and support substantial loads in vitro*. Nat Cell Biol **2006**, 8, 470-476.
105. Judge AD, Robbins M, Tavakoli I, Levi J, Hu L, Fronda A, Ambegia E, McClintock K, MacLachlan I. *Confirming the RNAi-mediated mechanism of action of siRNA-based cancer therapeutics in mice*. J clin invest **2009**, 119, 661-673.
106. Urban-Klein B, Werth S, Abuharbeid S, Czubayko F, Aigner A. *RNAi-mediated gene-targeting through systemic application of polyethylenimine (PEI)-complexed siRNA in vivo*. Gene Ther **2004**, 12, 461-466.
107. Judge AD, Bola G, Lee AC, MacLachlan I. *Design of noninflammatory synthetic siRNA mediating potent gene silencing in vivo*. Mol Ther **2006**, 13, 494-505.
108. Holohan C, Van Schaeybroeck S, Longley DB, Johnston PG. *Cancer drug resistance: an evolving paradigm*. Nat Rev Cancer **2013**, 13, 714-726.
109. Housman G, Byler S, Heerboth S, Lapinska K, Longacre M, Snyder N, Sarkar S. *Drug resistance in cancer: an overview*. Cancers **2014**, 6, 1769-1792.
110. Mantwill K, Köhler-Vargas N, Bernshausen A, Bieler A, Lage H, Kaszubiak A, Surowiak P, Dravits T, Treiber U, Hartung R, *et al. Inhibition of the Multidrug-Resistant Phenotype by Targeting YB-1 with a Conditionally Oncolytic Adenovirus: Implications for Combinatorial Treatment Regimen with Chemotherapeutic Agents*. Cancer Res **2006**, 66, 7195-7202.
111. Saad M, Garbuzenko OB, Minko T. *Co-delivery of siRNA and an anticancer drug for treatment of multidrug-resistant cancer*. Nanomed **2008**, 3, 761-776.

112. Devita VT, Serpick AA, Carbone PP. *Combination chemotherapy in the treatment of advanced Hodgkin's disease*. Ann Intern Med **1970**, 73, 881-895.
113. Baxevanis CN, Perez SA, Papamichail M. *Combinatorial treatments including vaccines, chemotherapy and monoclonal antibodies for cancer therapy*. Cancer Immunol Immunother **2009**, 58, 317-324.
114. Gandhi NS, Tekade RK, Chougule MB. *Nanocarrier mediated delivery of siRNA/miRNA in combination with chemotherapeutic agents for cancer therapy: current progress and advances*. J Control Release **2014**, 194, 238-256.
115. Ryser HJ-P, Shen W-C. *Conjugation of methotrexate to poly (L-lysine) increases drug transport and overcomes drug resistance in cultured cells*. Proc Natl Acad Sci **1978**, 75, 3867-3870.
116. Festing S, Wilkinson R. *The ethics of animal research. Talking Point on the use of animals in scientific research*. EMBO Reports **2007**, 8, 526-530.
117. Stei MM, Loeffler KU, Holz FG, Herwig MC. *Animal Models of Uveal Melanoma: Methods, Applicability, and Limitations*. BioMed Res Int **2016**, 2016, 4521807.
118. Schiffman JD, Breen M. *Comparative oncology: what dogs and other species can teach us about humans with cancer*. Phil Trans R Soc B **2015**, 370, 20140231.
119. Schuh JC. *Trials, tribulations, and trends in tumor modeling in mice*. Toxicol Pathol **2004**, 32, 53-66.
120. Harrington K, Rowlinson-Busza G, Syrigos K, Abra R, Uster P, Peters A, Stewart J. *Influence of tumour size on uptake of111In-DTPA-labelled pegylated liposomes in a human tumour xenograft model*. Br J Cancer **2000**, 83, 684.
121. https://www.lgcstandards-atcc.org/en.aspx
122. Cabral H, Matsumoto Y, Mizuno K, Chen Q, Murakami M, Kimura M, Terada Y, Kano MR, Miyazono K, Uesaka M*, et al. Accumulation of sub-100 nm polymeric micelles in poorly permeable tumours depends on size*. Nat Nanotechnol **2011**, 6, 815-823.
123. Beaney R, Lammertsma A, Jones T, McKenzie C, Halnan K. *In vivo measurements of regional blood flow, oxygen utilisation and blood volume in patients with carcinoma of the breast using positron emission tomography*. Clin Sci **1984**, 66, 16P-16P.
124. Davis ME. *The first targeted delivery of siRNA in humans via a self-assembling, cyclodextrin polymer-based nanoparticle: from concept to clinic*. Mol Pharm **2009**, 6, 659-668.
125. Bouchie A. *First microRNA mimic enters clinic*. Nat Biotech **2013**, 31, 577-577.
126. Maeda H. *The enhanced permeability and retention (EPR) effect in tumor vasculature: the key role of tumor-selective macromolecular drug targeting*. Adv Enzyme Regul **2001**, 41, 189-207.
127. Tietze N, Pelisek J, Philipp A, Roedl W, Merdan T, Tarcha P, Ogris M, Wagner E. *Induction of apoptosis in murine neuroblastoma by systemic delivery of transferrin-shielded siRNA polyplexes for downregulation of Ran*. Oligonucleotides **2008**, 18, 161-174.
128. Zhang W, Rodl W, He D, Doblinger M, Lachelt U, Wagner E. *Combination of sequence-defined oligoaminoamides with transferrin-polycation conjugates for receptor-targeted gene delivery*. J Gene Med **2015**, 17, 161-172.
129. Chollet P, Favrot MC, Hurbin A, Coll JL. *Side-effects of a systemic injection of linear polyethylenimine-DNA complexes*. The journal of gene medicine **2002**, 4, 84-91.
130. Burke RS, Pun SH. *Extracellular barriers to in Vivo PEI and PEGylated PEI polyplex-mediated gene delivery to the liver*. Bioconjug Chem **2008**, 19, 693-704.

131. Kos P, Lächelt U, Herrmann A, Mickler FM, Döblinger M, He D, Levačić AK, Morys S, Bräuchle C, Wagner E. *Histidine-rich stabilized polyplexes for cMet-directed tumor-targeted gene transfer*. Nanoscale **2015**, 7, 5350-5362.
132. Fleming RE, Migas MC, Holden CC, Waheed A, Britton RS, Tomatsu S, Bacon BR, Sly WS. *Transferrin receptor 2: Continued expression in mouse liver in the face of iron overload and in hereditary hemochromatosis*. Proc Natl Acad Sci **2000**, 97, 2214-2219.
133. Bartlett DW, Su H, Hildebrandt IJ, Weber WA, Davis ME. *Impact of tumor-specific targeting on the biodistribution and efficacy of siRNA nanoparticles measured by multimodality in vivo imaging*. Proc Natl Acad Sci **2007**, 104, 15549-15554.
134. Russ V, Frohlich T, Li Y, Halama A, Ogris M, Wagner E. *Improved in vivo gene transfer into tumor tissue by stabilization of pseudodendritic oligoethylenimine-based polyplexes*. J Gene Med **2010**, 12, 180-193.
135. Burke RS, Pun SH. *Extracellular barriers to in vivo PEI and PEGylated PEI polyplex-mediated gene delivery to the liver*. Bioconjug Chem **2008**, 19, 693-704.
136. Giannini EG, Testa R, Savarino V. *Liver enzyme alteration: a guide for clinicians*. Can Med Assoc J **2005**, 172, 367-379.
137. Kedmi R, Ben-Arie N, Peer D. *The systemic toxicity of positively charged lipid nanoparticles and the role of Toll-like receptor 4 in immune activation*. Biomaterials **2010**, 31, 6867-6875.
138. Finco D, Duncan J. *Evaluation of blood urea nitrogen and serum creatinine concentrations as indicators of renal dysfunction: a study of 111 cases and a review of related literature*. J Am Vet Med Assoc **1976**, 168, 593-601.

IX APPENDIX

4 Abbreviations

ALT	alanine transaminase
AST	aspartate transaminase
BUN	blood urea nitrogen
CCD	charge-coupled device
Cy7	cyanine 7
DNA	deoxyribonucleic acid
dsRNA	double-stranded RNA
e.g.	exempli gratia (for example)
EDTA	ethylenediamine tetraacetic acid
FolA	folic acid
FR	folate receptor
FELASA	Federation of European Laboratory Animal Science Associations
HBG	hepes buffered glucose
HE	haematoxylin and eosin
h	hour(s)

i.v.	intravenous(ly)
i.t.	intratumoral(ly)
MTX	methotrexate
min	minutes
miRNA	micro RNA
mRNA	messenger ribonucleic acid
PEG	polyethylene glycol
PBS	phosphate buffered saline
RNA	ribonucleic acid
RNAi	ribonucleic acid interference
RNase	ribonuclease
qRT-PCR	reverse transcription polymerase chain reaction
Stp	succinoyl tetraethylene pentamine
Sph	succinoyl pentaethylene hexamine
SD	standard deviation
SEM	standard error of the mean

Tf	transferrin
TfR	transferrin receptor

5 Publications

Lee D-J, Kessel E, Edinger D, He D, Klein P, Voith von Voithenberg L, Lamb D, Lächelt U, Lehto T, Wagner E. *Dual antitumoral potency of EG5 siRNA nanoplexes armed with cytotoxic bifunctional glutamyl-methotrexate targeting-ligand.* Biomaterials **2016**, 77, 98-110.

Zhang W, Müller K, Kessel E, Reinhard S, He D, Klein P, Höhn M, Rödl W, Kempter S, Wagner E. *Targeted siRNA Delivery Using a Lipo-Oligoaminoamide Nanocore with an Influenza Peptide and Transferrin Shell.* Advanced Healthcare Materials **2016**, 5(12), 1493-504.

Müller K, Kessel E, Klein P, Höhn M, Wagner E. *Post-PEGylation of siRNA Lipo-oligoamino Amide Polyplexes Using Tetra-glutamylated Folic Acid as Ligand for Receptor-Targeted Delivery.* Molecular Pharmaceutics **2016**, 13(7), 2332–2345.

Lee D-J, He D, Kessel E, Padari K, Kempter S, Lächelt U, Rädler J O., Pooga M, Wagner E. *Tumoral gene silencing by receptor-targeted combinatorial siRNA-polyplexes.* The Journal of Controlled Release **2016**, (Epub ahead of print).

Beckert, L, Kostka, L, Kessel, E, Krhac Levacic, A, Kostkova, H, Etrych, T, Lächelt, U, Wagner, E. *Acid-labile pHPMA modification of four-arm oligoaminoamide pDNA polyplexes balances shielding and gene transfer activity in vitro and in vivo.* European Journal of Pharmaceutics and Biopharmaceutics **2016**, 105, 85–96.

6 Abstracts and Poster

6.1 Poster

Lee D-J, Kessel E, He D, Klein P, Lächelt U, Lehto T, Wagner E. *Synergistic Antitumoral Potency Mediated by EG5 siRNA Nanoplexes with Bifunctional Glutamyl-MTX Targeting Ligand.* American Association of Pharmaceutical Scientists, Orlando, USA, October **2015**

Lee D-J, He D, Kessel E, Lächelt U, Wagner E. *Folate-Conjugated Oligomer-Based Combinatorial Nanocarrier for Tumor-Targeted siRNA Delivery.* European Symposium on Controlled Drug Delivery, Egmond aan Zee, Netherlands, April **2016**

Kessel E, Lee D-J, He D, Lächelt U, Wagner E. *Optimized Combinatorial Nanoparticles for Tumor-Specific siRNA Delivery and In Vivo Gene Silencing*. CeNS Workshop 2016: Nanoscale Matter – Novel Concepts and Functions, Venice, Italy, September **2016**

6.2 Abstract

Kessel E, Lee D-J, He D, Lächelt U, Wagner E. *Optimized combinatorial nanoparticles for systemic, tumor-specific siRNA delivery and in vivo gene silencing*. CeNS Workshop 2016: Nanoscale Matter – Novel Concepts and Functions, Venice, Italy, September **2016**

X ACKNOWLEDGEMENTS

There are many people to acknowledge who contributed to the completion of this thesis, either in a direct, scientific way or indirectly by keeping me motivated and happy.

First of all, I would like to express my gratitude to Univ.-Prof. Dr. Ernst Wagner, the mentor of this thesis and my supervisor at the chair of Pharmaceutical Biotechnology of the Ludwig-Maximilians-University Munich. I would like to thank him for his professional advice and support over the last years of experiments, including the careful proofreading of this thesis. Furthermore, I want to express my appreciation for the trust he has put in me regarding experimental and organizational tasks.

I would like to thank Univ.-Prof. Dr. Eckhard Wolf for being my veterinary supervisor and for accepting this doctoral thesis at the veterinary faculty.

Many thanks to Dian-Jang Lee, Katharina Müller and Wei Zhang for their reliable teamwork throughout the experiments.

Markus Kovac deserves my gratitude for his reliable work and experienced support in the animal facility, moreover I would like to thank him for his team spirit that enabled the positive working atmosphere, even in busy times.

Thanks a lot to Wolfgang Rödl for his inexhaustible patience and help with technical issues and for always lending a sympathetic ear to all the group members' needs.

My gratitude goes to Miriam Höhn for her great scientific support concerning the histological experiments and cell culture.

Thanks to Dr. Martina Rüffer for her help concerning the practical courses and her scientific support regarding histology.

I would like to thank all group members for their scientific contributions and for the great time I have experienced in our AK Wagner.

There are three more people in our AK that deserve special gratitude for contributions to this thesis and even more important for the great time we spent together.

Therefore, I like to thank Dominik Wendel for the funny conversations during our coffee breaks and moreover for introducing me into the magical world of key combinations for the efficient use of Word.

I am grateful for the company of Ines Truebenbach and Jasmin Kuhn, who have become far more than colleagues but dear friends to me, lifting my spirits at all times! Special thanks to Ines for proofreading of this thesis and Jasmin for many fabulous lunch meals.

My dissertation would not have been possible without the encouragement of my family and friends, many thanks to my mother and my father for the trust and confidence in me and their tireless support! Furthermore, I like to thank Anna and the my beloved flatmates Stefan, Jakob and Martin who have made my start in Munich as cool as I could have possibly hoped for!
I am grateful for my best friends Markus, Janina und Michi who have enriched my life for already more than a decade. Thank you for the support, energy and happiness that I have always found in your friendship. I am sure, we will accompany each other in the coming decades, too.
Samir, you believe in me when I don't even believe in myself, I am lucky you entered my life!